TOPICAL REVIEW · **OPEN ACCESS**

Engineered nanomaterials and microstructures for tissue engineering and regenerative medicine

To cite this article: Chiara Martinelli *et al* 2026 *Nano Futures* **10** 032001

NANO FUTURES

OPEN ACCESS

RECEIVED
7 April 2026

REVISED
7 June 2026

ACCEPTED FOR PUBLICATION
10 July 2026

PUBLISHED
11 August 2026

TOPICAL REVIEW

Engineered nanomaterials and microstructures for tissue engineering and regenerative medicine

Chiara Martinelli[1,2,*], **Claudio Conci**[1,2,*] and **Manuela Teresa Raimondi**[1,*]

[1] Politecnico di Milano, Department of Chemistry, Materials and Chemical Engineering 'Giulio Natta', Piazza Leonardo da Vinci 32, 20133 Milano, Italy
[2] These authors contributed equally to this work.
[*] Authors to whom any correspondence should be addressed.

E-mail: chiara.martinelli@polimi.it, claudio.conci@polimi.it and manuela.raimondi@polimi.it

Keywords: nanomaterials, microstructures, tissue engineering, regenerative medicine

Abstract

Tissue engineering stands at the forefront of regenerative medicine, offering innovative solutions to replace, repair, and enhance damaged or lost tissue functions. The key to its success lies in the careful selection of biomaterials. Mechanobiology plays a pivotal role in tissue regeneration, and recent advances have revealed the profound impact of mechanical cues on cell behavior and tissue development. Indeed, biomaterials have been engineered to provide structural support and mimic the mechanical features of native tissues. This topical review provides an in-depth exploration of the pivotal nanomaterials and microstructures related to the field, emphasizing the critical role of biocompatibility and mechanical properties, and describing the strategies for enhancing cellular interactions at the nano/microscale. Engineered nanomaterials developed to meet these essential criteria are analyzed, encompassing inorganic and organic nanoparticles. We discuss how they facilitate the controlled release of bioactive molecules, and provide mechanical support for cellular adhesion, proliferation, and differentiation. In the context of microstructures, we describe the microfabrication techniques and analyze innovative and recent materials for microscaffolds, their role in creating tissue-specific microenvironments, and their drug-release properties. Finally, open challenges in the field are addressed, including translation to clinical applications, and the potential impact of biocompatible engineered nanomaterials and microstructures.

1. Introduction

In the last decades, the increased aging of the world population has brought to the rise of diseases characterized by a growing request for organ replacement and tissue repair. Currently, organ failures are treated with transplants but unfortunately, they are greatly limited by the availability of immunologically compatible donors, with success rates that remain very low because of immune and transplant rejection [1]. According to the U.S. Government report on organ donation and transplantation, about 103 223 people are on the 2023 waiting list for organ transplantation and around 13 people die in the U.S. each day waiting for an organ transplant [2]. Presently, a person every eight minutes in the U.S. is added to the transplant waiting list and organ donor deficiency is at its highest point ever [2]. In Europe, the situation is not brighter: demand for organs exceeds their availability in all E.U. Member States, and the need increases faster than organ donation in most of them [3].

Tissue engineering, as defined by The National Science Foundation, is a discipline 'combining principles and methods of engineering and life sciences for understanding the structure-function of tissues and for developing biological substitutes to restore, maintain and improve tissue functions'. This approach holds great promise and in 2019, the global tissue engineering market has accounted for $9.88 billion with a prediction to reach around $25.68 billion by 2026 [4].

The main methodologies employed in tissue engineering are at the nano/microscale interface and typically involve (i) the use of acellularized scaffolds able to induce endogenous tissue regeneration and repair when implanted in the patient, or (ii) cell growth and differentiation into specific biocompatible tridimensional (3D) scaffolds, providing physiological mechanical stimuli and giving rise to newly formed functional tissues able to regenerate and/or replace injured tissues and damaged organs upon implantation [5–7].

The possibility to produce miniaturized artificial structures resembling native tissues and organs, combined with the introduction of biomaterials for fabricating scaffolds mimicking tissue microenvironment structure (i.e. the physiological niche), has revolutionized this field of research [8]. Moreover, integration of biomaterials, cells, and biochemical signaling molecules regulating their interactions can stimulate and promote tissue regeneration as evaluated both in *in vitro* and *in vivo* models [7, 9]. In the last years, many kinds of biomaterials have been developed, based on the following properties: i) biocompatibility, ii) surface topography and morphology, iii) degradation trends suitable to new tissue formation rates, and iv) 3D structure. These features can influence the capacity of cells to adhere, proliferate, migrate, and display a physiological behavior, finalized at developing a regenerated tissue even more performing than the original one [10, 11]. There are plenty of nano/micro materials of natural or artificial origin devised for tissue regeneration purposes.

The extracellular matrix (ECM) represents the main structural component of tissues. It has a prominent role in tissue modeling, providing signals and stimuli for influencing cell phenotype, behavior, and fate, and is mainly composed of collagen, fibronectin, elastin, and proteoglycans [12]. The most critical features of ECM are stiffness, surface topography, geometry, and chemical composition, and all of them dynamically influence cells in terms of mechanical stimuli and molecular activation, impacting correct tissue formation and organization [13]. Cells physically interact with the ECM and once detected its mechanical properties, they transduce signals to the intracellular components, such as cytoskeletal proteins, in a process called mechanotransduction. The main key players involved in this signaling cascade are integrins, transmembrane receptors able to bind ECM proteins on the extracellular domain, and the cytoskeleton localized in the intracellular domain. Upon specific binding, many other proteins are recruited in small focal complexes present on membrane protrusions, that successively mature into focal adhesions responsible for transducing the mechanical intracellular tension across the cell membrane to the surrounding ECM [14].

Considering these observations, materials to be used as cell matrices must present a wide range of stiffnesses depending on the degree typical of each target tissue (i.e. from GPa for hard glass and polystyrene to MPa for elastomeric polymers and kPa for hydrogels). When fabricating 3D scaffolds, it is equally important to consider specific properties such as surface topography, fiber orientation, and porosity to favor the efficient transport of molecules necessary for cell proliferation and tissue regeneration [15].

An essential feature of any foreign body artificially introduced into a tissue or organ is to not elicit immune responses leading to inflammation, which might delay healing or may result in the rejection of the implant by the body. Ideally, tissue engineering aims at replacing the implanted material with the patient's cells, promoting the creation of a natural ECM. Therefore, the implant might be fully degradable, breaking down at a controlled rate aligned with the pace of new tissue formation and releasing by-products nontoxic to normal physiology [16]. Biomaterials can be considered foreign bodies capable of eliciting an inflammatory response upon implantation. Thus, fine regulation is required to obtain successful wound healing and inflammation resolution while avoiding tissue fibrosis [17]. The main steps of a foreign body reaction can be summarized into (i) haemostasis and inflammation, (ii) stimulation of cell proliferation and repair, and (iii) tissue remodeling. Upon tissue injury and within minutes, plasma proteins and ECM components are adsorbed on the biomaterial's surface, and a provisional matrix is formed. In terms of hours, innate immune cells, and in particular neutrophils, are recruited to the damaged site and lead to the onset of acute inflammation (figure 1(a)). The release of ROS and specific cytokines attracts monocytes, that can differentiate into macrophages polarizing into M1 pro-inflammatory or M2 anti-inflammatory phenotypes, eventually fusing with foreign body giant cells [18]. Specific release of inflammatory signals facilitates fibroblast infiltration and formation of a fibrotic capsule with subsequent implant rejection [19].

In this process, the architecture of the designed scaffold holds significant importance: highly porous structures with interconnected pores are essential for facilitating cell migration, new blood vessel formation, and diffusion of nutrients to the cells while removing waste products. Pore size plays a critical role, and it must be large enough to enable cell migration, yet small enough to maintain a considerable surface area for binding a suitable number of cells to the structure [20]. In this case, the acute inflammatory process can promote integration of the implant and tissue repair. Indeed, in terms of days, cells

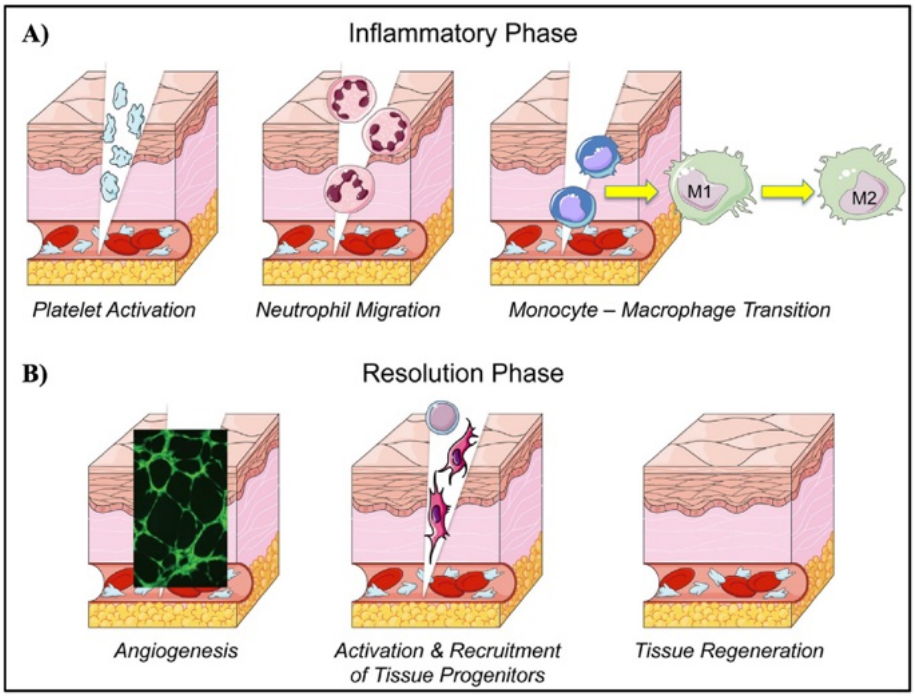

Figure 1. Main events and phases of the wound healing process. In the inflammatory phase (A), platelets activate, and neutrophils start migrating at the wound site. Upon release of specific signals, monocytes are recruited and undergo polarization into M1, pro-inflammatory or M2, anti-inflammatory phenotypes. The resolution phase (B) is characterized by angiogenesis, involving endothelial cell proliferation, activation, and recruitment of progenitor cells, and culminates in the complete tissue regeneration. Reproduced from [23]. CC BY 4.0. Copyright 2017 the authors, published by frontiers media SA.

start dividing replacing the damaged tissue, and specific factors, such as cytokines, growth factors, and extracellular vesicles carrying nucleic acids, proteins, and lipids released by macrophages induce migration and proliferation of endothelial cells creating new blood vessels [21, 22]. Finally, inflammation is resolved, the provisional granulation tissue matures, and the temporary ECM is substituted by a collagen matrix (figure 1(b)). The remodeling process can last from weeks up to months depending on the specific tissue damage [23].

Engineered biocompatible materials, specifically tuned with nanoparticles (NPs), have been developed as vehicles for controlled drug delivery, enhancing the mechanical properties of 3D scaffolds, providing functionalized surface area, improving cell adhesion and interaction, mimicking the tissue microenvironment architecture, and for modulating immune cells' behavior. Parameters such as nanomaterials' size [24, 25], shape, stiffness, surface roughness, topography, charge, degradability, and ligand functionalization have been studied for modulating the stiffness of the regenerated tissue [26], and mixing between two or more nanomaterials has been exploited for achieving hybrid multifunctional devices for reducing inflammatory outcomes [27].

Nanostructured materials with optimized mechanical properties and surface nanotopography can control the switch from M1 pro-inflammatory macrophages, toward M2 anti-inflammatory macrophages [28]. A central mechanism underlying this process is mechanotransduction and the ability of macrophages to convert physical stimuli from the microenvironment into biochemical signals. Integrin-mediated adhesion complexes represent the primary mechanosensing machinery, and upon interaction with nanostructured surfaces, they cluster and activate focal adhesion kinase (FAK), leading to downstream signaling mediated by Src, PI3K/Akt, MAPK/ERK, and RhoA/ROCK pathways. These cascades regulate the cell cytoskeleton that contributes to determine macrophage phenotype. Generally, increased cytoskeletal tension and matrix stiffness trigger the RhoA/ROCK–FAK axis and influence inflammatory genes expression, whereas biomimetic matrices tend to favor a pro-regenerative M2 profile [29]. Among the most important mechanotransduction effectors are the Hippo pathway co-activators YAP (Yes-associated protein) and TAZ. Mechanical signals generated by nanomaterial stiffness and nanotopography can regulate YAP/TAZ nuclear translocation, and their subsequent interaction with transcription factors controlling genes involved in inflammation, metabolism, proliferation, and tissue remodeling. Increasing evidence indicates that YAP/TAZ act as key molecular switches linking mechanical cues to macrophage polarization, by means of their coupling to integrin-FAK-RhoA signaling

and cytoskeletal dynamics [30]. Furthermore, mechanosensitive ion channels such as Piezo1 and TRPV4 respond to substrate stiffness and nanomaterial-induced membrane deformation, triggering Ca^{2+} influx and activation of NF-κB, mitogen-activated protein kinase (MAPK), and STAT signaling. These pathways modulate cytokine production and macrophage phenotype [31]. Currently, the design of immunomodulatory nanomaterials is increasingly focusing on integrating structural and mechanical features regulating these pathways. Such strategies allow timely modulation of macrophage polarization, promoting an initial M1 response for pathogen clearance followed by a switch toward the M2 phenotype to enhance tissue regeneration, vascularization, and healing [32]. In the last years, emerging mechanobiological theories have been developed, with high relevance to the field of nanomaterials for immunomodulation. One of these is the motor-clutch model, which describes how integrins, focal adhesions, and the actomyosin cytoskeleton cooperate to convert nanoscale mechanical cues into intracellular forces. This framework predicts how variations in ligand spacing, nanotopography, and substrate stiffness regulate force transmission, influencing macrophage polarization and YAP/TAZ activation. Recent reviews have proposed this model as a unifying theory for mechanobiology and mechanomedicine, making it particularly relevant for the design of immunomodulatory biomaterials [33]. Another highly relevant model is the cellular tensegrity theory, originally proposed by Ingber *et al* and recently revisited through computational and multiscale models [34]. Tensegrity describes the cell as a prestressed mechanical network in which cytoskeletal tension and extracellular forces are globally integrated. In macrophages, this framework helps explain how nanomaterial-induced changes in cytoskeletal architecture can transmit mechanical signals to the nucleus and alter inflammatory gene expression. Modern tensegrity-based models provide quantitative tools to predict cellular responses to engineered nano- and microenvironments [35]. Recent advances also emphasize YAP/TAZ-centered computational mechanotransduction models, which integrate matrix mechanics, focal adhesion dynamics, RhoA signaling, and nuclear mechanosensing into predictive systems-level frameworks. These theories are increasingly used to identify design procedures for biomaterials capable of controlling immune-cell phenotypes through mechanical regulation of transcriptional programs. Notably, these approaches are expected to enable *in silico* optimization of nanomaterial properties before experimental testing, accelerating the development of next-generation immunomodulatory biomaterials [30]. Finally, the theory of dynamic reciprocity has been developed, which views cells and biomaterials as a continuously evolving feedback system. According to this concept, macrophages not only sense nanomaterial properties but also actively remodel their microenvironment, generating adaptive mechano-immune responses. This perspective supports the development of responsive nanomaterials that can dynamically modulate M1–M2 transitions during healing [36].

Also, microscaffolds can provide a controlled microenvironment to modulate inflammation in terms of polarization and changing behavior of macrophages, and their characteristics including composition, chemistry, and stiffness play a critical role in these processes.

In recent years, fabrication techniques like inkjet bioprinting have been extensively used for precise control over drug deposition, making it potentially suitable for developing scaffolds with drug loading capabilities for targeted therapies, including possibly controlling macrophage responses. By incorporating drugs into scaffold materials, these created smart scaffolds would release therapeutic agents in a controlled manner, minimizing inflammation and immune response at the implant site. This innovative approach not only provides greater control over drug release kinetics but also ensures that drugs are delivered directly to the target tissue, optimizing therapeutic outcomes while minimizing side effects. As research in this field continues to advance, nanomaterials optimization and smart scaffold technology hold great promise for revolutionizing the management of foreign body reactions and enhancing the efficacy of implanted medical devices [37].

In this review, we will provide an overview of the biocompatible nanomaterials and microstructures presently applied in the tissue engineering field. Their applications in the regeneration of tissues, such as bone, skin, cartilage, and wound healing will be described. The state of the art in the clinical context will be also discussed, highlighting their impact on the development of functional, integrated tissues.

2. Tissue engineering in the current age

Tissue engineering has evolved from meticulous material selection for scaffold manufacturing to the current emphasis on nano and micrometric materials and growth factors technology, to stimulate and maintain cells in their physiological environment.

Crucial to this process are materials that are both biocompatible and biodegradable and, for assessing these features and evaluating their safety and effectiveness, rigorous *in vitro* tests have been

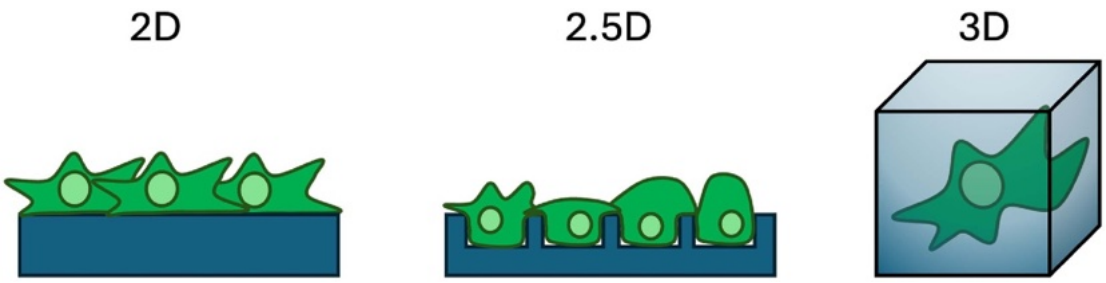

Figure 2. Schematic representation of the 2D, 2.5D, and 3D cell culture substrates classified based on their geometry and on how cells interact with their surrounding environment.

developed [38]. Current approaches face challenges such as using inappropriate materials that fail to accurately mimic the physiological properties of tissues and may induce undesired and uncontrolled immune reactions.

Additionally, cell growth is often ineffective, because of the limited production of growth factors required to stimulate cell communication and the non-effective mechanical stimulation typical of native tissue. *In vivo*, cells are significantly influenced by the surrounding ECM in terms of stiffness, surface topography, geometry, and specific composition, all of which regulate their behavior. Chemical stimulation of the tissue microenvironment is another fundamental aspect determining the success of tissue engineering, and many challenges in terms of efficiency and reproducibility remain to be addressed.

The integration of tissue engineering and nano/microstructures may solve these issues; materials, including NPs, hydrogels, and 3D-printed scaffolds, have been explored for their potential to enhance effectiveness in regenerative medicine applications.

In the field of biomaterials and tissue engineering, cell culture substrates are typically classified into 2D, 2.5D, and 3D based on their geometry and on how cells interact with their surrounding environment (figure 2) [39]. 2D substrates consist of flat surfaces where cells adhere and spread in a single plane. These systems provide a simplified and highly controlled environment, even though they poorly reproduce the complexity of native tissues. Cell-substrate interactions occur mainly at the basal membrane, and cells display a flattened morphology, altered cytoskeletal organization, and gene expression profiles that often differ from those observed *in vivo*. 2.5D substrates represent an intermediate configuration, characterized by surface features such as grooves, pillars, wells, or multilayered architectures that introduce partial three-dimensionality without fully embedding the cells. These topographies provide additional mechanical and geometrical cues, influencing cell adhesion, orientation, migration, and force generation. Cells can interact with multiple surfaces and are spatially confined, more closely resembling physiological conditions respect to conventional 2D cultures. Finally, 3D substrates, including porous scaffolds, hydrogels, and ECM-like networks, allow cells to interact with their environment in all spatial directions. Cells are surrounded by a 3D architecture characterized by defined stiffness, porosity, and mass transport properties, and this configuration promotes more realistic cell morphology, cell–cell communication, mechanotransduction, differentiation, and tissue-specific functions. 3D systems provide the most representative model of tissues and thus they are the preferred substrate for regenerative medicine.

NPs present a small size (1–1000 nm), they can easily cross cell membranes and, thanks to their high surface-to-volume ratio and physical-chemical properties, they have revealed versatile agents in many biomedical applications, from therapeutic agents to imaging tools and contrast agents, to targeted drug delivery systems [40–42]. Most NPs are biocompatible, biodegradable, present low immunogenicity, and are relatively easy to fabricate [43, 44], and nowadays, most of them are synthesized from inorganic and organic materials (figure 3).

Microscaffolds, which have complex porosity architectures intended to imitate the natural ECM, can be made from natural or synthetic materials. The mechanical strength, porosity, and degradation kinetics of scaffolds are some of the characteristics that have a significant impact on tissue regeneration and cell activity. Nanotechnology (for the materials used) and 3D microstructuring represent advances in scaffold design that allow for fine control over the architecture and characteristics of the scaffold. Furthermore, by creating a supportive microenvironment, the idea of 'living scaffolds', in which cells are enclosed within the scaffold or scaffold-free environments (such as spheroids or cell sheets), has the potential to improve tissue regeneration.

In this context, nanomaterials can readily interact with cell membranes and modulate cellular responses favoring cell adhesion, proliferation, migration and differentiation, essential for achieving

efficient tissue and organ regeneration. Moreover, when combined with microstructured scaffolds, that mimic tissue microenvironments through controlled porosity and mechanical properties, they actively contribute, thanks to their chemical–physical features, to the creation of supportive regenerative conditions. This synergistic interaction not only facilitates tissue regeneration but also enhances the activation of biological pathways, ultimately improving the efficacy of tissue engineering approaches.

Currently, some of the main tissues object of research in tissue engineering and repair are bone, skin, cartilage, and blood vessels. Pathologies involving these organs have become very common and there is an increasing need for possible alternatives to standard medical and surgical approaches. Concerning bones, apart from conventional implants, innovative bone grafts have been developed by using advanced nano and biomaterials. The introduction of bioactive and biocompatible scaffolds with surfaces able to support cell growth, promote differentiation, and mimic the biological microenvironment and the mechanical forces necessary to provide physiological stimuli has been fundamental for successful bone regeneration [45].

Skin trauma is an injury involving the epithelial layers of this tissue. When large areas need to be covered, it becomes difficult to promote wound healing, avoiding visible scars. Currently, autologous skin transplantation is the most common type of intervention; with the advent of tissue engineering, the artificial creation of functional skin tissues has been made possible, overcoming some of the well-known limitations linked to conventional approaches [46].

Cartilage does not present blood vessels and nerves, and its defects can be repaired by patient's or donor's tissue transplantation, chondrocyte/mesenchymal stem cells (MSCs) transplantation, delivery of cellularized scaffolds, and filling with biomaterials. Although many efforts have been made in the direction of repairing this tissue, unfortunately, current strategies present many drawbacks among which are limited autologous cell sources and transplant rejection [47].

The increase in cardiovascular diseases has brought a continuous need for functional blood vessels to be used in bypass and transplant procedures. However, allogeneic transplantation brings increased risks of thrombosis, stenosis, and vascular degeneration. Thanks to tissue engineering, many systems have been developed for stimulating blood vessel regeneration with the support of *ad hoc* devised nanomaterials and 3D microstructures [48]. In the following sections, the roles of NPs and microstructures in tissue engineering will be reported, emphasizing their contribution in solving specific issues.

3. Inorganic nanomaterials in tissue engineering

Inorganic nanomaterials have gained rising interest in tissue engineering thanks to their biocompatibility, magnetic, antibacterial, and mechanical properties. Moreover, they can be functionalized with fluorescent and bioactive molecules [49], such as growth factors, and are easily uptaken by living cells; they can deliver molecules and drugs with specific targeting and finely modulate cell activity.

Inorganic NPs are exploited because of their biocompatibility and degradability; they can be used as carriers for poorly soluble drugs and as calcium sources for bone repair [50, 51]. Iron oxide NPs (IONPs) have been approved by the Food and Drug Administration (FDA) [52]; they present superparamagnetic properties and are very versatile as drug delivery carriers and contrast agents [53]. Cerium oxide NPs (i.e. nanoceria), thanks to their reactive oxygen species (ROS) scavenging activity have demonstrated efficient in regenerative therapies [54]. Moreover, they present anti-inflammatory, antibacterial, and angiogenic properties and have been incorporated into polymeric scaffolds for promoting wound healing [55].

The main inorganic nanomaterials employed in tissue regeneration belong to the following categories: (i) metal NPs, (ii) magnetic NPs, (iii) cerium oxide NPs, (iv) calcium phosphate-based NPs, and (v) carbon-based NPs (figure 3(a)), (table 1).

4. Metal NPs

Gold NPs (AuNPs) are a colloid of nanometric particles of gold. Turkevich was the first to synthesize spherical AuNPs in 1951 [74]. From then, many modifications to the protocol have been introduced for obtaining multiple shapes and many procedures for functionalization with different ligands, from proteins to antibodies, to fluorophores and small chemical groups such as thiols and amines were set [74, 75]. Thanks to their unique optical and physical properties, such as surface plasmon resonance [76], and high biocompatibility, AuNPs application has spread in disparate fields of research and medicine.

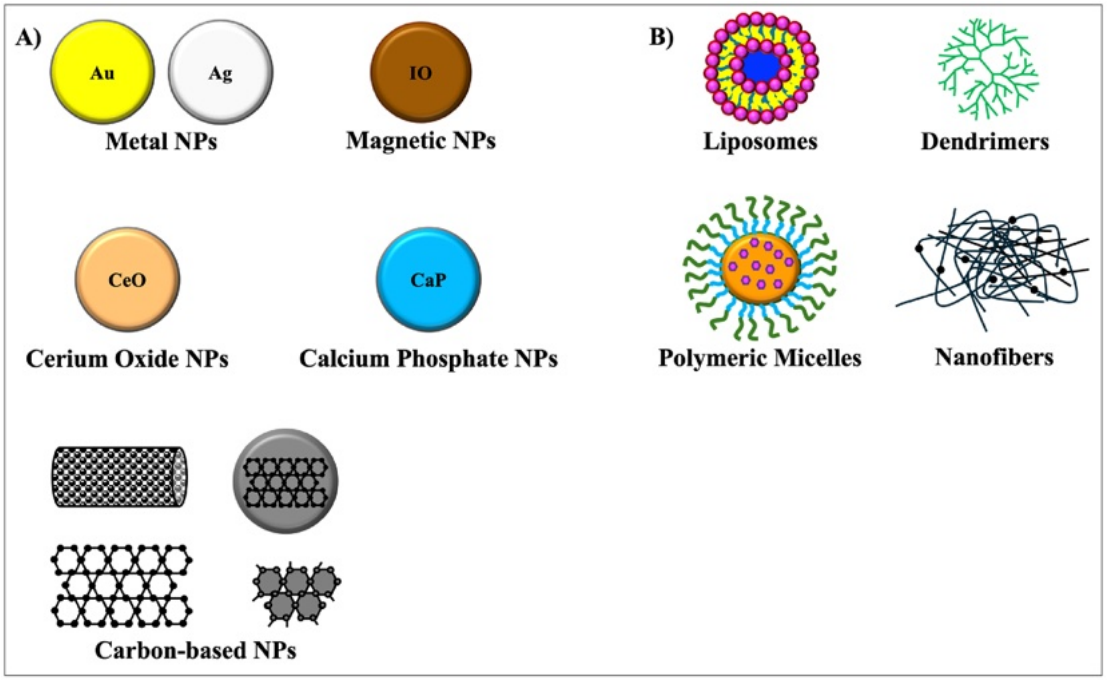

Figure 3. Scheme of the main inorganic and organic nanomaterials investigated in nanomedicine and employed in tissue engineering. (A) Inorganic nanoparticles: from top to bottom, metal nanoparticles (NPs), magnetic NPs, cerium oxide NPs, calcium phosphate NPs, carbon-based NPs. (B) Organic nanoparticles: from top to bottom, liposomes, dendrimers, polymeric micelles, nanofibers.

Table 1. Inorganic nanomaterials applied to tissue engineering.

Nanoparticle	Fabrication approach	Targeted organ	Results	Ref.
AuNPs	Homogenization	Myocardium	Electrical conductivity; *ex vivo* non-invasive monitorization by computer tomography	[56]
AuNPs	Reduction	Bone	Size-dependent induction of osteogenic differentiation; upregulation of β-catenin and p-GSK-3β; *in vivo* stimulation of bone regeneration	[57]
AuNCs	Reduction	Skin	Rapid detection of gram-positive and gram-negative bacteria; *in vivo* biocompatibility and biosafety	[58]
AuNPs	Reduction	Skin, bone	Size dependent induction of M2 macrophage polarization; promotion of osteogenic differentiation; degradation of *S. aureus*	[59]
AuNPs	Reduction	Skin	Bactericidal and antioxidant activity; biocompatibility; *in vitro* promotion of cell proliferation and migration; *in vivo* accelerated vascularization and collagen deposition upon combination with electrical stimuli	[60]
AgNPs	Aqueous solution mixture and precipitation	Skin	Antibacterial activity against *S. aureus* and *K. pneumoniae* infection; *in vivo* accelerated wound regeneration; enhanced expression of TNF-α IP8, Cox2, MHCII; Col I and αSMA	[61]
AgNPs	Incorporation into a matrix of catechol-modified hyaluronic acid	Skin	Antibacterial activity against *S. aureus* infection; M2 macrophage polarization; down regulation of IL-6 and TNF-α; upregulation of Il-10; promotion of mature blood vessels formation	[62]
SPIONs	Co-precipitation	Bone	Stimulation of cell adhesion, proliferation, and ALP expression	[63]
IO-NPs	Chemical bonding of carbon–carbon double bonds between GelMA and IO-NPs	Cartilage	*In vitro* promotion of oxidative phosphorylation of mitochondria; facilitated lipids catabolism in chondrocytes; *in vivo* tissue remodeling	[64]

(Continued.)

Table 1. (Continued.)

Nanoparticle	Fabrication approach	Targeted organ	Results	Ref.
IO-NPs	Not specified	Cartilage	Efficient MSCs labeling without affecting viability and differentiation ability; enhanced MRI tracking; *in vivo* defect regeneration and proteoglycan formation	[65]
Nanoceria	Hydrothermal synthesis	Bone	Increased proliferation and migration of MSCs; stimulation of osteogenic differentiation; ROS scavenging; upregulation of genes related to cell growth, migration, osteogenesis, ROS metabolism; *in vivo* bone regeneration	[66]
Nanoceria	Nanoemulsion	Skin	*In vitro* enhanced antibacterial, antioxidant and wound healing properties; *in vivo* full thickness wound contraction and increased collagen synthesis	[67]
Nanoceria	Modified cerium oxide nanorods crosslinked to the hydrogel	Skin	*In vitro* ROS scavenging ability; *in vivo* biocompatibility and biodegradability; *in vivo* enhanced wound healing and epithelium regeneration	[68]
CaP NPs	Co-precipitation	Skin, bone	Efficient bFGF release; promotion of fibroblasts and osteoblastic cells proliferation	[69]
CaP NPs	Precipitation from aqueous solution	Bone	Efficient TNF-α gene silencing and VEGF-A and BMP-7 gene expression mediated by transfection; *in vivo* bone healing	[70]
CNPs	Hydrothermal carbonization of alginate biopolymer	Bone	*In vitro* hemocompatibility and cytocompatibility; *in vivo* induction of bone formation	[71]
Carbon dots	One-pot hydrothermal synthesis	Skin	*In vitro* biocompatibility, low cytotoxicity, antibacterial activity, enhanced cell proliferation and migration	[72]
MWCNTs	Commercially available	Bone	Biocompatibility and biodegradability; promotion of biomineralization; osteogenic differentiation	[73]

Recently, gold NPs have been applied in tissue engineering, especially for improving scaffold structure, inducing cellular responses finalized at repair and regeneration, and for intracellular delivery of molecules [77]. The electrical conductivity of AuNPs has been exploited in multiple ways. Researchers have incorporated AuNPs into polymers to create conductive scaffolds and elicit precise responses in cells [78, 79]. Carvalho *et al* have developed an injectable nanocomposite hydrogel composed of gelatin and hyaluronic acid (GHA) and incorporating lysozyme nanofibrils, obtaining enhanced mechanical and antioxidant properties, together with *in situ* synthesized gold NPs, giving electrical conductivity. These nanomaterials demonstrated excellent in myocardial regeneration as shown in *ex vivo* computer tomography [56].

AuNPs have been widely applied in the field of bone tissue regeneration. Osteogenesis is a very complex process involving many key players and cellular mechanisms, among which differentiation of osteoblasts, vascularization, and immunomodulation. A finely regulated balance must be established between progenitor cells belonging to the osteoblastic lineage that are responsible for tissue mineralization and calcium deposition, and osteoclasts that resorb mineralized bone. In the presence of a bone defect, it is of fundamental importance to enhance stem cells' functions, while repressing inflammation due to increased oxidative stress. Biomaterials, thanks to their properties, can influence the regulation of these processes. The use of biodegradable scaffolds displaying mechanical cues, prompting cell attachment, proliferation, and differentiation together with the introduction of AuNPs that can enhance the scaffold features, promote cell adhesion and response, deliver bioactive molecules, reduce inflammation, and support vascularization, has brought tremendous advancements [80, 81]. More in detail, gold NPs can efficiently participate in bone regeneration by (i) stimulating cells with a pulsed electromagnetic field [82], and (ii) inducing efficient cell differentiation [83]. For instance, different sizes of NPs have been able to elicit distinguished responses in pre-osteoblasts and stem cells [57].

MSCs typically differentiate into osteocytes, adipocytes, and chondrocytes upon proper stimuli [84], and many mechanisms are involved in their osteogenic differentiation. AuNPs can (i) interact with specific proteins activating precise differentiation pathways through mechanical forces [85], (ii) activate the extracellular signal-regulated kinase (ERK)/ MAPK) pathway promoting osteoblasts differentiation [86], or (iii) work as antioxidants reducing the production of ROS and negatively affecting osteoclasts formation [87]. The size, shape, and concentration of AuNPs have been demonstrated fundamental for

regulating MSCs and pre-osteoblasts differentiation towards osteogenesis [57, 88]. Generally, smaller sizes between 20 and 50 nm and spherical NPs have been revealed to be more efficient in promoting osteogenesis [83].

Incorporation of AuNPs into polymer scaffolds can be exploited for modulating their properties, for better mimicking the bone tissue ECM, favoring cell proliferation, and differentiation, for providing mechanical and electrical stimuli, and for regulating the degradation of the scaffolds upon *in vivo* implantation [80]. For instance, scaffolds often present poor mechanical properties, and incorporating AuNPs enhances their mechanical strength. An injectable chitosan/k-carrageenan hydrogel added with AuNPs was demonstrated to be efficient in supporting cell adhesion and growth [89].

Currently, one of the most critical clinical health issues concerns the problem of wound healing. Indeed, skin regeneration is a complex process involving many key players and it presents difficult challenges to overcome. Strategies for eliminating possible infections, promoting cell proliferation, and accelerating healing are currently top priorities. Although electrical stimulation has been used as a therapy, this technique is not sufficient to cover large areas. Moreover, the high risk of bacterial infection poses a threat because it usually destroys newly generated tissues and induces an inflammation cascade that can reduce treatments' efficacy. In wound-healing applications, gold nanostructures have therefore been exploited along a common path: combining their intrinsic antibacterial and antioxidant activity with a polymer or peptide matrix, and frequently potentiating it through photothermal or electrical stimulation, to clear infection while simultaneously promoting M2 macrophage polarization, cell proliferation and angiogenesis [58–60, 90–92].

An imaging-guided antibacterial platform constituted by ultra-small gold nanoclusters (AuNCs) protected with an antimicrobial peptide HHC10 and glutathione co-ligand was applied for selective detection of bacteria and antibiotic effect, showing great potential for wound healing *in vivo* [58]. Gold nanorods functionalized with the antimicrobial peptide C-At5 have been developed for selectively contrasting gram-positive and gram-negative infection. These NPs were demonstrated to be highly biocompatible in human skin fibroblasts and were able to enhance wound healing in mice models upon near-infrared photothermal therapy [90]. Gold NPS with a diameter of 50 nm were able to polarize macrophages toward an M2 phenotype and favored their phagocytic activity toward *Staphylococcus aureus*, thus inducing an anti-inflammatory response. Moreover, they promoted differentiation of bone marrow stromal cells *in vitro* showing great promise for future application *in vivo* [59].

Gold NPS have also been successfully integrated into matrices and polymers. An anti-microbial polymer constituted by poly hexamethylene biguanide and gold NPs for photothermal therapy has been developed and demonstrated effective in killing *S. aureus*, promoting wound healing in *in vivo* models, and enhancing M2 polarization and tissue angiogenesis [91]. Poly (ε-caprolactone) (PCL)/gelatin nanofibrous matrices loaded with gold NPs showed good mechanical properties and porosity favoring cell proliferation *in vitro* and *in vivo* in a rat model on a full- thickness excisional wound [92]. We report here a recent work, exemplifying the use of gold NPs as agents to modify a material and promote regeneration in an *in vivo* model. Poly(lactic-co-glycolic acid) (PLGA) membranes have been modified with gold NPs and antibacterial peptides enhancing their anti-inflammatory, antibacterial, and biocompatibility properties. Upon electrical stimuli, the nanomaterial efficiently promoted cell proliferation *in vitro* and displayed bactericidal and antioxidant properties. In *in vivo* models of full-thickness skin defect, the composite membrane showed significantly accelerated vascularization and collagen deposition supporting wound healing (figure 4) [60]. The results obtained led the authors hypothesize that the antimicrobial peptides efficiently improved the antibacterial properties of the membranes by inhibiting infections caused by pathogens and promoting full thickness skin defects in rats. Silver NPs (AgNPs) present great antimicrobial properties, being able to inhibit bacterial function by binding their surface and promoting ROS formation [93]. They are ideal candidates for being incorporated or synthesized *in situ* in scaffolds, especially for wound healing applications, when the probability of developing an infection is very high. Different kinds of polymers have been combined with AgNPs, and configured in different shapes, from nanofibrous to porous scaffolds. Interesting research reported the design of an antibacterial hydrogel, composed of AgNPs and poly (gamma-glutamic acid) (γ-PGA), meeting two of the most important requirements for wound healing: antibacterial and moisturizing capacities. *In vitro* and *in vivo* experiments revealed its efficient activity and showed optimal prevention of wound contraction in mice [94].

Chitosan hydrogels loaded with AgNPs and calendula extract were shown to be efficient as haemostatic, antibacterial, and anti-inflammatory materials, obtaining a controlled release of the natural compound [95]. Composite hydrogels constituted by chitosan, poly (vinyl alcohol) (PVA), and silver NPs together with ibuprofen were able to give sustained release of the molecule and showed antibacterial activity *in vitro*. *In vivo*, wound healing was promoted as indicated by the expression of specific

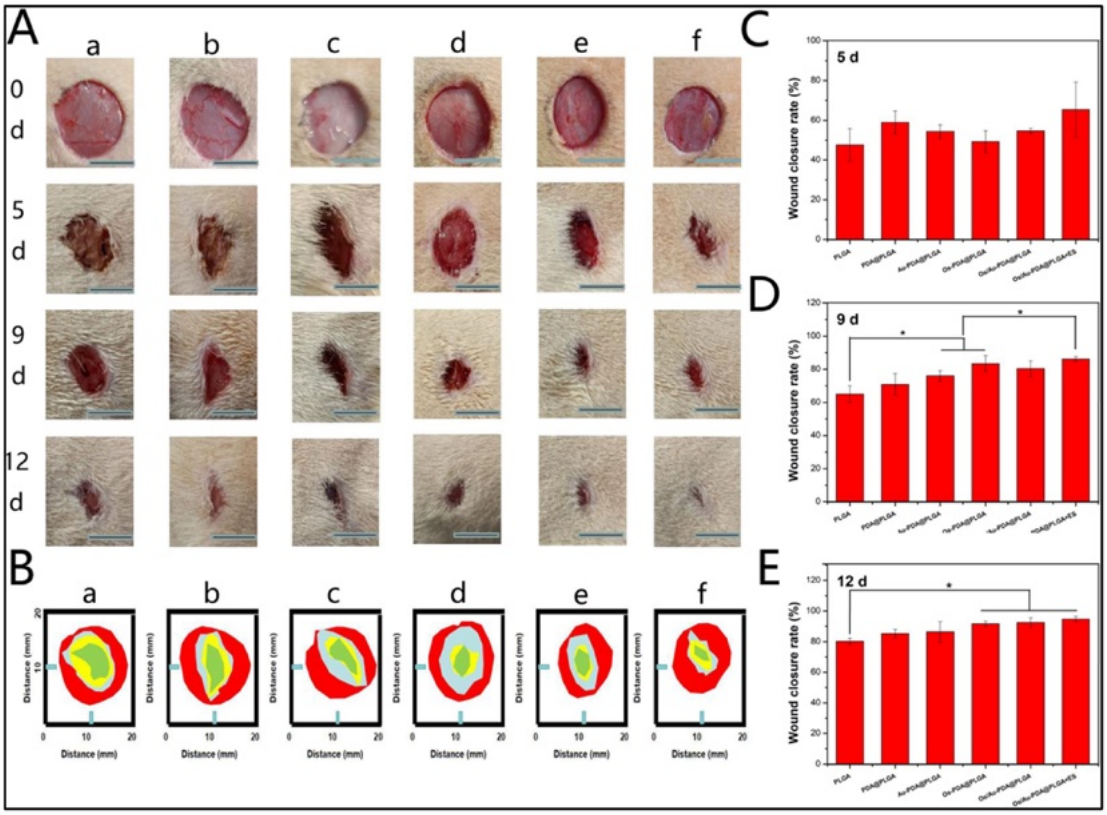

Figure 4. Evaluation of the effects of different membrane materials and electrical stimulation on skin wound healing in a rat skin defect model. (A) The closure rate of the wound defects with different treatments at days 0, 5, 9, and 12. (B) Schematic diagram of wound closure at different time points. (a) PLGA, (b) PDA@PLGA, (c) Au-PDA@PLGA, (d) Os-PDA@PLGA, (e) Os/Au-PDA@PLGA and (f) Os/Au-PDA@PLGA + ES. (C–E) Quantitative statistical analysis of wound closure for different treatments at 5, 9 and 12 d. Scale bar = 1 cm, $p < 0.05$, $n = 3$. PDA, polydopamine; Os, antibacterial peptides; ES, electrical stimulation. Reproduced from [60]. CC BY 4.0. Copyright 2024 the authors, published by Springer Nature.

markers of cell migration and proliferation [61]. Similarly, a nanocomposite of hyaluronic acid and silver NPs displayed a potent antibacterial activity against *S. aureus* and favored sustained release of basic fibroblast growth factor. This nanomaterial was able to induce M2 macrophage polarization, upregulation of anti-inflammatory cytokines, and regulate the deposition of collagen and vessel formation [62]. A nanoporous composite of chitosan and fibrin encapsulating silver NPs has been developed for wound healing. *In vitro* experiments validated the prepared bandage for safety, biocompatibility, and antibacterial properties against multiple microorganisms. *In vivo*, efficacy was proven in rats presenting postoperative abdomen wounds [96]. Interestingly, gold, and silver NPs bioactive glasses have been combined in biopolymer composites for application in bone regeneration. Proliferation and migration of human fibroblasts and osteoblast cells were favored, and new bone formation was promoted *in vivo* [97].

Summarizing the reported research concerning metal NPs, they have been widely applied as efficient tools for improving the mechanical properties of scaffolds, for stimulating cells to differentiation, for delivering molecules and for obtaining efficient antibacterial activity, avoiding undesired immune reactions.

5. Magnetic NPs

IO-NPs have been widely applied in the diagnostic and therapeutic fields, thanks to their biocompatibility in aqueous solutions and ease of functionalization [98]. These nanomaterials present a magnetically oriented core and can be exploited for targeted delivery and local release of drugs in the presence of an applied magnetic field [99, 100].

Collagen membranes have been modified by incorporating FDA-approved IO-NPs, greatly improving their osteo-conductivity and osteo-inductivity properties. This modified scaffold showed good biocompatibility *in vitro* on pre-osteoblast cells and efficiently stimulated their differentiation. Encouraging

results have been obtained upon implantation of the construct in rabbits carrying radial defects, where rapid bone repair was observed [101].

The loading of IO-NPs into polymeric scaffolds has been exploited for preparing devices for magnetic hyperthermia. *In vitro* experiments demonstrated that cell adhesion and proliferation were enhanced, and the expression of alkaline phosphatase (ALP) was stimulated, leading the way for their use in bone regeneration [63].

In the last years, many wound dressing polymers have been used for wound healing thanks to their biodegradability, biocompatibility, and haemostatic properties. The advent of nanomaterials, and IO-NPs, have been exploited to enhance the features of polymer-based hydrogels. In recent work, chitosan-dextran-glycerol hydrogels have been enriched with IO NPs and displayed decreased porosity and increased antibacterial activity, paving the way to a possible application for wound regeneration [102].

Daya *et al* modified IO-NPs with the pro-angiogenic natural molecule curcumin and then dispersed them in hyaluronic acid hydrogels. The nanomaterial showed a sustained release of the drug and biocompatibility upon culture of bone marrow-derived MSCs. Moreover, the NPs were magneto-responsive, and vascular endothelial growth factor was secreted in the presence of the magnetic hydrogel, thus demonstrating a promising strategy for tissue regeneration [103]. The use of magnetic NPs has been applied also to cartilage regeneration by modifying a hydrogel constituted by methacrylate gelatin with IO-NPs, that provided tuneable stiffness to the material based on their concentration. Upon interaction with chondrocytes, the biomaterials modulated their properties and promoted their metabolic activity, and upon *in vivo* implantation it demonstrated successful as a means for regeneration [64]. Suryadevara *et al* developed a labeling strategy for tracking MSCs and chondrogenic pellets based on the mechanoporation of MegaPro iron NPs. Upon cell labeling, their features were investigated by imaging and spectroscopy and successively, upon implantation in pig knee joints, by magnetic resonance imaging (MRI). NPs did not influence physiological cell behavior while displaying a better MRI performance with respect to cells labeled with ferumoxytol NPs [65].

Summarizing the reported findings concerning magnetic NPs, thanks to their physical chemical properties, they have been successfully used for improving tissue regeneration, for stimulating cell proliferation, for enhancing biomaterial mechanical features, for releasing drugs, and for gaining specific cell labeling.

6. Cerium oxide NPs

Cerium is a rare earth metal that can exist both as CeO_2 and Ce_2O_3. Cerium oxide (CeO) NPs (nanoceria) present both Ce^{3+} and Ce^{4+} on their surface and, as small as they become, the number of 3+ increases while oxygen vacancies are created. This peculiar feature gives to this nanomaterial specific properties, allowing it to act as a scavenger of hydroxyl and nitric oxide radicals, and peroxynitrite [104, 105].

Bone is currently one of the most transplanted tissues in the world and the exponential increase in bone fractures requires more effort to find effective therapies for repair and full functional recovery. During this process, the generation of free radicals is a known challenge that remains to be overcome. Tissue engineering approaches based on the use of scaffolds loaded with cerium oxide NPs able to scavenge free radicals and counteract oxidative stress contributing to a slowing of the healing process are currently a potential choice.

Generally, porous scaffolds favor bone healing and regeneration. Nanoceria incorporated into gelatin alginate scaffolds enhanced their mechanical features and biomineralization properties. Moreover, these composite scaffolds favored MSC differentiation together with reducing the presence of free radicals *in vitro* [106] and *in vivo* [107].

A nanocomposite scaffold carrying nanoceria effectively supported cell growth of human osteoblasts and their proliferation and mineralization. Upon oxidative stress induction, it efficiently reduced cytotoxicity and upon implantation showed good biocompatibility properties with minimal induction of immune response [108]. Kurian *et al* applied nanoceria and their properties as agents able to modify the surface properties of a material and facilitate stem cells proliferation. Indeed, the inclusion of uniform layers of nanoceria into gelatin methacryloyl (GelMA) matrices enhanced their mechanical properties and gave an antioxidant response to the microstructure. The scaffolds confirmed to be efficient in scavenging radicals *in vitro* by acting as antioxidants able to capture ROS. Moreover, rat bone marrow MSCs (BMSCs) were successfully cultured on the scaffolds and underwent enhanced proliferation and viability, thus demonstrating their high biocompatibility (figure 5) [66]. Chitosan scaffolds modified

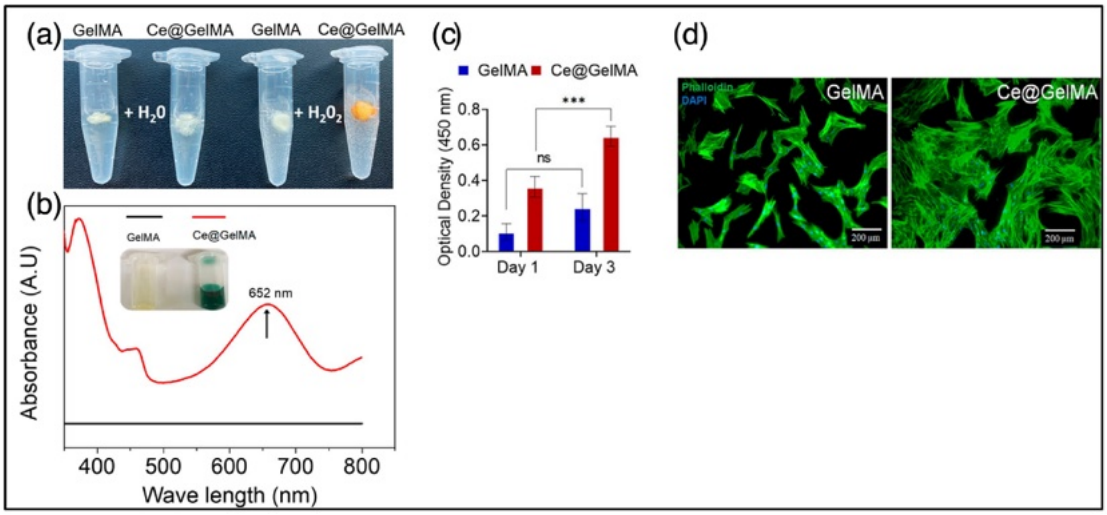

Figure 5. ROS scavenging nature of the hybrid scaffolds and cell proliferation and cytoskeleton/nuclear staining images of cells cultured on GelMA and Ce@GelMA scaffolds. (a) Images showing GelMA and Ce@GelMA scaffolds treated with non-ROS-like (H_2O) and ROS-like (H_2O_2) solutions. Scaffolds incubated in H_2O_2 showed an instant color change due to the presence of antioxidant nCe, while noncoated scaffolds remained the same. (b) The oxidase like nature of the hybrid scaffolds was confirmed by TMB assay. The characteristic UV absorbance peak observed at 652 nm indicates the antioxidant property of the Ce@GelMA scaffolds. (c) The cell proliferation rate was measured using a CCK-8 assay. The Ce@GelMA scaffolds exhibited a significantly higher cell proliferation rate as compared to GelMA for up to 3 d of culture. (d) Fluorescence images of rMSCs seeded on scaffolds stained with phalloidin (green) for F-actin and DAPI (blue) for nuclei, after 3 d of culture. The statistical significance was calculated using two-way ANOVA multiple comparison tests ($^*P < 0.05$). Reprinted with permission from [66]. Copyright (2022) American chemical society.

with iron-doped dicalcium phosphate dihydrate minerals and nanoceria efficiently prevented infection and allowed the proliferation of human BMSCs [109].

The presence of high levels of ROS in the wound microenvironment is responsible for the slowdown of wound repair and induction of fibrotic reaction. Therefore, it is fundamental to modulate free radical levels to obtain fast tissue healing and regeneration. A hydrogel incorporating curcumin and cerium oxide has been developed and characterized showing controlled release, favoring cell migration, and reducing oxidative stress *in vitro* and inflammation *in vivo* [110]. An ECM gel was emulsionated with nanoceria and curcumin and showed antioxidant antibacterial properties and a good ability to penetrate the wound site accelerating the healing rate [67]. Similarly, cerium oxide NP incorporated poly-L-lactic acid (PLLA)-gelatin composite fiber membranes were fabricated showing great biocompatibility *in vitro* [111]. An interesting formulation composed of an injectable self-healing hydrogel coated with cerium oxide nanorods showed good ROS scavenging activity, biocompatibility, and biodegradability upon implantation. Skin epithelium regeneration was enhanced together with accelerated wound healing [68]. Nanocapsules composed of a core carrying pirfenidone as an anti-fibrotic drug and cerium oxide in the shell were demonstrated to be highly biocompatible and with good ROS scavenging activity. Upon adhesion to Polylactic acid (PLA) fiber membranes, this nanocomposite was applied *in vivo* to the wounds inducing tissue epithelialization, favoring collagen fiber arrangement, and reducing scar formation [112].

In conclusion, cerium oxide NPs have been widely applied as free radicals' scavengers, for supporting cell growth and differentiation, enhancing the mechanical properties of scaffolds and accelerating the wound healing processes.

7. Calcium phosphate-based NPs

Due to their high similarity to the mineral part of the bone tissue, biocompatibility, and high surface area, calcium phosphate NPs (CaP NPs) have been employed in tissue engineering [113, 114]. A kind of calcium phosphate, hydroxyapatite (HA), has been studied and developed, thanks to its biocompatibility with bone cells. HA, known for its osteoinductive properties, promotes cell adhesion and proliferation, facilitating bone tissue regeneration. Many studies have been performed also focusing on the combination of these NPs with other molecules and drugs.

Hydroxyapatite nanospheres have been designed and loaded with bone morphogenetic protein-2 (BMP-2) showing rapid regeneration upon implantation in rats presenting femoral bone defects [115].

In another research, layer-by-layer assembled biomimetic calcium phosphate particles have been synthesized carrying BMP-2. Upon implantation into 8 mm diameter rat cranial critical-sized bone defects and, when combined with coprecipitated biphasic calcium phosphate (BCP), they induced new bone formation with a higher degree of BCP biodegradation as compared to the effect obtained when used alone [116].

To give stability to the basic fibroblast growth factor, a molecule essential for the promotion of angiogenesis and wound healing, multifunctional versatile calcium phosphate NPs loaded with this molecule, together with heparin and ferucarbotran have been developed. *In vitro* experiments demonstrated their ability to specifically promote mouse fibroblasts and osteoblastic cell proliferation [69].

Tenkumo *et al* developed a system of calcium phosphate NPs with multiple functionalizations for bone repair. In detail, tumor necrosis factor alpha inhibition by siRNA and release of VEGF-A and BMP-7 by plasmid DNA were evaluated in a rat model of femoral head defects. Upon implantation, the multifunctional NPs revealed efficient in promoting bone healing [70].

8. Carbon-based NPs

Carbon NPs (CNPs) can be easily functionalized and loaded with specific drugs. Moreover, they display remarkable electrical and mechanical properties, and they have been successfully applied to tissue engineering [117]. Indeed, 3D scaffolds composed of alginate hydrogels have been filled with CNPs, creating a porous structure as a niche for improved bone cell proliferation and migration. Upon *in vivo* implantation into an induced bone defect, the scaffold promoted bone formation [71]. Carbon quantum dots, graphene, carbon nanotubes (CNTs), and nanodiamonds are the most used nanomaterials in this category. In the last decade, carbon dots have been exploited thanks to their fluorescence properties, high biocompatibility, and low toxicity.

Environmental factors are known to contribute to the upregulation of enzymes involved in the loss of elasticity and skin aging. Carbon quantum dots have been fabricated with specific optical properties, high biocompatibility, and antioxidant/antiaging features, by carrying multiple phenolic moieties, that demonstrated to be able to lower detrimental enzymatic activity. These nanomaterials can suppress free radical accumulation induced by UV radiation, and once incorporated in hydrogels, favor wound healing [118]. Commonly, they are chemically synthesized and only a few studies have been focused on the possibility of extracting them from natural sources. In recent work, Cheng *et al* extracted carbon dots from resveratrol, and their features and activities were deeply investigated *in vitro* in human umbilical vein endothelial cells and *in vivo* in a rat skin defect model of inflammation. Carbon dots performed better than resveratrol itself and promoted cell migration and tube formation while stimulating vessel formation and wound healing *in vivo* [119].

Ghataty *et al* used fluorescent carbon dots as agents able to promote tissue regeneration both *in vitro* and *ex vivo*. Carbon dots synthesized from bovine serum albumin have been designed as fluorescent carriers of linezolid, an antibiotic used for reducing wound infections. *In vitro* experiments such as metabolic activity assays, antibacterial activity evaluation, elastase, collagenase, and tyrosinase activity inhibition assays were performed together with *ex vivo* hemolysis tests. The nanomaterials revealed to be biocompatible when used in normal human skin fibroblasts promoting their proliferation and migration in a scratch wound healing assay. Treated cells display significantly higher contraction and closure of the wound gap respect to control cells. Overall, the results demonstrated their great potential for use in wound healing and tissue regeneration (figure 6) [72]. Garlic peel-derived carbon quantum dots have been combined with synthetic hydrogels of dimethylaminoethyl methacrylate and acrylic acid to promote rapid chondrogenesis [120].

The introduction of graphene oxide has brought great advancements in the field of tissue engineering because of its mechanical strength, optical transparency, electrical conductivity, and biocompatibility, essential features for bone regeneration. Scaffolds of chitosan, gelatin nanobioglass, and graphene oxide have been fabricated and characterized. With an average pore size of a hundred micrometers, good incorporation of the biomaterial, and thermal stability they were investigated for their capacity to interact with the human MG-63 osteosarcoma cell line. These cells proliferated, were metabolically active and were induced to osteogenic differentiation [121]. Multiwall CNTs (MWCNTs) have been used for bone regeneration applications. By combining gelatin methacryloyl, bioactive glass, and MWCNTs, a nanocomposite hydrogel has been obtained. Biological experiments demonstrated that it supported MSCs interaction and differentiation into osteogenic lineage and provided the electrical and mechanical features necessary for bone physiological repair and regeneration [73].

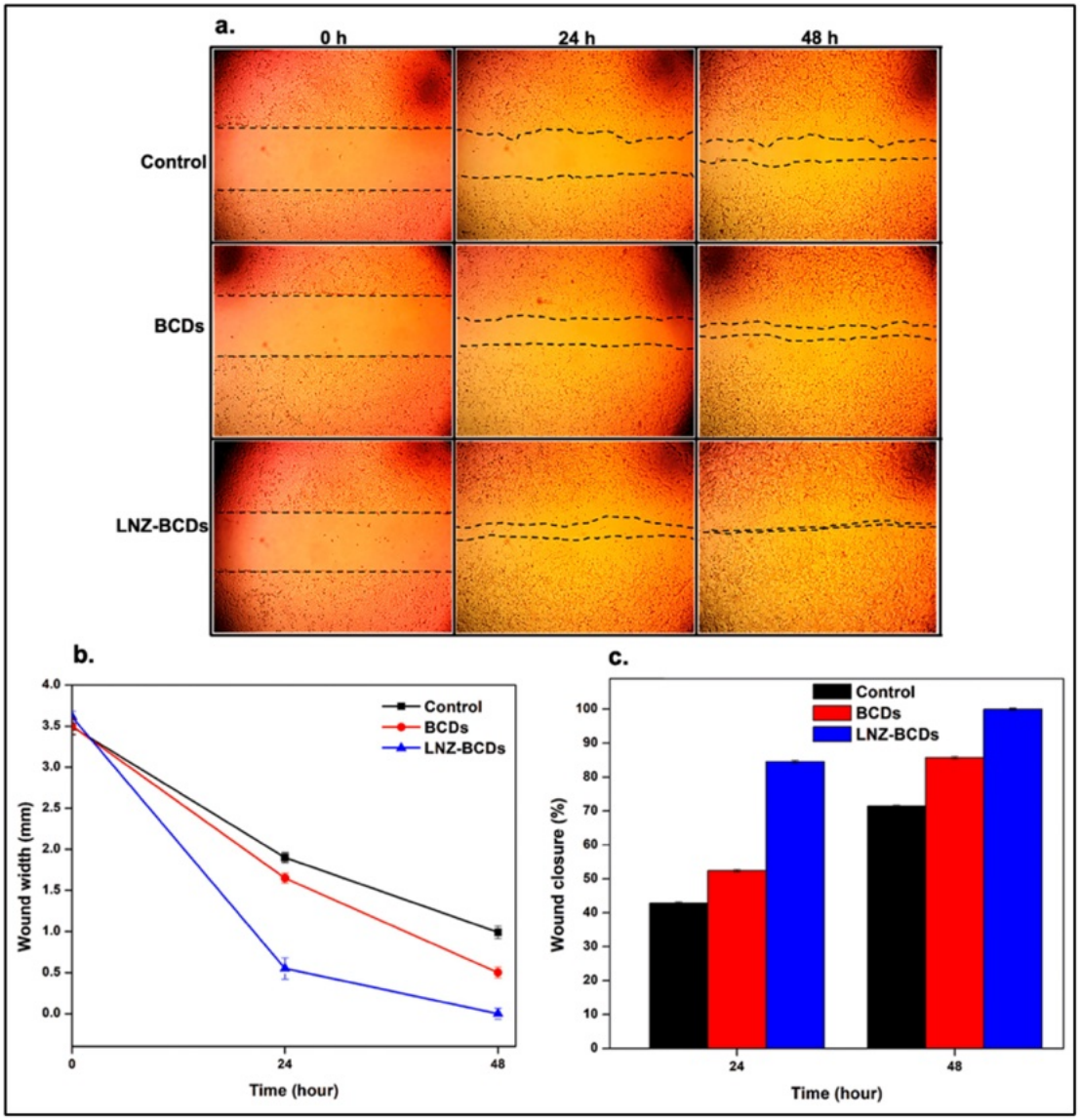

Figure 6. Evaluation of the effectiveness of the BCDs and LNZ-BCDs nano-biomaterials in the wound healing process determined *in vitro* by scratch wound healing assay. (a) Images at 1 mm scale bar, (b) profile of changes in the width of wounds with time, and (c) wound closure percentages of untreated control and treated normal human skin fibroblast (HSF) cell line with BCDs nano-biocarrier and LNZ–BCDs nano-bioconjugate at 24 and 48 h. BCD, bovine serum albumin carbon dots; LNZ, linezolid. Reproduced from [72]. CC BY 4.0. Copyright 2023 the authors, published by MDPI.

Composite scaffolds potentiated by the inclusion of nanodiamonds carrying the antibiotic vancomycin have been produced for the treatment of infected bone defects. Experiments conducted demonstrated that they performed excellently in terms of biocompatibility and antibacterial activity and promoted osteogenesis. *In vivo* experiments showed that, upon implantation, the scaffold was biocompatible and efficiently carried out its functions [122].

From the reported research, we can state that both calcium phosphate-based and carbon-based NPs have been successful in treating different issues related to tissue engineering by efficiently promoting cell adhesion and proliferation, by delivering specific cargos thanks to their relative ease of loading, and by displaying exceptional properties in terms of biocompatibility, antibacterial activity and low toxicity.

In summary, inorganic NPs have been demonstrated as efficient systems in tissue engineering, by improving scaffold structure, delivering bioactive molecules, acting as triggered release agents in response to external stimuli, as ROS scavengers, and by providing a niche for specific cell proliferation and differentiation (figure 7). Further developments and design refinement will guarantee obtaining even more specific and functional NPs. Concerning their translation from basic research to the clinical context, it is important to underline that much more effort is still needed to standardize the fabrication and characterization procedures and warrant their wide and safe medical application following compliance with the main regulatory frameworks.

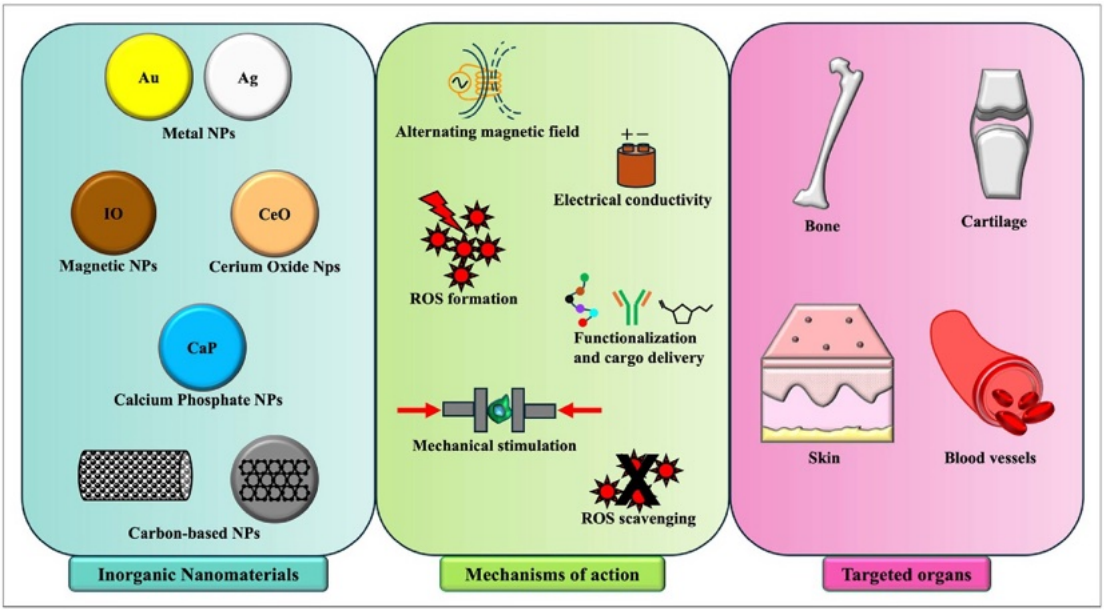

Figure 7. Overview of the main inorganic nanomaterials investigated in nanomedicine and employed in tissue engineering. The main mechanisms of action are indicated, together with the targeted organs.

9. Organic nanomaterials in tissue engineering

Organic NPs constituted by natural or synthetic materials have been widely employed for tissue regeneration because they are highly biocompatible, can incorporate multiple kinds of molecules, and can be easily fabricated. However, they generally present high clearance by the reticuloendothelial system *in vivo*. Therefore, surface modification by using biocompatible polymers (e.g. polyethylene glycol (PEG), a hydrophilic molecule with low immunogenicity) is commonly carried out to reduce phagocytosis by macrophages and subsequent organ clearance. Lipid NPs are widely applied in drug delivery, and thanks to their small size, they have demonstrated the ability to cross the blood-brain barrier [49]. Polymeric NPs can be fabricated by using natural or synthetic materials and can efficiently incorporate a plethora of hydrophobic and hydrophilic drugs [123, 124]. PLGA has been approved by the FDA for its safety, biodegradability, and high versatility and it has been successfully employed as a therapeutic agent in different pathologies, such as diabetes, neurodegenerative diseases, and cancer [125–130]. Another biomaterial that has raised increasing interest is the hydrophilic component of silk, sericin [131]. This protein presents low immunogenicity [132], displays antioxidant properties [133], and has been used as a nanomaterial, both for producing nanocarriers for insoluble molecules [134, 135] and as a biomineralization matrix [136]. Natural materials like fibroin, collagen, and chitosan as well as synthetic carriers, are currently widely utilized and have shown to be highly biocompatible. Different kinds of organic NPs have been developed for tissue repair applications, from liposomes to dendrimers, polymeric micelles, and nanofibers (figure 3(b)), (table 2).

10. Liposomes

Liposomes are constituted of a bilayer of amphiphilic lipids and form closed structures in water able to carry both hydrophobic and hydrophilic molecules. They display high biocompatibility thanks to their similarity to the cell membranes, low immunogenicity, and can be functionalized for increased targeted delivery [12]. However, despite the many advantages, their ability to store and maintain proper drug concentration at the site of interest is yet an open challenge. These nanomaterials have been widely applied to bone repair and wound healing, but also to cartilage regeneration. They have been developed for transporting growth factors, hydrophilic, and very unstable molecules that make it difficult to target injured sites within a reasonable time and many natural and synthetic bioactive molecules, providing their sustained release.

Melatonin, which displays beneficial antioxidant effects and has been shown able to promote osteoblast differentiation and bone formation, needs very high amounts to achieve clinical results when

Table 2. Organic nanomaterials applied to tissue engineering.

Nanoparticle	Fabrication approach	Targeted organ	Results	Ref.
Liposomes	Reverse phase evaporation	Bone	Increased ALP and osteocalcin expression in osteoblasts; formation of mineralized nodules	[137]
Liposomes	Phospholipids mixture in organic solvent and extrusion	Bone	*In vivo* increased *de novo* bone formation and bone-to-implant integration; increased transition M1-to-M2 phenotype	[138]
Liposomes	Thin-film hydration	Skin	*In vitro* efficient drug delivery; no cytotoxicity; cell proliferation and migration; *in vivo* reduced inflammation; increased re-epithelialization; collagen deposition and angiogenesis	[139]
Dendrimers	Hydrothermal synthesis of nanoceria and conjugation with dendrimers	Bone	*In vitro* increased proliferation and migration ability of MSCs; upregulation of genes associated to cell growth, migration, osteogenesis, and ROS metabolism; *in vivo* implant integration and effective bone regeneration	[140]
Dendrimers	Mixture of GelMA and methacrylic anhydride-modified poly(amidoamine)	Cartilage	*In vitro* biocompatibility; promotion of cartilage regeneration by ASCs; *in vivo* articular cartilage defect repair	[141]
Polymeric micelles	Nanoprecipitation	Bone	Cytocompatibility; tunable and continued drug release	[142]
Polymeric micelles	Solid dispersion	Skin	*In vitro* controlled and sustained drug release; cytocompatibility; *in vivo* biocompatibility; enhanced cell migration and proliferation	[143]
Nanofibers	Electrospinning	Bone	Biocompatibility; proliferation of hASCs; increased levels of ALP, osteocalcin and osteopontin	[144]
Nanofibers	Electrospinning	Bone	Increased cell adhesion, enhanced ALP activity; upregulation of osteopontin, Col-1 and BMP-2	[145]
Nanofibers	Electrospinning	Bone	Increased ALP activity; enhanced cell–cell interaction and calcium content; biocompatibility	[146]
Nanofibers	Electrospinning	Bone	Recruitment of BMSCs; induction of BMCs differentiation to chondrocytes and osteoblasts with enhanced related gene expression; *in vivo* cartilage and new bone formation	[147]
Nanofibers	Electrospinning	Cartilage	Improved mechanical properties; drug sustained release; *in vitro* BMSCs proliferation; *in vitro* and *in vivo* enhanced chondrogenesis and promotion of neocartilage formation	[148]

systemically administered. Xiao *et al* developed a composite adhesive GelMA system loaded with liposomes carrying this molecule for local administration. The authors observed a reduction of osteoblasts' apoptosis in the presence of induced oxidative stress and near the implant in animal models [149].

A 3D scaffold has been designed to carry liposomes of a cholesterol analogue together with smoothened agonist as a drug, for stimulating the Hedgehog pathway, fundamental for the release of signals promoting bone regeneration. *In vitro* experiments demonstrated that bone marrow stromal cells underwent osteogenic differentiation and *in vivo* research showed successful calvarial bone healing [150]. Minhua *et al* have fabricated liposomes loaded with scutellarin. The authors showed that osteoblasts expressed increased levels of alkaline phosphatase and osteocalcin and formed mineralized nodules *in vitro* [137].

Immune cells are the main players involved in the response to a biomaterial implant into a living tissue. Macrophages polarize into M1 pro-inflammatory or M2 anti-inflammatory phenotypes and are essential in determining its fate through a foreign body reaction, leading to integration and tissue repair. Strategies for immunomodulation and for inducing macrophage pro-healing response are at the top of the current research in the field. In a recent work, multilayered liposomes composed of artificial apoptotic cell mimetics phosphatidylserine induced an M1 to M2 transition and, upon their integration into titanium implants, helped in promoting bone regeneration. In a rat model of femur implantation, the formation of new bone tissue and successful promotion of M2 macrophage polarization were observed [138].

Much research on the use of liposomes has been performed also in the field of wound healing, based on the encapsulation of natural therapeutic molecules. Across these studies the liposome serves as a common platform to stabilize and locally deliver otherwise poorly bioavailable cargoes, consistently yielding faster re-epithelialization, reduced inflammation and increased angiogenesis in rodent wound models [139, 151–154].

For instance, highly hydrophilic madecassoside has been loaded into liposomes optimized for topical administration. The formulation excellently performed *in vivo* in rat models showing a good healing potential [151]. Similarly, in a rat model of open skin ulcers, liposomes carrying curcumin were applied together with adipose tissue-derived stem cells demonstrating efficient wound healing [152]. More recently, PEGylated liposomes encapsulating the antioxidant compound oleuropein improved wound healing capacity with respect to not-modified liposomes, as proven by scratch assay [153]. A liposomal formulation of the chemokine stromal cell-derived factor-1 alpha released from hydrogels demonstrated efficient in promoting skin regeneration. Pro-healing M2 macrophages were recruited at the site of the open wound in mouse models and increased dermal angiogenesis was appreciable [154]. Kiani *et al* developed a system for PEGylated liposomal delivery of microRNA-21 and simvastatin. The nanomaterial presented a high efficiency of encapsulation and cellular uptake. *In vivo* experiments showed a fast re-epithelialization, wound closure, and a consistent reduction in inflammation [139].

As mentioned before, the treatment of infections arising from tissue damage is one of the major concerns in wound healing. We report here a work exploiting the use of liposomes as drug delivery agents able to promote tissue regeneration *in vivo*. A hydrogel loaded with liposomes carrying berberine hydrochloride for evaluation on wound tissue in mice was prepared. Notably, inflammation was reduced by acting as an antimicrobial agent, and efficient dermis regeneration was obtained. Moreover, treated samples showed a continuous migration of keratinocytes from the dermis to the epidermis, thus suggesting an active role of the drug in promoting physiological regeneration. Liposomes showed to be biocompatible and reduced inflammation normally induced in the organism by the administration of drugs, thanks to the efficient delivery of berberine hydrochloride and high affinity to cell membranes. Finally, enhanced angiogenesis was observed with increased secretion of VEGF (figure 8) [155]. A versatile tool constituted by polymyxin B targeted liposomal photosensitizers for photodynamic therapy has been developed. It acted against multidrug-resistant *A. baumannii* burn infections by disrupting its membrane and increasing ROS. This approach worked also *in vivo*, efficiently stimulating tissue regeneration by modulating the polarization phenotype of macrophages [156].

Concerning the most recent application of liposomal formulations to cartilage tissue repair, we report here two studies. In the first one, the authors developed liposomes composed of phospholipids or covered by macrophage membrane proteins that were intravenously administered in mouse models of post-traumatic osteoarthritis showing a localization at the site of injury and presenting an immunomodulatory effect on infiltrating immune cells [157]. The second one reports an innovative multifunctional hybrid system developed by Kryuchkova *et al* composed of i) a matrix of spider silk, ii) a coating of ferromagnetic NPs for drug release upon a thermal trigger given by exposure to alternating magnetic fields, and iii) liposomes as drug carriers. The study demonstrated a high potential for cartilage regeneration because of the perfect match between the biocompatible physiological and mechanical properties of the biomaterials and the system for controlled drug release upon specific external stimuli [158].

From the reported research, we can conclude that liposomes have been successfully applied for inducing cell differentiation and tissue repair, for encapsulating and delivering a plethora of natural therapeutic molecules and drugs, for promoting anti-inflammatory responses and as components of multifunctional devices.

11. Dendrimers

Dendrimers are ordered branched polymers that can be exploited to bind multiple ligands on their protruding arms improving their bioavailability while giving necessary protection until they reach their target site [159]. An innovative material composed of BCP NPs and dendrimers presenting phosphoserine, known to stimulate mineralization and differentiation of stem cells toward bone tissue, has been employed *in vitro* and injected *in vivo* in an osteoporotic model, demonstrating successful integration and bone regeneration [160]. An interesting approach for promoting bone regeneration is based on the use of functionalized composite hydrogels combining the biocompatibility of the biomaterial with the mechanical properties given by the incorporated dendrimers. A recent study reported the beneficial application of a GelMA hydrogel combined with dendrimer (G3)-functionalized nanoceria. MSCs adhered and proliferated showing an increased capacity to migrate and were able to survive oxidative

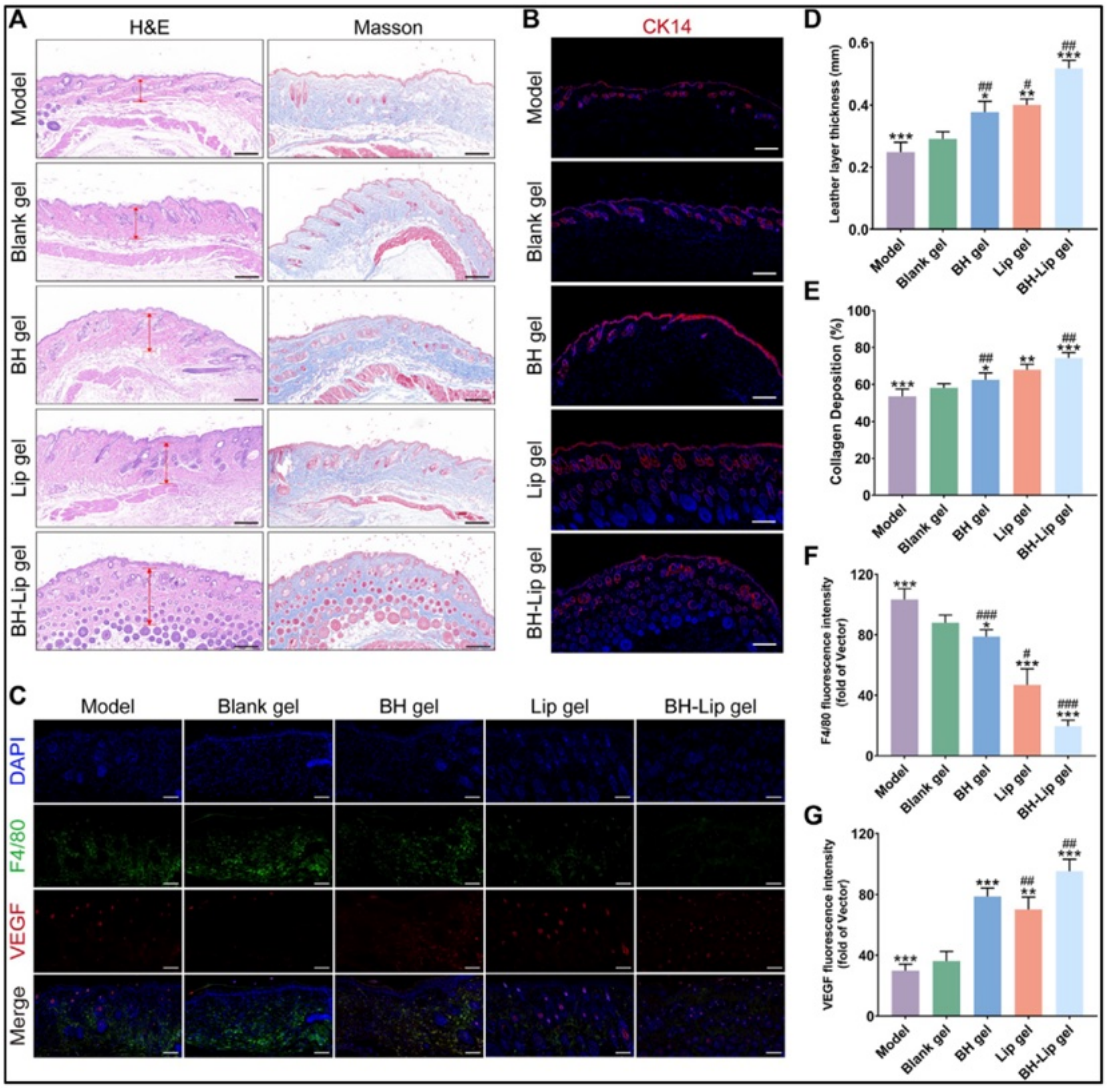

Figure 8. Evaluation of wound healing by H&E and Masson staining of wound tissues of different groups (Scale bar = 200 μm) (A). Immunofluorescence staining of CK14 (red) for the wounds at days 14 (Scale bar = 200 μm), cells were stained with CK14 and nuclei were re-stained with blue DAPI (B). Immunofluorescence staining of F4/80 (green) and VEGF (red) for the wounds at day 14 (Scale bar = 100 μm) (C). Quantification of the length of the new leather layer of the wound ($^{***}p$, $^{**}p < 0.01$, $^{*}p < 0.05$ when compared with the model group, $\#\#p < 0.01$, $\#p < 0.05$ when compared with the BH-Lip gel group, $n = 6$/group) (D). Maturity of collagen fibers in different groups ($^{***}p$, $^{**}p < 0.01$, $^{*}p < 0.05$ when compared with the model group, $\#\#p < 0.01$ when compared with the BH-Lip gel group, $n = 6$/group) (E). Quantification of F4/80 fluorescence intensity ($^{***}p < 0.01$, $^{*}p < 0.05$ when compared with the model group, $\#\#\#p < 0.01$, $\#p < 0.05$ when compared with the BH-Lip gel group, $n = 6$/group) (F). Quantification of VEGF fluorescence intensity ($^{***}p$, $^{**}p < 0.01$ when compared with the model group, $\#\#p < 0.01$ when compared with the BH-lip gel group, $n = 6$/group) (G). BH, berberine; lip, liposome. Reproduced from [155]. CC BY 4.0.

stress thanks to the scavenging properties of nanoceria. Upon implantation, a very low inflammatory response was induced, and bone regeneration was shown to be effective in a rat model of bone defect [140]. A recent example of PEG-based hydrogel modified with dendrimer-like poly-lysine has been reported as a scaffold for promoting osteogenesis. Human BMSCs were able to differentiate and secrete BMP-2 [161].

Dendrimers have been successfully applied also to wound healing. Zhu *et al* have reported the development of a L-Arginine-rich amphiphilic dendritic peptide, acting as a nitric oxide donor favoring angiogenesis and epithelialization, and facilitating bacterial infection elimination in combination with photodynamic therapy thanks to the presence of the photosensitizer chlorin e6 [162]. An injectable GelMA hydrogel scaffold has been produced and loaded with methacrylic anhydride-modified poly(amidoamine) as a stem cell delivery system for the induction of chondrogenic differentiation for cartilage repair. ASCs were encapsulated proving the scaffold's biocompatibility and ability to promote cartilage regeneration *in vitro* and *in vivo* [141].

12. Polymeric micelles

Polymeric micelles are constituted by the self-assembly of amphiphilic block copolymers in water and present a stable structure able to encapsulate hydrophobic and hydrophilic drugs [163], such as chemotherapeutics, reducing their heavy side effects while enhancing their pharmaceutical properties [164]. An example of PLA-PEG-PLA polymeric micelles loaded with the hydrophobic drug simvastatin for promoting osteogenesis has been reported by Cisneros *et al.* The NPs have been mixed with N-methacryloyl chitosan and PEG dimethacrylate for fabricating a hydrogel. Sustained release of the molecule over a 17 week time frame was observed confirming its potential clinical application [142]. Biodegradable polymeric micelles composed of methoxy-poly(ethylene glycol)-di-hexyl-substituted-poly(lactic acid) have been developed for carrying the mineralocorticoid receptor antagonist spironolactone. This molecule is used to block the off-target effects of treatment with glucocorticoids that impair efficient cutaneous wound healing. The NPs accumulated and preferentially delivered the drug to the epidermis and upper dermis [165]. Great relevance in skin tissue engineering is devoted to stimulating chronic wound repair, for instance in diabetic patients. In particular, the development of multifunctional hydrogels is on top of the strategies in this field. Curcumin micelles have been fabricated and loaded into an injectable chitosan-carboxymethyl cellulose-g-Pluronic F127 hydrogel to obtain a controlled release of the molecule while promoting wound healing. The profile of release and biocompatibility were evaluated *in vitro* on fibroblast cell lines and *in vivo* in diabetes rat models upon subcutaneous injection. The composite induced efficient cell migration and proliferation together with the delivery of curcumin, a well-known natural compound involved in angiogenesis, collagen deposition, and antioxidant activities [143].

A novel field of interest in tissue engineering is based on the design of gels with self-assembling abilities. Self-assembly of P311 peptide micelles and diblock copolymer poly (ethylene glycol)-block-poly (propylene sulfide) successfully promoted epidermal cell migration and efficiently reduced ROS presence. Moreover, the nanomaterials were proven to accelerate diabetic wound healing and new tissue formation [166]. A carrier composed of amphiphilic polyurethane (PU) has been designed to obtain an efficient and reversible self-assembly into micelles in aqueous medium. A triple-charged peptide, commonly found in human collagen type IV and displaying self-assembly properties, was added to the PU solution. The strong interactions promoted the formation of a gel carrier, and the properties of the complex were then investigated. It presented a reversible sol-gel transition at physiological temperature, thus proving to be a versatile material with great potential for *in situ* applications in tissue regeneration [167].

Summarizing the findings reported concerning dendrimers and polymeric micelles, thanks to their high biocompatibility, biodegradability, and versatility have been specifically functionalized for stimulating tissue regeneration, for delivering molecules *in vitro* and *in vivo*, and for reducing possible pharmaceutical-related side effects while providing sustained release of drugs.

13. Nanofibers in tissue engineering

Nanofibers are very versatile biomaterials suitable for scaffold fabrication because of their high surface-to-volume ratio, porosity, and ability to mimic the tissue microenvironment in terms of morphology. They are typically composed of natural (e.g. collagen, gelatin, chitosan, and alginate) or synthetic polymers. The latter present a plethora of advantages, among which are low immunogenicity, biodegradability, low costs of production, high versatility in terms of mechanical properties, and easy tuning of degradation rates [168]. Commonly, PLA, PGA, PCL, PU, PVA, and poly- (ethylene oxide) (PEO) are used. Nanofibers can be produced by phase separation self-assembly and electrospinning. With the second technique, the polymeric solution is subjected to an electrostatic force beyond its surface tension under applied voltage. Upon ejection, the solution undergoes multiple stretching and splitting, creating nanoscale fibers upon solvent evaporation [169].

Some of the most important properties of these nanomaterials, related to the field of tissue regeneration, are the possibility of tuning their (i) spatial orientation, (ii) stiffness, and (iii) size for obtaining specific cell orientation, differentiation, and morphology. Moreover, they can be functionalized with active molecules, such as growth factors and ECM proteins to better control cell behavior [170]. To reduce the hydrophobicity of nanofibers and promote cell attachment, specific incorporation of hydrophilic materials, such as PEG [171], or treatment of scaffold surfaces with plasma can be used [172].

Bones are composed of organic and inorganic materials and present a structure consisting of collagen-mineralized fibrils coated by hydroxyapatite. To efficiently regenerate this tissue, scaffolds

mimicking the physiological ECM must be designed. For bone, electrospun nanofiber scaffolds have followed three complementary design routes. Specifically, core–shell architectures that deliver osteogenic growth factors in a sustained or sequential manner [173–176], the incorporation of bioactive or antioxidant nanofillers (such as calcium silicate, hydroxyapatite nanowires, montmorillonite or MgO/g-C3N4) to add osteoinductivity, mechanical reinforcement and ROS scavenging [144–146, 177, 178], and finally the engineering of aligned, channeled or multilayered geometries that recruit and guide marrow-derived stem cells toward the defect [147].

Core–shell nanofibers have been loaded with multiple growth factors for promoting bone regeneration, among which are platelet-rich plasma [173], BMP-2, and dexamethasone [174]. Core–shell silk fibroin/PCL/polyvinyl alcohol nanofibrous mats have been proven to stimulate bone regeneration by releasing connective tissue growth factor and regulating the release of BMP-2 [175], essential for bone regeneration [179]. Core–shell silk fibroin/poly (L-lactide-co-ε-caprolactone) (PLCL), carrying an osteogenic peptide and hydroxyapatite, promoted differentiation into osteoblasts of human-induced pluripotent stem cell-derived MSCs and proved to be effective in bone regeneration *in vivo* [176].

The accumulation of ROS in the presence of bone defects is one of the main challenges that prevent a fast osteogenesis process. Therefore, strategies for producing scaffolds carrying antioxidant molecules together with nanomaterials responsible for providing mechanical strength and controlled drug release have been implemented. One research reported the development of nanofibers composed of PLA/organophilic montmorillonite/resveratrol. *In vitro*, experiments showed biocompatibility towards human adipose MSCs together with efficient free radicals scavenging activity and pro-osteogenic stimulation [144]. Recently, it has been reported the design and fabrication of sandwich mesh structures by electrospinning carrying naringenin and vitamin K2 that synergistically stimulated osteogenesis, as assessed by *in vitro* experiments [177]. An electrospun PLLA nanofiber scaffold integrated with calcium silicate nanowires, facilitated cell adhesion and activation of osteopontin, collagen I, and BMP-2 gene expression [145].

GelMA cryogel microspheres integrated with hydroxyapatite nanowires and calcium silicate nanofibers presented a microstructured porous conformation and a rough surface, greatly enhancing cell biocompatibility and injectability, showing osteogenesis and bone regeneration *in vivo* [178]. A work by Danagody *et al* demonstrated the prominent role of surface topography in obtaining physiological cell growth and activity. A nanofibrous membrane constituted of polyacrylonitrile (PAN)/PEG and incorporated with MgO/gC_3N_4 induced tissue healing and bone regeneration *in vitro* [146]. In the presence of long bone defects, it is essential to provide scaffolds able to support the BMSCs confined inside the bone marrow, for obtaining efficient damage repair. A 3D vertically aligned nanofiber scaffold presenting long channels and large pores has been developed for recruiting stem cells from the bone cavity. Upon implantation, BMSCs differentiated into chondrocytes and osteoblasts, favoring bone regeneration [147].

Scaffolds composed of nanofibers have also been used for wound healing, acting as skin substitutes [180]. Hyaluronic acid-silk fibroin/zinc oxide nanofibers successfully promoted wound regeneration while suppressing any undesired inflammatory response [181]. Chitosan-PCL/PVA-melatonin/chitosan-polycaprolactone three-layer nanofiber wound dressing was fabricated by electrospinning and its effects in the regeneration of the epithelial layer together with the remodeling of wounds, collagen deposition, and decreased inflammation were evaluated *in vivo* [182]. Notably, other types of nanofiber dressings have been produced (i) containing berberine as an antibacterial molecule [183], (ii) as bilayers with keratin and vascular endothelial growth factor [184], and iii) composed of gelatin and *Astragalus* polysaccharides for joint wound healing [185].

An innovative study demonstrated the feasibility of creating methacrylamide chitosan/PCL nanofibers delivering tannic acid as an inhibitor of microorganisms' proliferation and promoter of wound healing, and curcumin, at a later stage, for relieving inflammation and promoting dermal tissue maturation *in vivo* [186]. The use of nanofibrous membranes composed of recombinant spider silk protein and PLCL allowed to obtain scaffolds with ideal properties for skin regeneration, such as higher hydrophilicity and enhanced mechanical, and thermal properties. This nanomaterial efficiently delivered human epidermal growth factor to cultured mouse fibroblasts [187]. Another material widely used in tissue regeneration, silk fibroin, has been integrated into electrospun nanofibers, showing improved tensile strength, Young's modulus, swelling capability, and thermal stability. Upon addition of deferoxamine and ciprofloxacin, high antibacterial activity was observed together with enhanced wound healing [188].

A research by Liu *et al* showed a new strategy for cartilage regeneration, by designing a nanofiber composite microchannel-containing injectable hydrogel. These scaffolds were constituted of thermosensitive gelatin microrods, for forming pores, and PLA/gelatin fibers carrying kartogenin, a small molecule

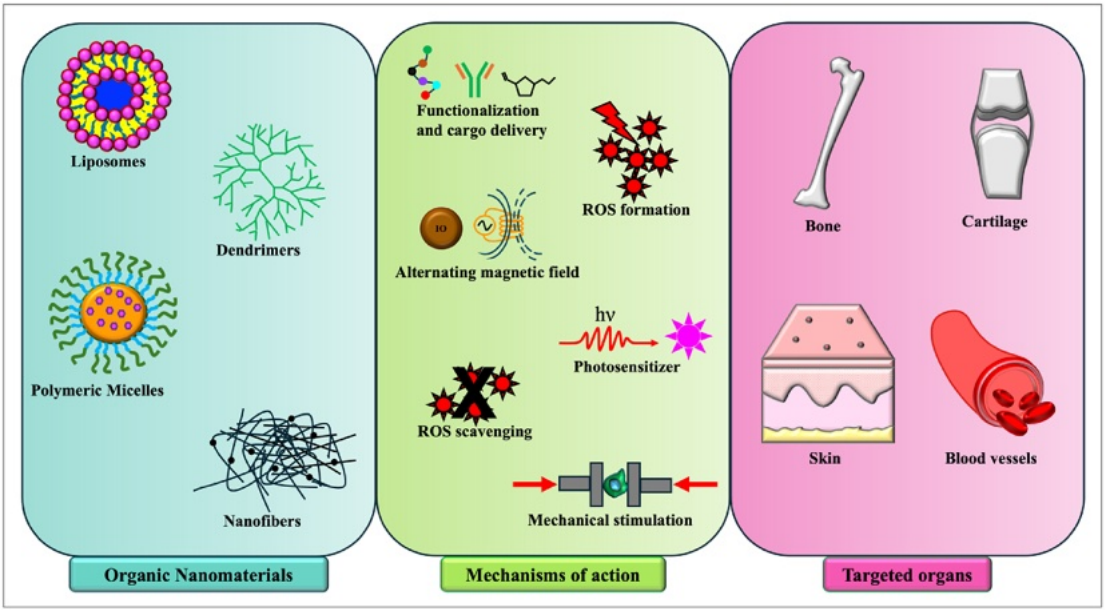

Figure 9. Overview of the main organic nanomaterials investigated in nanomedicine and employed in tissue engineering. The main mechanisms of action are indicated, together with the targeted organs.

that emerged as a promising agent for cartilage regeneration. The structure efficiently supported the proliferation of BMSCs and promoted the formation of novel tissue in a rabbit model of cartilage defect [148].

Although nanofiber scaffold design has been improved in recent years, however, some more studies are needed to reduce the costs and the time-consuming preparation protocols and to increase scaffold porosity, which is essential not only for giving mechanical support to cell growth and proliferation but also to allow oxygen and nutrients diffusion and waste products excretion. Further work will be required in the future to optimally combine all these factors.

Summarizing the reported findings, nanofibers, thanks to their physical properties, have been applied for modulating cell spatial orientation and differentiation. Upon functionalization with growth factors, specific molecules, and drugs they have been exploited for facilitating cell adhesion, promoting proliferation, and for obtaining antioxidant and antibacterial activities. Moreover, 3D scaffolds composed of aligned nanofibers have demonstrated highly efficient in recruiting stem cells, contributing to specific tissue regeneration.

In conclusion, organic NPs are efficient agents for transporting growth factors, drugs, and bioactive molecules and ligands, improving their bioavailability, while providing sustained and controlled release upon specific triggers. Moreover, they have been applied as systems for spatially orienting cells, giving mechanical support and inducing a controlled cell behavior (figure 9). Future efforts will be devoted to improving their fabrication protocols in a timely and cost-effective manner, making the most of their properties for optimally supporting tissue regeneration, and for adhering to the regulations required for their clinical translation.

A summary of the main applications of inorganic and organic nanomaterials in tissue engineering is reported in figures 10 and a comparative analysis between the two categories in terms of performance, toxicity profile, cost level, scalability and main advantages *versus* limitations is reported in table 3. As it can be seen, metal NPs exhibit strong antimicrobial properties, making them highly effective in biomedical applications. However, their relatively high toxicity and cost, particularly for noble metals, limit a large-scale implementation. Magnetic NPs show excellent scalability and low toxicity, offering promising opportunities for targeted delivery and industrial processes. Cerium oxide NPs present unique redox-switching ability and antioxidant behavior, although their safety profile remains dependent on the synthesis conditions and dosage. Calcium phosphate-based NPs display high biocompatibility and biodegradability, making them particularly suitable for biomedical applications. Carbon-based NPs provide high adsorption capacity and multifunctionality but face concerns regarding toxicity and regulatory approval. Among organic nanocarriers, liposomes, dendrimers, polymeric micelles, and nanofibers demonstrate excellent potential for drug delivery and regenerative medicine. Liposomes present strong

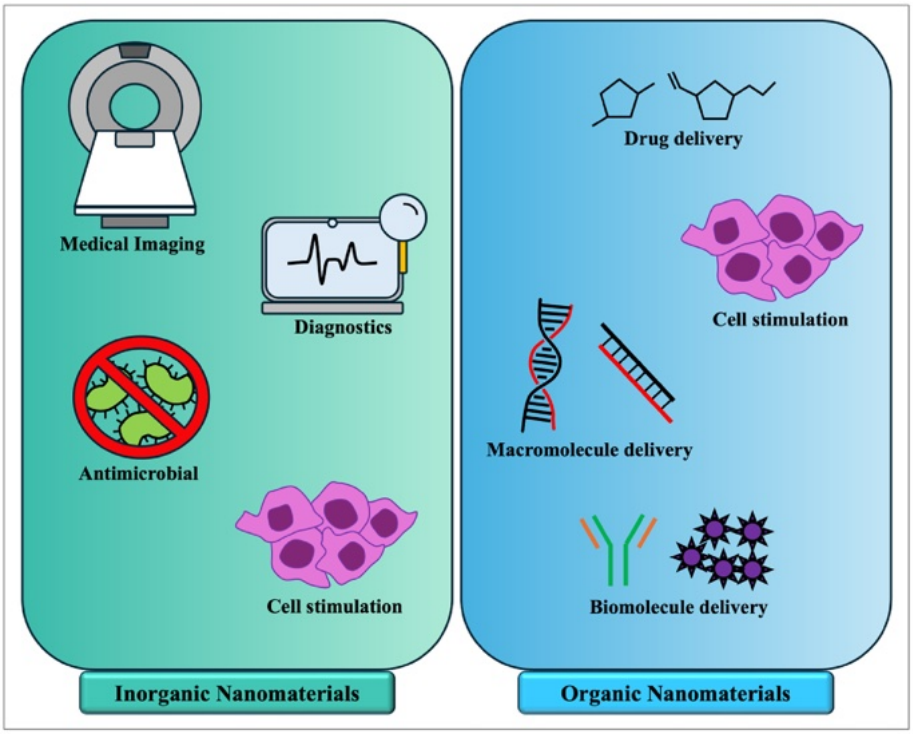

Figure 10. Overview of the main applications of inorganic (left) and organic (right) nanomaterials employed in tissue engineering.

clinical maturity and biocompatibility, whereas dendrimers provide highly controlled and targeted delivery at the expense of higher production costs. Finally, polymeric micelles and nanofibers combine good scalability with low toxicity, although stability and application range can be limiting factors.

Importantly, long-term toxicity, biodistribution, and clearance are key factors to be considered for the clinical translation of both inorganic and organic NPs. Biodistribution is mainly determined by the physicochemical properties of the nanomaterial, such as size, surface charge, shape, and functionalization [189, 190]. Inorganic NPs such as gold and iron oxide often exhibit strong tissue retention because of their low biodegradability, raising concerns about their potential long-term accumulation and chronic toxicity, including oxidative stress and inflammatory responses [191, 192]. Concerning organic NPs, such as liposomes and polymeric systems, they are generally more biodegradable, enabling enzymatic or hydrolytic degradation into nontoxic byproducts, which improves their safety profiles but may limit long-term stability and sustained delivery applications. Clearance pathways strongly depend on NP size: if below 5–6 nm, they can undergo renal excretion, whereas larger ones are predominantly cleared *via* hepatobiliary routes and sequestered in the liver and spleen [193]. Importantly, protein corona formation in biological fluids can significantly alter NPs, affecting both biodistribution and immune recognition. One of the main challenges that remain open in the view of NP clinical translation is finding the optimal balance between prolonged circulation for therapeutic efficacy and efficient clearance to minimize long-term toxicity, in other words the possibility to combine controlled degradation with optimized targeting properties. It must be considered that the interaction between nanomaterials and cells is governed by complex molecular mechanisms that begin when NPs are exposed to biological fluids inside our body and continue through cellular uptake and intracellular processing. Initially, the rapid adsorption of proteins onto the NP surface modulates its recognition by cell-surface receptors [194]. This step influences successive uptake pathways, such as clathrin-mediated endocytosis, caveolae-dependent internalization, macropinocytosis, and phagocytosis, that strongly depend on particle size, shape, and surface chemistry [189]. Receptor-mediated interactions are particularly important for uptake by immune cells, such as macrophages, while electrostatic interactions between positively charged NPs and negatively charged cell membranes contribute further to their internalization. Successively, NPs are directed to the endo-lysosomal compartments, where acidic pH and enzymatic activity may trigger degradation for organic systems or promote persistence for inorganic materials. Once inside the cell, NPs can activate oxidative stress pathways *via* ROS generation, leading to mitochondrial dysfunction and activation of signaling cascades such as NF-κB, or they may trigger inflammasome activation, contributing to inflammatory

Table 3. Comparative analysis between inorganic and organic nanoparticles applied to tissue engineering.

Nanoparticle	Performance	Toxicity profile	Cost level	Scalability	Key advantages	Main limitations
Metal NPs	Strong antimicrobial and redox behavior	Moderate-high (ion release, ROS generation; Ag highest risk)	High (noble metals)	Moderate	Exceptional reactivity, strong antimicrobial effects, versatile chemistry	Aggregation, instability, cost (noble metals)
Magnetic NPs	High in enhancing mechanical properties of biomaterials, drug release	Low-moderate (generally biocompatible iron metabolism)	Low	Very high	Magnetic recovery, biomedical safety, industrial maturity	Aggregation, instability
Cerium oxide	High redox switching (Ce^{3+}/Ce^{4+}), antioxidant/pro-oxidant activity	Context-dependent (low-moderate; dose and coating dependent)	Moderate-high (rare earth dependency)	Moderate	Unique ROS modulation, strong biomedical potential	Complex safety profile, sensitive to synthesis conditions
Calcium phosphate-based NPs	Moderate performance (drug delivery, bone regeneration)	Very low (biomimetic, biodegradable)	Low	Very high	Excellent biocompatibility, natural degradation pathways	Weak functional versatility beyond biomedicine
Carbon-based NPs	High adsorption capacity, tunable surface chemistry	Variable (low-high depending on structure and functionalization)	High (graphene/CNTs)	High	High surface area, multifunctionality, strong environmental applications	Toxicity uncertainty, structural variability, regulatory concerns
Liposomes	High efficiency in encapsulating drugs, strong clinical translation, and controlled release	Very low (biomimetic phospholipid composition)	Moderate-high (phospholipids, sterility, stability requirements)	High (industrialized, several FDA-approved systems)	Excellent biocompatibility, clinical maturity, flexible loading	Poor physical stability, leakage, oxidation, storage constraints
Dendrimers	Very high precision delivery, multivalent surface functionalization. controlled/triggered release	Low-moderate (surface charge-dependent cytotoxicity)	High (multi-step synthesis, purification complexity)	Moderate (synthetic complexity limits scale-up)	High drug loading control, gene delivery efficiency, imaging multifunctionality	Cytotoxicity (cationic surfaces), cost, regulatory barriers
Polymeric micelles	High solubilization of hydrophobic drugs, stimuli-responsive release, efficient tumor penetration	Low-moderate (depends on polymer composition)	Low-moderate	Moderate-high (self-assembly scalable but stability issues)	Small size, high tumor penetration, responsive release systems	Dilution instability, burst release risk
Nanofibers	High surface area for local drug delivery, tissue engineering, wound healing	Very low (depends on polymer used, often biodegradable)	Low-moderate	High (electrospinning scalable industrially)	Structural mimicry of ECM, localized sustained release, regenerative medicine applications	Limited systemic delivery, mostly implant/local applications

responses [192, 195]. Overall, these mechanisms determine cellular fate, nanomaterials toxicity, and therapeutic efficacy, thus their understanding is essential for designing safe nanomaterials for biomedical applications.

As mentioned above, the physicochemical properties of nanomaterials, particularly size, shape, and surface chemistry, quantitatively determine their biological fate and functional outcomes. Size is one of the strongest factors: particles below approximately 10 nm often show rapid renal clearance with circulation half-lives in the order of minutes to hours, whereas particles in the 20–100 nm range typically exhibit maximal tumor accumulation *via* the enhanced permeability and retention effect, with uptake efficiencies varying by more than an order of magnitude depending on tumor type and vascular permeability [193]. Above approximately 200 nm, sequestration by the mononuclear phagocyte system increases, with liver and spleen uptake often exceeding 60%–80% of injected dose *in vivo*. Shape also influences these outcomes with nanorods, nanowires, and nanotubes showing prolonged circulation and reduced phagocytic uptake compared to spherical particles of equivalent volume, while discoidal particles may increase endothelial interaction probability by several folds under flow conditions [196]. Concerning surface chemistry, PEGylation can extend blood half-life from minutes to many hours by reducing opsonin adsorption by up to 90%, while positively charged surfaces can increase cellular uptake rates but also raise nonspecific protein binding and cytotoxicity [189]. In conclusion, all these parameters interact, and even small physicochemical modifications can lead to significant differences in biodistribution, clearance half-life, and target-site accumulation of nanomaterials, determining their potential for clinical translation.

14. Microstructures

Microscaffolds are essential tools for the success of tissue engineering. They provide a surface for cells to attach, grow, and in some cases differentiate into committed cells or in others to maintain their stem fate. They also help to preserve or recreate the shape of the final tissue structure. To be effective, microscaffolds design for *in vitro* or *in vivo* tissue engineering must meet specific biological and structural criteria in terms of biocompatibility [197, 198], pore size [199–201], degradability [202, 203], and optical [204, 205], and mechanical properties [206–210].

Their microfabrication for biological applications can be grossly divided into two main approaches: i) top–down and ii) bottom–up technologies.

15. Top–down microscaffold fabrication approaches

Top–down fabrication technology in the context of tissue engineering refers to a strategy where large structures are shaped or subtractive patterned to create small ones. This approach is often used to create complex 3D tissue structures (table 4). The process involves the use of external forces or stimuli to manipulate biomaterials into desired patterns. These external forces can be physical, chemical, or biological. For instance, physical forces could include mechanical pressure, electrical fields, or light beam, chemical stimuli could involve pH or temperature changes, and biological stimuli might include the presence of certain drugs or enzymes. We can also find stimuli such as light, magnetism, or acoustic waves, to pattern biomaterials and cells within a single construct. Examples include laser micromachining, 3D photopatterning, pattern-guided electrospinning and other types of coupled micropatterning (like magnetic assembly or acoustic patterning coupled with bioprinting). Patterns that are created through this fabrication approach try to mimic the complex architecture of natural tissues, which often have intricate 3D structures.

15.1. Photopatterning

Photopatterning can be used to manage (i) the cross-linking of synthetic, natural, organic, or even organic/inorganic polymers, (ii) the degradation of hydrogels, or to control the display and release of biochemical signals like adhesive patterns and growth factors (figure 11(a)). By combining elements that respond to different light wavelengths, it is possible to fine-tune multiple parameters within a single system, enabling the creation of intricate patterns. Photopatterning of large surfaces can be achieved by using a photomask to selectively light up areas of a sample. While this method is better suited for patterning on a 2D surface, it can also be exploited to create 3D structures by employing a layer-by-layer approach. 3D patterning can be achieved by using more complex techniques like interference, or two-photon lithography which can create an environment with a scale down to the cellular level. In the last

Table 4. Top–down fabrication approaches applied to tissue engineering.

Top–down approaches	Description	Targeted organ	Detailed applications	Ref.
Photopatterning and Two-photon polymerization	A technique that uses light to control material cross-linking, degradation, or functionalization in 3D	Vascular system /skin /bone /cartilage	- Creating 3D channels and pores for tissue engineering - Patterning of biochemical cues to guide cell migration and differentiation - Optogenetics to control signaling pathways and cell fate	[202, 203, 211–224]
Laser micromachining	A process that uses a focused laser beam to remove material from a bulk material at a microscopic scale. The laser ablates, melts, or modifies the material to create desired patterns, holes, or structures. Different laser types and pulse durations offer varying levels of precision and thermal effects, allowing for processing of a wide range of materials from hard and brittle ceramics to soft polymers.	Vascular system / skin/nerve	- Creating micro and nano holes in various materials (e.g. catheters, stents) - Cutting thin materials - Creating patterning for modulating material properties like hydrophobicity or adhesion - Selectively removing or patterning thin layers - Creating 3D micro scaffolds through layer-by-layer ablation or by combining with other techniques	[225, 226]

10 years, 3D patterning has been largely and easily achieved through two-photon polymerization (2PP). 2PP is a direct laser writing technique that promotes the curing of a photosensitive material inducing radical reactions between chain precursor and photo-initiator molecules. This method implies the focusing of the light into a point, allowing it to act on molecular bonds into both solid and liquid bulk materials. One of the advantages of two-photon patterning is that the rate of absorption into a material (i.e. photoresist) relies on a nonlinear dependence, being proportional to the incident light intensity squared times the number of reactive molecules in the material cross-section. Therefore, being inversely proportional to the area, the greatest density of excited molecules arises in the highly focused regions only, generating features with a resolution lower than the Rayleigh–Abbe diffraction limit (100 nm for scaffolds and recently, down to 22 nm for a single feature) [206–210, 212, 213]. The choice of the photosensitive material is crucial for the performance and functionality of the fabricated structures [203, 209, 216, 227]. Different materials that can be polymerized, or in the case of the top–down approaches degraded, in 2PP include organic photopolymers, such as acrylates, commercial IP-series, stimuli-responsive materials for 4D printing, hydrogels, epoxy, hybrid polymers, such as metallic containing materials, inorganic dielectric materials, and emitting materials [217–220].

15.2. Photodegradation

Between the physical methods that exploit two-photon absorption, we can mention as top–down approach the photodegradation. This technique uses light-sensitive moieties, such as ortho-nitrobenzyl or coumarin, to break bonds and degrade hydrogel structures, creating channels or pores that can be used for microchannels [202, 228]. Photocoupling is another light patterning technique that uses light to activate functional groups, such as thiols or amines, that can react with biomolecules, such as peptides or proteins, to pattern them within the hydrogel [229].

15.3. Laser micromachining

Laser micromachining is a top–down microfabrication technique that employs highly focused laser beams usually in the form of ultrafast (down to femtosecond) pulses, to remove material with nanometric precision. In the biomedical scenarios, this approach is used to create complex microstructures in biocompatible materials as metals, polymers or ceramics commonly employed to realize implantable devices, microfluidic systems, and tissue scaffolds. Due to the nonlinearity of the process, any thermal

damage is minimized, preserving the integrity of the material. Laser micromachining in the biomedical scenario has been used so far to produce texturized implant surfaces to improve osseointegration by creating biomimetic roughness on metallic implants, microfluidic channels, usually realized in fused-silica glasses or polymers for point-of-care diagnostics and lab-on-a-chip devices, or to create trenches or microneedles [225, 226].

In summary, top–down fabrication technology is a powerful tool that allows for the creation of complex 3D tissue structures by precisely controlling the arrangement of cells and biomaterials. This approach holds great promise for the development of engineered tissues that can replicate the structure and function of natural tissues.

16. Bottom–up microscaffold fabrication approaches

To produce patterning inside a larger 3D build, bottom–up techniques rely on the controlled assembly of small-scale elements at first. This can be accomplished by building small structures, such as spheroids or microgels, or through 3D bioprinting. Examples include 3D bioprinting, photolithography, laser assisted techniques, microfluidics, cell sheet technology, and self-assembly (table 5).

16.1. 3D bioprinting

In tissue engineering, 3D bioprinting is used to create biocompatible constructs in a wide range of materials. Some of the widely used methods for fabricating 3D scaffolds are inkjet, pressure-assisted, laser-assisted bioprinting, and extrusion-based bioprinting (figure 11(e)–(e')). These techniques have shown a significant impact on cell adherence, proliferation, and differentiation in both *in vitro* and *in vivo* studies. Additionally, 3D-printed constructs with growth factors enhance ECM production, collagen I content, and glycosaminoglycan content for cell growth and bone formation. This technology can also be employed to create individualized biological constructs for various tissues, including cartilage, vascular grafts, skin, neural tissue, heart tissue, liver tissue, lung tissue, etc. The different bio-fabricating approaches will result in different physical approaches. Inkjet-based bioprinting uses thermal or piezoelectric actuators to generate droplets of biocompatible substances (bioink) onto a substrate [236]. It has advantages such as high-throughput, high resolution (10–50 μm), and high cell viability, but it requires bioink to be in a liquid state and have appropriate viscosity [237–239, 275]. Laser-assisted bioprinting uses continuous wavelengths (or femtosecond ones) to selectively crosslink bioinks onto a substrate [241–244, 276], while pressure-assisted bioprinting uses pressure forces bioinks through nozzles to create patterns (figure 11(e')) [245–248].

16.2. 2PP

The distinction between top–down and bottom–up fabrication approaches is peculiar, particularly when discussing 2PP. When 2PP is employed to add or modify features on existing bulk material, it aligns with the top–down approach, which typically involves the removal or addition of material to create structures. Conversely, when 2PP is utilized to construct complex three-dimensional structures from the ground up, one voxel at a time, it embodies the bottom–up approach. This method aims at building molecular Lego blocks, where each voxel represents a unit structure, and their sequential polymerization leads to the formation of intricate scaffolds or constructs. The bottom–up approach allows for the creation of microscaffolds with complex geometries and gradients of properties that mimic the natural ECM, facilitating cell attachment, proliferation, and differentiation. In contrast, the top–down approach using 2PP might be more suited for applications where modifications to existing structures are needed, such as creating microfluidic channels within a bulk material or modifying the surface properties of a device for enhanced functionality. This demonstrates the adaptability of 2PP as a fabrication technique, capable of both subtractive and additive processes, and highlights the importance of defining the approach based on the end goal of the fabrication process.

16.3. Electrospinning

Between the fabrication techniques, electrospinning is a highly versatile technique that allows the production of ultrathin fibers with diameters as small as nanometers (figure 11(c)). This technique starts with bulk fiber, which is then processed into nanostructures through the controlled application of electric forces. The process begins with a polymer solution or melt loaded into a spinneret. Then, an electric field is applied, causing the polymer to form a charged jet that elongates and solidifies into nanofibers as it travels to a collector. The resulting fibers can have various morphologies, including porous, hollow, helical, aligned, multilayer, core–shell, and multichannel structures [230–235, 277].

Table 5. Bottom–up fabrication approaches applied to tissue engineering.

Bottom–up approaches	Description	Targeted organ	Detailed applications	Ref.
Two-photon polymerization	A technique that uses light to control material cross-linking in 3D	Bone /vascular system /skin /cartilage /nerve	- Creating 3D scaffold for controlling cellular fate or for maintaining cellular functionalities	[202, 203, 206, 209, 211–224, 227–229]
Electrospinning	A technique to produce ultrathin fibers by using an electric field that is normally labeled as bottom–up. The process starts with a polymer solution or melt loaded into a spinneret. An applied electric causes the polymer to form a charged jet that elongates and solidifies into nanofibers. When combined with patterned collectors or masks, it can function as a top–down technique to impose micro-organization onto fibers	Bone /skin vascular system /Nerve	- Creating nanofibrous scaffolds that replicate the native extracellular matrix in terms of composition and architecture - Controlling drug delivery with loaded fibers - Creating filtration or sterile membranes	[224, 230–235]
Inkjet bioprinting	A method that precisely dispenses bioink onto the target surface, utilizing thermal or piezoelectric mechanisms to produce droplets	Bone /skin /cartilage /vascular system /ligament	- Creating biological constructs with a resolution ranging from 10 to 50 μm - Fabricating various tissue types, including cartilage, vascular grafts, skin, neural tissue, heart tissue, liver tissue, and lung tissue - Contactless bioprinting for both hard and soft tissue regeneration - Creating biocompatible constructs using a wide range of materials, including bioinks loaded with cells, growth factors, drugs and other bioactive molecules	[210, 218, 236–240]
Laser-assisted bioprinting	A technique that uses a pulsed laser beam to transfer biological material from a donor layer to a receiving substrate	Bone /skin /cartilage /vascular system /ligament	- Depositing living cells and biomaterials to create functional tissues and organs - Creating and depositing *in situ* biocompatible constructs using a wide range of materials, including bioinks loaded with cells, growth factors, drugs and other bioactive molecules - Producing skin constructs for wound healing and burn treatment	[232, 241–244]
Pressure-driven bioprinting	A technique that combines a fluid-dispensing system and an automated robotic system to extrude and print bioink in continuous cylindrical lines	Bone /skin /cartilage /vascular system /ligament	- Creating 3D scaffold for tissue defect healing or for tissue replacement - Creating organ-on-a-chip systems, - Creating organoids, - Employing high cell densities and highly viscous inks during bioprinting processes	[245–250]

(Continued.)

Table 5. (Continued.)

Bottom–up approaches	Description	Targeted organ	Detailed applications	Ref.
Microfluidics	A technique that uses microscale channels and droplets to control the flow and mixing of cells and biomaterials in the 3D environments	Bone /skin /cartilage	- Separating specific cell types from a mixture for diagnostics or therapeutics (cell sorting) - Creating gradient of biomolecules for studying cell migration - Generating 3D structures with defined cell patterns or material gradients - Developing microencapsulated 3D constructs with complex cell organoid and tissue culture environments (with a control on the microenvironmental cues)	[251–259]
Magnetism	A technique that uses magnetic fields to manipulate the position and orientation of cells or particles in 3D	Vascular system /cartilage	- Patterning of cell aggregates and spheroids - Labeling of cells with magnetic nanoparticles for remote control - Negative magnetophoresis to shuttle cells to low field regions	[260–262]
Acoustic patterning	A technique that uses acoustic forces to modulate the distribution of cells or particles in 3D	Skin /cartilage /bone	- Large-scale manipulation of cell aggregates - Precise single cell positioning and grouping - Dynamic and programmable cell manipulation	[263–267]
Cell origami	A technique that uses stimuli-responsive biomaterials and folding principles to create complex 3D cell structures	Bone	- Producing intricate 3D microstructures, including micro-sized containers and scaffolds for artificial tissues - Creating 3D tissue constructs with complex geometries for regenerative medicine and drug testing	[268, 269]
Cell sheet and self-assembly	A process that relies on the spontaneous organization of molecules or cells into ordered structures	Skin /cartilage /bone	- Patterning cells to create functional *in vitro* tissue construct - Creating exogenous material-free 3D microenvironments - Creating thick (up to 0.5 mm in height) constructs for bone, cartilage, and skin tissue engineering	[270–274]

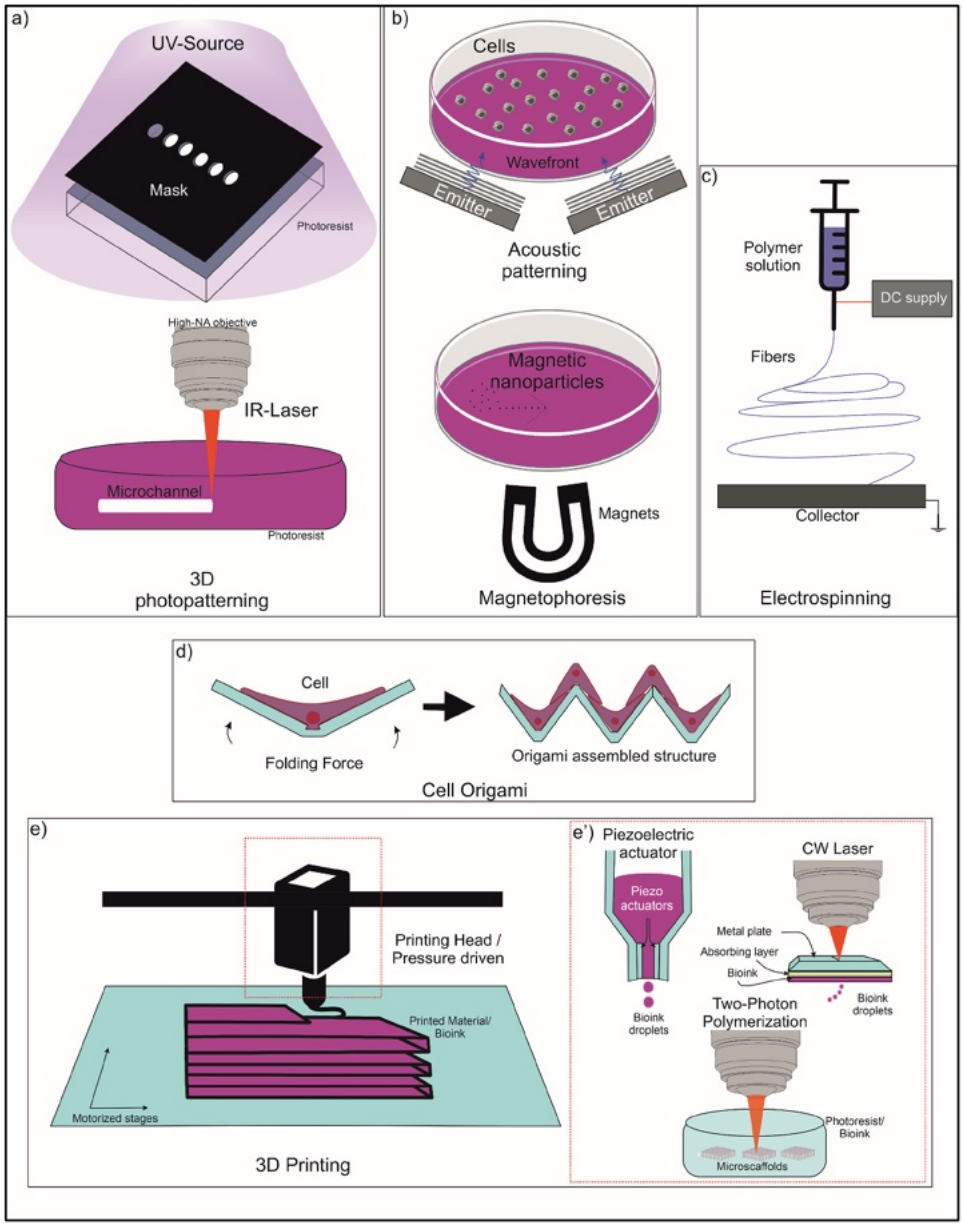

Figure 11. Top–down and bottom–up technologies to realize 3D microscaffolds or 3D micro-architectures. (a) Two-dimensional and three-dimensional photopatterning/photodegradation. Two-dimensional photopatterning is typically achieved using continuous wave (CW) ultraviolet (UV) light, which allows for the precise manipulation of polymer surfaces. On the other hand, three-dimensional structuring within a polymer is facilitated by multiphoton illumination, a technique that enables the creation of complex shapes and patterns at a submicron scale. This method is not only used for the cross-linking or degradation of polymer networks but also for the uncaging of bioactive molecules within the scaffold. (b) Acoustic patterning and magnetophoresis. Acoustic patterning employs sound waves (provided by emitters) to organize cells into a cohesive strategy for constructing complex tissue structures, while magnetophoresis utilizes static or modulated magnetic fields to manipulate particles and living cells. The sketch likely illustrates the precise control over cell placement and alignment, which is crucial for replicating the intricate architecture of natural tissues. (c) Electrospinning in action: sketched view of the electrospinning process, showing the intricate formation of ultra-fine polymer fibers as they are drawn from a charged liquid droplet to create a nanoscale fiber material. This innovative technique employs electric forces to produce fibers with tunable properties for tissue engineering applications. (d) Cell origami is based on the principles of the ancient art of paper folding applied to cellular structures. This technique utilizes the natural traction forces exerted by cells to induce the folding of specially designed microstructures into three-dimensional shapes. The process involves the use of biocompatible materials to which cells can attach and manipulate. As cells adhere to these substrates, their inherent traction forces (generated as they attempt to move) cause the flat, two-dimensional surfaces to bend and fold along pre-determined creases, transforming into complex, three-dimensional forms. (e) Bioprinting and 3D-printing processes. This process allows for the precise spatial arrangement of different materials or cell types dispersed within a bioink. Motorized stages allow for positioning the printing head with a precision close to 100 nm. (e') Pressure-driven bioprinting utilizes pneumatic or mechanical forces to extrude biomaterials through a nozzle, allowing for the construction of three-dimensional structures. Piezoelectric bioprinting, on the other hand, employs electric charges to control the deposition of biomaterials, offering high-resolution printing capabilities. Inkjet Dropping allows for depositing droplets layer by layer to form multilayered tissues. Lastly, two-photon bioprinting involves the use of laser-focused photons to solidify light-sensitive materials, creating intricate structures with cellular-level detail.

16.4. Microfluidics

Microfluidics, the well-known *in vitro* category of devices, in recent years, has become an emerging bioprinting branch, known as 'organoid formation on a chip', that has the potential to create simple 3D structures with specific cell patterns and mimic complex biophysical/biochemical parameters of 3D cellular/tissue microenvironments. Because of the micro-scaled geometries, high surface area to volume ratio, dynamic fluid flow, and low reagent consumption, this technique has been applied to fabricate 3D constructs with cell-like functionalized micro-fibers hollow, complex micro-spheroids, gel microspheres, and high-viscous inks (jammed gels) [251–259].

16.5. Magnetophoresis

Magnetophoresis can be used to pattern and create three-dimensional structures by using magnetic forces to control the 3D location of cells. This technique does not directly physically move cells, making it gentler than other methods, while it uses the interaction of intrinsically magnetic properties of certain cells and external magnetic fields (figure 11(b)). There are two main types: positive and negative. In positive magnetophoresis, cells move towards stronger magnetic fields, while in negative magnetophoresis, they move away. Positive magnetophoresis requires special magnetic cells, while negative magnetophoresis only needs a magnetic environment [260–262].

16.6. Acoustic wave techniques

In addition, surface acoustic wave techniques garnered significant attention in the field of tissue engineering. This technique is a biocompatible, easily accessible, label-free, and non-invasive tool that has gained prominence by enabling precise sorting, manipulation, cell patterning, and rapid spheroid formation (figure 11(b)) [263–267].

16.7. Cell-based technologies

Origami-based methods have emerged as effective strategies for creating 3D microstructures due to their simplicity and efficiency compared to other top–down fabrication techniques (figure 11(d)). These methods have been utilized to develop various 3D cell-laden microstructures, including micro-containers and scaffolds for artificial tissues. The folding process often relies on surface tension, stress-induced forces, and hinge shrinkage triggered by external stimuli such as temperature and electrical/chemical signals. Cells themselves can drive this folding through their natural contractile forces, known as cell traction forces, facilitated by actomyosin interactions and actin polymerization. Patterning cells on microplates allows them to stretch and adhere, leading to the self-folding of 3D structures. The advantage of cell origami is its biocompatibility, as it does not require special materials for folding. This innovative technique holds significant potential for applications in tissue engineering, drug delivery, and other biomedical fields [269, 278].

Cell sheet and self-assembly fabrication techniques are two relatively mature scaffold-free tissue engineering approaches that use cells as a biomaterial. The first method involves the creation of micrometric sheets, which are layers of cells that can be used for composing complex tissue portions [270]. While some research has suggested a more sophisticated approach [271], in which numerous cell types were cocultured inside a single sheet, the most straightforward method of using cell sheets to create 3D tissues is to stack monoculture cell sheets of distinct cell kinds layer by layer [272]. Instead, the latter method relies on cells organizing themselves spontaneously, that is, without external direction or control, into an equilibrium-preserving structural arrangement [273].

Nonetheless, the scaling up of both technologies for 3D tissue fabrication is still limited. Thick 3D tissues cannot survive for very long time *in vivo* or *in vitro* due to inadequate nutrition and waste product buildup. Stacked cell sheets can only be as thick as 70–80 μm *in vivo*. One way to solve the issue for *in vivo* applications is by creating hybrid 3D structures to be used with cell sheets, which makes it simple to construct potentially up to 0.5/1 mm thick cell-dense tissue. One method could be to include bioprinted blood capillary-like networks into tissue-engineered structures to build thicker tissue *in vitro*.

17. Microfabrication technologies and normative scenario

The use of microstructures (extended also to materials and nanomaterials based on inorganic and organic NPs) into tissue engineering products may provide increased functionality, such as regulated biocompatibility, degradability, and better mechanical and optical properties. However, bringing these advances from the research laboratory to clinical practice necessitates complete compliance to regulatory

frameworks intended to assure safety, performance, and quality. For example, the European Union's regulatory environment is primarily determined by the E.U. Medical Device Regulation (MDR) 2017/745, which puts mandatory performance standards and safety measures on medical devices. This regulation revised the Medical Device Directive 93/42/EEC and made significant changes to enhance the regulatory framework for medical devices. This regulation classifies devices into four categories (I, IIa, IIb, and III) depending on the danger they represent to patients and users. Depending on the classification, producers or even scientists must go through a conformity assessment procedure, which frequently includes the participation of a notified body and the creation of extensive technical paperwork (like the Biological Evaluation Report), including specific design and production information. This information must satisfy ISO 10993 biocompatibility and safety criteria, which include several studies such as cytotoxicity, sensitization and irritation, genotoxicity, and so on. Furthermore, the E.U. MDR emphasizes quality management systems that adhere to ISO 13485 standards. ISO 13485 sets standards for an organization to show its capacity to supply medical devices and related services that consistently fulfill customer and regulatory requirements, such as process validation and quality control.

For instance, to comply with ISO 10993, biofabrication procedures based on light-matter interaction that employ resist, or custom-made biomaterials must undergo final testing to show compound stability. Photoinitiators and bioinks, for example, must be examined for their capacity to produce DNA damage, whereas resins must be tested for their impact on cellular survival and function, including cytotoxicity and immunogenicity. Similarly, standardizing bioink formulations, employed in most of the bottom–up techniques, is critical for ensuring consistent performance over several batches and over a determined amount of time (i.e. shelf-life). This entails extensive testing and quality control procedures to verify that the bioinks do not cause undesirable biological reactions. Furthermore, the mechanical qualities of the printed structures, such as tensile strength and elasticity, must be examined to ensure that they fulfill the performance requirements. Similarly, fabrication processes which may employ thermal and mechanical effects that may damage cells or material (like laser assisted techniques or piezo/pressure driven ones) must mitigate risks by selecting appropriate fabrication parameters and by using materials that may not degrade. Finally, the process validation must be assessed by using a quality management system compliant with ISO 13485. In this regard, the manufacturing process must consistently generate structures with predetermined specifications and attributes. Maintaining high quality and safety standards requires regular equipment calibration and maintenance, as well as extensive documentation and a control system alongside the fabrication line (e.g. real-time machine-vision inspection or sensors' data collection). Advanced imaging methods, including scanning electron microscopy and atomic force microscopy, should be used to ensure the structural integrity and accuracy of the scaffolds produced. Similarly, scaffold-free techniques like self-assembly and cell origami must ensure the stability and functionality of the assembled biological structures over time, crucial factors for clinical applications.

18. Materials for microscaffolds in tissue engineering

Scaffolds play a crucial role in bone tissue engineering, providing a structural framework for cell attachment, proliferation, and differentiation to regenerate damaged or lost bone tissue. Ideal scaffolds should mimic the ECM of natural bone, possess mechanical strength, promote vascularization, and support the growth of new bone tissue. Various materials and fabrication techniques have been explored to design scaffolds tailored for bone tissue engineering applications. However, engineered biomaterials for bone grafts are still behind natural bone grafts in regenerative potential, especially for weight-bearing applications. To address this problem, there is an immense need for implantable scaffolds that support bone regeneration with load-bearing capacity. Emerging approaches involve using scaffolds with stem cells, drug addiction, or reinforced fibers with NP embedding or fiber coating, which are showing promising outcomes in generating new bone and repairing segmental defects in animal studies.

The studies summarized in this section illustrate a small set of recurring strategies for engineering load-bearing and tissue-specific microscaffolds, such as reinforcing soft matrices with ceramic or carbon fillers and bioactive coatings to raise mechanical properties [279–281]. Moreover, we presented bioprinting cell-, vesicle- or drug-laden inks by inkjet, extrusion or laser-assisted methods to reconstruct multi-layered tissues [239, 243, 245, 247]. Then, we made an insight on electrospinning composite membranes that combine high porosity with antibacterial for wound coverage [234, 277], and the assembly of hybrid constructs from fibers, spheroids or self-folding units used to introduce three-dimensional microarchitecture [269, 282, 283].

One of the most promising approaches is the coating method, such as hydroxyapatite and fiberglass coating, which have been employed to enhance the mechanical properties of PLA scaffolds. Moghimi

et al realized a concentric core–shell structure with a hard shell. The first one is the stiffer material: PLA microfibers coated with HA NPs and encapsulated with the cells. The soft core is a mixture of GelMA (8%), PLA microfibers, and platelet-rich factors extracted from human blood, which makes the composite material with growth factors incorporated to mimic the bone marrow or induce osteogenesis [279]. Incorporating short fibers coated with HA improves biological activity and reinforces mechanical strength in bioinks. The scaffold has been bioprinted by extrusion bioprinting and by UV exposure. The scaffold diameter was 6 mm, and the height was 3 or 6 mm. The core diameter was 2 mm, while the scaffold porosity was about 80%. PLA short fibers with an average length of 600 μm and an average diameter of 40 μm were obtained.

Wound healing scaffolds are designed to completely rejuvenate skin functionality and architecture by overcoming existing challenges in the development of skin analogues through cellular engineering and the integration of biochemical and biomechanical elements. In this domain, Ferroni *et al* crafted a 3D-printed construct using a methacrylated hyaluronic acid bioink. This construct was specifically engineered to administer small extracellular vesicles derived from human MSCs, thereby augmenting the cutaneous regeneration process. The scaffold, characterized by a pore size of 1.34 mm, facilitated the release of these diminutive vesicles within a live pressure ulcer model, leading to improved wound healing in diabetic rodents, as demonstrated through assays of re-epithelialization, vascular formation, and neural tissue integration [245].

Inkjet printing technique primarily targets the construction of cellular multilayers, where the bioink is precisely deposited onto a base material. In this context, Kang *et al* developed a triple-layered pulmonary structure utilizing a specially formulated bioink that integrates collagen, pulmonary cells, and vascular cells. This innovative approach resulted in an inkjet-printed pulmonary structure with a notable thickness of approximately 12 $\pm$ 1.1 μm and its structural details were examined through histological analysis [239].

PCL is a semi-crystalline, biocompatible, and biodegradable polyester having mechanical characteristics comparable to those of biological tissues. However, PCL is a synthetic polymer missing biological patterns for cell recognition, hence it is frequently used with natural polymers such as chitosan and gelatin [93]. Viera *et al* used PCL blended with chitosan, a natural polysaccharide derived from chitin for fabricating the scaffold in electrospinning to realize thin-fiber structures having a high porosity as to enhance cellular migration and fibroblast infiltration. They produced fibrous membranes having a mean fiber diameter of 3.4 $\pm$ 0.7 μm, an overall thickness of 227 $\pm$ 65 μm, and a porosity of about 88% [277].

In the field of wound healing, the research by Khan *et al* introduced an innovative two-layered scaffold structure. The base layer consists of a gelatin-based hydrogel created through lyophilization, while the upper layer features a nanofiber mesh composed of bacterial cellulose and polyvinyl alcohol, formed through the electrospinning process. This dual-layered hydrogel-nanofiber construct exhibits a network of pores with 70%–80% porosity (pore sizes ranging from 100 to 150 μm, which promotes effective fluid uptake and cellular movement. It also enhances the diffusion of nutrients, supports the growth of new tissue due to its expansive surface area, and possesses robust antibacterial properties [234].

In one study by Huang *et al* a highly biomimetic 3D-printed porous scaffold made of multi-walled CNTs with the same dimensions as collagen fibers and primarily aligned along the printing direction was combined with HA and blended with a PCL matrix to create scaffolds using a screw-based extrusion production system resulting in a filament diameter of 330 μm [280]. This mixture led to increasing the storage modulus, the elastic modulus of the filament (compressive modulus was nearly 90 MPa), and the yield strength (almost 3 MPa) of the scaffold, the surface roughness increased, which promoted bone differentiation, helped to adjust the path of the hard surface transfer mechanism, and enabled high protein absorption. The obtained pore size was 350 μm [280].

To reduce the scaffold size while maintaining mechanical properties, carbon-based nanomaterials can be employed to modify pre-existing biocompatible materials. Carbon-based nanomaterials such as graphene oxide, CNTs, fullerenes, carbon diamond, and their derivatives improve the mechanical stability of scaffolds, which play an important role in bone regeneration. Specifically, the mechanical properties of graphene oxide and reduced graphene oxide have been extensively studied in the context of tissue engineering scaffolds. Nonetheless, few researchers were able to fabricate by additive manufacturing techniques [208]. One notable study by Kadhim *et al* focused on reinforcing electrospun PCL-gelatin nanofiber scaffolds with bone morphogenetic protein-modified graphene oxide to increase mechanical stability. Therefore, the mix of PCL and graphene oxide decreased the strain at break from 116% $\pm$ 6.2% to 90% $\pm$ 2.9% due to the stiffness increase, while the swelling ratio rose significantly, from 150% to 218%. The obtained fibers had a diameter of 270 nm [281].

To promote fully vascularized bone regeneration using laser-assisted bioprinting, researchers initial improvements focused on enhancing bioprinted layers quality, both mechanically and physiologically. In conjunction with Washio *et al,* Kérourédan produced gelatin hydrogel sponges integrating bioactive glass, which demonstrated mechanical and chemical efficacy as scaffolds, including the production of hydroxyapatite crystallization in the setting of dental pulp and dentin regeneration. They highlighted that those bioactive glasses induced bone regeneration more quickly than other bioactive ceramics (e.g.hydroxyapatite) due to their osteoconductivity and osteoinductivity. Furthermore, angiogenesis or neovascularization was not impaired, thanks to the scaffold made of Gel 5 wt % bioactive glass 1 wt %, porosity of 385 μm, porosity of 91.7 $\pm$ 1.55%, and an overall height of 500 μm with a scalable lateral size [243]. Another study combines electrospinning technology with origami methods to produce a 3D complex of nanofiber scaffolds and cells and investigates its potential applications in bone tissue engineering. This method's primary features are the utilization of electrospun nanofiber boxes and the twofold seeding of human fetal osteoblasts on nanofiber films. The nanofiber boxes are predicted to provide a constrained environment for the nanofiber films, whilst the twofold seeding of cells may assist the bonding of neighboring nanofiber films *via* ECM secretion. To improve mechanical qualities, nanohydroxyapatite particles were incorporated into polycaprolactone nanofibers. Finally, origami was used to generate 3D nanofiber structures in a variety of basic and complicated shapes [269].

A bioresponsive hydrogel made of GHA can be cross-linked with genipin, making it suitable for 3D bioprinting of tissue engineering scaffolds that maintain high shape accuracy and resolution in extrusion bioprinting. The cross-linking of genipin with gelatin polymers enhances the hydrogel's stability and makes it extrudable as it was demonstrated by Khatun and colleagues [247].

To further reduce the bottom–up starting point, self-assembly methods can be used to generate spheroids. These can be used as modular tissue units, facilitating bottom–up tissue engineering approaches. However, using bare spheroids as building blocks presents challenges such as difficulty in achieving defined geometry and mechanical stability. To address these issues, researchers have explored the use of microscaffolds, such as buckyballs, which are highly porous cage-like structures capable of carrying cells and supporting spheroid formation within their core. This approach integrates cellular spheroids cultured within robust micro scaffolds, offering synergistic benefits of both scaffold-based and scaffold-free strategies. These structures were produced using 2PP in a biodegradable PCL-based resin, with a diameter of 350 μm, a volume of 0.014 mm^3, a truss thickness of 35 μm, and a porosity of about 95%. Since one buckyball was produced in 10 s, Guillaume and colleagues estimated it feasible to manufacture enough hybrid spheroids to fill defect volumes up to 1 cm^3 within 6 d [282].

An example from Wang *et al* investigated the incorporation of conductive nanofiber yarns, synthesized from polycaprolactone, silk fibroin, and CNTs, into a GelMA hydrogel. This integration promoted the alignment of cardiomyocytes and the expression of mature cardiomyocyte markers while maintaining their functionality. Similarly, composite materials comprising PCL nanofibers in an HA hydrogel have been studied [283].

Fibers exhibit distinct effects on the alignment and organization of various cell types, including hepatocytes, neural cells, tendons, and ligaments, among others. This strategy holds potential across a range of tissue types, particularly considering the feasibility of bioprinting inks containing nanofibers or particles. This enables the combination of macroscale patterning with micro- or nanoscale features of fibers and NPs, facilitating precise control over tissue engineering constructs [284–286].

2PP initially utilized acrylic photopolymers and a wide variety of commercial photoresists specifically designed for tissue engineering applications, like IP-L 780, Ormocomp® (produced by micro resist technology GmbH), PEGda, SR368, and SR499 triacrylate blends (from Sartomer), Accura® SI10 (from 3D Systems Corporation), ORMOCER®s (from The Fraunhofer ISC), hydrolytically degradable polycaprolactone-based polymers, enzymatically degradable methacrylamide-modified gelatin (known as gelMOD), and water-soluble PI-Irgacure [219, 287].

However, recent research shifted towards photosensitive sol-gel hybrid materials, such as ORMOCER®, Polyethylene Glycol diacrylate, poly(trimethylene-carbonate), SZ2080 or towards naturally derived materials like GelMa in tissue engineering applications.

The choice among these photoresists is dictated mainly by the property required of the final scaffold, such as biodegradability for transient bone constructs (e.g. PTMC and methacrylated PLLA) [203, 211], crosslinking efficiency for high-resolution woodpile and grid architectures (CHic and chitosan/gelMOD) [212, 288], long-term biocompatibility and optical quality for implantable niches (SZ2080) [206, 289–292], and stimuli-responsiveness or on-demand degradation for dynamic, '4D' constructs (like host–guest photoresists and photodegradable PEG) [202, 209].

A peculiar polymer is poly(trimethylene-carbonate) (PTMC). Due to its degradation mechanism given by surface erosion driven by enzymatic erosion, PTMC has shown to be a highly suitable polymer for the fabrication of scaffolds for bone tissue engineering and hence poses a great potential for the realization of biocompatible and biodegradable scaffolds with an unprecedented large size. In this regard, Weisgrab and colleagues realized a (PTMC)-based bulky balls scaffold of large size ($18 \times 18 \times 0.9$ mm^3) with a volume of 292 mm^3, a volumetric porosity of 96%, a structure width of around 20 μm, and a thickness of approximately 30 μm (figures 12(a)–(h)) [203]. Similarly, Song and his team introduced a unique one-component, polymer-based photoreactive material system that relies on carbon-hydrogen (C, H) insertion crosslinking (named CHic) to create 3D microstructures for bone tissue engineering. The material is locally crosslinked through a C, H insertion and is composed entirely of one component, specifically the prepolymer molecules themselves. The prepolymer can undergo the process of multi-photon polymerization, which leads to the formation of active intermediates. These intermediates can bond with neighboring aliphatic components, some of which are integral to the prepolymer's main structure. Consequently, when stimulated, this CHic-capable photoreactive substance can establish a network of crosslinks independently, without relying on monomers, photoinitiators, or sensitizers. The resulting structures were fabricated in the form of woodpile patterns, with pore sizes measuring 10 μm, 25 μm, and 50 μm, achieving a lateral precision as fine as 2.5 μm. This was accomplished by employing an objective lens with low magnification (20x) and a numerical aperture of merely 0.7, designed for water immersion [212]. In the study conducted by Rodimova *et al* a three-dimensional scaffold was engineered using methacrylated poly(L-lactic acid) within a supercritical carbon dioxide environment. This scaffold was designed for the purpose of enhancing osteogenic differentiation and the efficacy of bone formation in human MSCs that were introduced to the structure. The scaffold is composed of three stratified cylindrical layers with uniform diameters, while the variant with gradient pore sizes features a central layer with enlarged cylinders, replicating the porous architecture of natural trabecular bone. The uniform scaffold has internal and external diameters measuring 180 μm and 250 μm respectively, with a height of 80 μm. In contrast, the gradient scaffold boasts internal and external diameters of 300 μm and 400 μm respectively, and a height of 100 μm [211].

SZ2080, a biocompatible photopolymer frequently used for microscaffold realization was employed by Raimondi and her team for different biological purposes. As an example, they used a 100x oil-immersion objective with a numerical aperture of 1.4 to create artificial stem cell niches. These niches had two different heights (20 and 80–100 μm) and four lattice pore sizes (10, 20, 30 μm, and graded). They aimed to study the impact of purely structural cues on stem cell behavior. Then, the team created a new substrate with approximately 400 niches to ensure the proliferation and stemness maintenance of cultured cells [289].

Additionally, SZ2080 stem cell niches were coated with thin layers of hyaluronic acid-based and gelatin-based hydrogels to explore the interactions between structural and chemical biomimicry and their impact on stem cell responses. Parodi *et al* demonstrated the efficacy of this kind of scaffold in chondrogenic differentiation of seeded rat MSCs [290].

Additionally, SZ2080 has been employed in ten years' old preclinical studies. Mačiulaitis *et al* created hexagonal-pore-shaped microscaffold having a rod height and width of about 15 and 10 μm, respectively, a pore size of 40×40 μm^2 and a maximum dimension of $2.5 \times 2.5 \times 0.22$ mm^3. These constructs were then *in vitro* seeded with isolated allogeneic rabbit chondrocytes and *in vivo* implanted into laboratory rabbits for one, three, and six months. They achieved a degree of biocompatibility comparable to the one of commercially available collagen membranes [291]. Another application of SZ2080 was demonstrated by Conci and colleagues, where two works showed the possibility of realizing microscaffolds having sufficient mechanical and optical characteristics to control and trace over time a foreign body reaction against microstructures implanted in living chicken embryos (figures 12(a')–(f')) [206, 292].

Moreover, besides the reduced achieved resolution (10 μm), a water-soluble photosensitive derivative of chitosan and its hybrid biopolymer-based hydrogel with gelatin methacrylamide has been used as the photoresist to realize scaffolds for bone remineralization. This hybrid hydrogel was utilized to construct grid-like scaffolds of $400 \times 400 \times 75$ and $500 \times 500 \times 75$ μm^3 with a pore size of 80–100 μm. The fabricated 3D biopolymer-based scaffolds were loaded with dental pulp stem cells, after being functionalized with an osteoinductive protein. The findings indicate promising potential for these hybrid photo-cross-linkable materials when used with femtosecond pulse lasers, for *in situ* bioprinting of biocompatible and functional scaffolds for tissue engineering [287]. The team led by Hippler introduced a photoresist that responds to stimuli, which is created through noncovalent, directional bonds between β-cyclodextrin and adamantane components. The hydrogel microstructures produced through 2PP can significantly alter their volume when exposed to soluble guest molecules of low molecular weight in

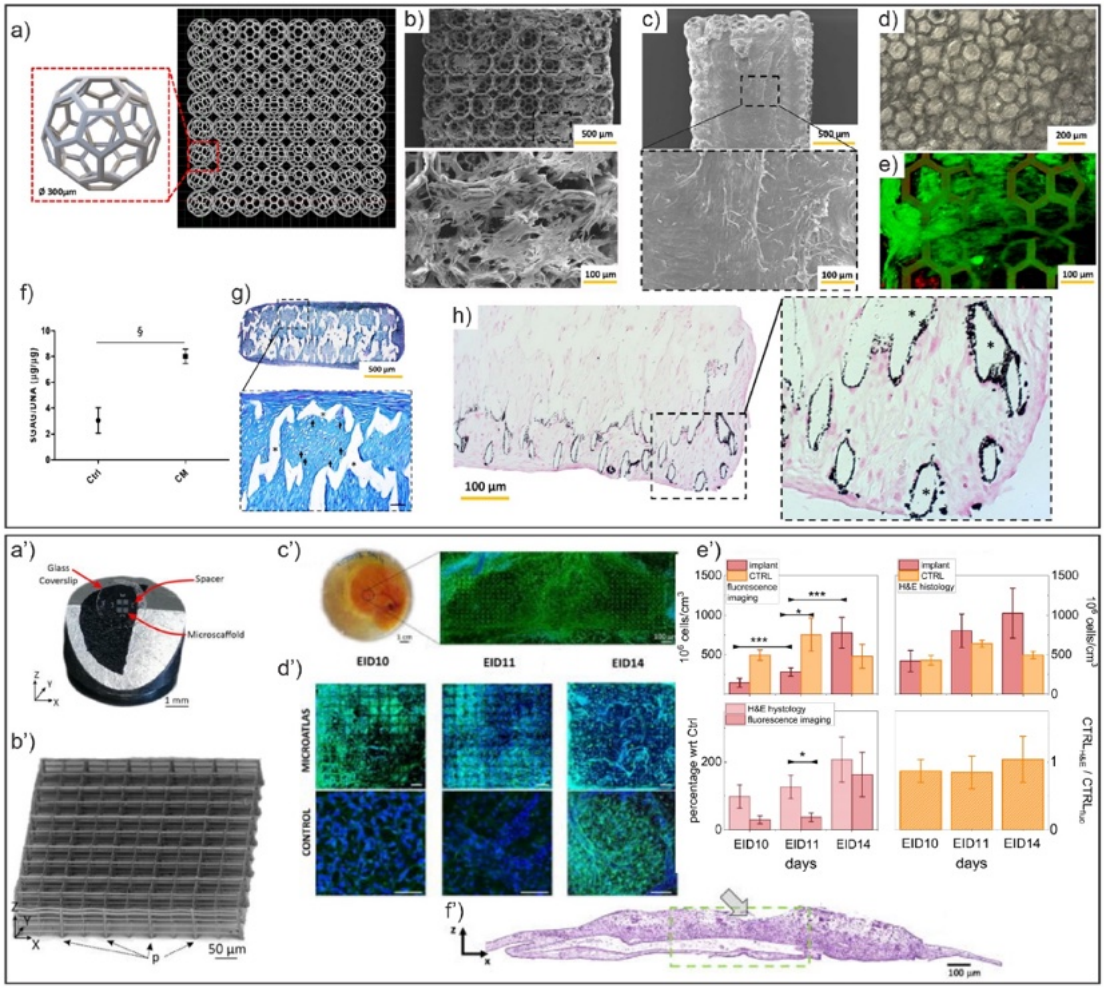

Figure 12. Panel (a) design of buckyball-based scaffold. 3D render of the scaffold consisting of an 8 × 8 × 3 array with a diameter of 300 μm each. Panel (b) 2PP-produced PTMC-MA scaffolds support cell invasion and proliferation. SEM images of cell-seeded scaffolds day 2 (b) and day 28 (c) post seeding. Panel d) bright field and (e) live/dead illustrations of the colonized scaffold at day 28 post-seeding. Panel (f) quantification of sulfated glycosaminoglycans secretion by cells (§ indicates significance) in control medium versus chondrogenic medium and (g) histological staining of sulfated glycosaminoglycans using Alcian Blue at day 28. Black arrows show the chondrocytes embedded in the secreted extracellular matrix. (h) Von Kossa staining showing in black the calcium mineralization after 28 d of cells cultivation in osteogenic medium. Cross-sections of the scaffold are marked with black asterisks. Reproduced from [203]. © The author(s). Published by IOP publishing Ltd CC BY 4.0. Copyright 2020 The authors, published by IOP publishing Ltd panel (a') photograph of a whole device composed of four Microatlas, four spacers on a 5 mm diameter glass slide. Panel (b') SEM micrograph of one Microatlas lattice, with the details of the thicker pillars (*P*) and the microgrid. Panel (c') Microatlas implanted ex ovo in the respiratory membrane and a wide field of view of the implant taken under two-photon excitation ($\lambda = 800$ nm). Panel (d') details of a Microatlas grid, imaged by two-photon excitation, at embryonic incubation days 10, 11, and 14 (top row, bar size = 50 μm) and of control tissue (bottom row, bar size = 50 μm). Signals are fluorescence from cytoplasm and vessels (green, Exc: 800 nm, Em: 535/50 nm) and second harmonic generation from collagen I (blue, Exc: 800 nm; Em: 400/40 nm). Panel (e') cell counting in the Microatlas and control tissue: cellular volume density measured on 3D fluorescence images in the Microatlas and in the control samples, cellular volume density measured on H&E stained tissue sections measured around the Microatlas and in the control samples, percentage increase in cellular density in the Microatlas as measured on fluorescence images and as measured on the H&E sections around the Microatlas, and ratio of the cell counting on the control samples as measured on the histological sections over the cell counting as measured on the fluorescence images. Panel (f') H&E stained cross section (x–z plane) of the respiratory membrane. The pocket in which the Microatlas was implanted is indicated by the arrow. Reproduced from [292]. CC BY 4.0. Copyright 2023 the authors, published by AIP publishing.

physiological environments. Following this, the team integrated this innovative material with standard photoresists to construct composite scaffolds. These scaffolds were composed of a base that repels proteins, sections that attract proteins, and the responsive hydrogel and were tested with fibroblasts [209]. Multiphoton-assisted photodegradation allows for the creation and subsequent alteration of complex 3D networks with personalized intraluminal patterns in the presence of encapsulated cells. In the study conducted by Arakawa *et al* a novel approach for fabricating biocompatible 3D vascular structures within hydrogel matrices is introduced, leveraging the precision of molecular photolysis. The creation of photodegradable hydrogels was achieved through the process of strain-promoted azide-alkyne cycloaddition,

utilizing poly(ethylene glycol) tetrabicyclononyne in conjunction with a diazide-modified synthetic peptide. Subsequently, the research illustrated the capability to engineer perfusable microvessels with varying dimensions by fabricating a series of five photodegraded channels with progressively diminishing widths and heights. Microvessels with cross-sections as large as 200 × 200 μm^2 and as small as 10 × 10 μm^2 were realized [202].

Nonetheless, microscaffolds may fail in supporting cell migration, cell–cell interactions, and in supporting 3D mechano-transduction within their pores. In addition, all the presented microscaffolds suffer from reduced scalability. In this regard, cell sheet engineering revealed as an emerging technology designed to overcome these limitations. It involves growing cells to confluence on a cell sheet, after which they can be detached from the culture dish surface thanks to external forces like temperature-responsive polymers [270]. In certain studies, osteogenic layers derived from rabbit BMSCs were generated *via* a mechanical technique and subsequently implanted into the subdermal cavities of immunodeficient mice, which promoted the formation of new bone tissue without the need for an external scaffold. Similarly, the implantation of multi-tiered MSC layers from humans, crafted using a magnetic methodology, into the cranial defects of nude rats, led to the development of new bone encircled by cells resembling osteoblasts. While the creation of osteogenic layers through mechanical means and their implantation into facial skeletal defects has been shown to enhance bone tissue formation, there are instances where factors such as biological or mechanical disruptions may cause a delay or absence in bone fusion. In such challenging scenarios, the solitary use of cell layers has demonstrated potential efficacy. Research has delved into the application of osteogenic layers from rat BMSCs in addressing non-union fractures and critical bone healing. The introduction of these layers into the femoral fractures of rats has been observed to augment bone tissue formation at the site of the fracture, culminating in a stable union of the bone. Moreover, in models of critical femoral fractures in rats, the administration of these osteogenic layers has been instrumental in fostering bone tissue regeneration, ultimately achieving bone fusion. Additionally, the encasement of pre-differentiated osteogenic layers from rabbit BMSCs around a fracture gap of 2 mm in the mandible has shown to expedite the healing process of delayed bone fractures and diminish the presence of fibrous tissue at the fracture location [255, 271].

Similarly, Forghani *et al* eliminate the need for biodegradable scaffolds by using thermoresponsive hydrogels made of methylcelluse and poly(N isopropylacrylamide) for bone adipose tissue regeneration [293]. By following the same detaching methods, a critical bone defect model of a load-bearing bone on mice was assessed by Kazuaki Mito. His team implanted 25 mm diameter BMSC sheets one on each side of the defect [272]. Moreover, in self-assembly production, Decoene *et al* demonstrated significant progress made in automating aspects of tissue-engineered advanced therapy medicinal products like the creation of industrial setups for cartilage cell aggregates with a focus on skeletal tissue engineering [273].

Innovations in biomaterials have led to the development of a novel technique for three-dimensional cellular arrangement utilizing magnetic matrices. The research spearheaded by Goranov *et al* has expanded upon previous methods by employing strategically engineered magnetic matrices. These matrices exhibit intense magnetic gradients on a microscale (ranging from 100 to 200 μm) which can effectively direct and secure cells that have been magnetically tagged to a predetermined side of the matrix filaments (figure 13(a)). Such magnetic micro-patterning paves the way for constructing three-dimensional cellular structures with finely tuned textural properties. For the magnetic labeling of cells, commercially available magnetic particles were utilized, and the matrices themselves were crafted from cutting-edge magnetic substances, incorporating iron-doped bioabsorbable hydroxyapatite into poly(ε-caprolactone) (figure 13(b)). The three-dimensional matrices were precisely crafted by the methodical injection, extrusion, and placement of the filaments in a prearranged pattern, which allowed for the segregation of two distinct cellular groups, MSCs and human umbilical vein endothelial cells, on opposing facets of the magnetic osteogenic matrix filaments. This strategic placement of cellular types is anticipated to enhance the regeneration of bone structures at the micro-level, with a particular focus on fostering vascularization within the engineered bone tissue (figures 13(c) and (d)) [260].

Moreover, Kamei *et al* cultured BMSCs with superparamagnetic IO-NPs (SPIONs, ferucarbotran), allowing for incorporation of NPs into the MSC cytoplasm. MSCs containing ferucarbotran were then attracted and guided by a magnet. Consequently, MSCs injected into a joint can be controlled and accumulated at the cartilage defect area using magnetic forces [261].

Acoustic forces can also be used to create cell patterning to control the three-dimensional generation of tissues *in vitro* and *in vivo*. In this regard, Comeau *et al* demonstrated the possibility of repositioning endothelial cells for tissue vascularization in a living organism. This study opens also to the possibility of composing, in the same way, complex structures or 3D scaffolds by moving *in situ* micro and NPs injected in an organism [265]. In addition, this method can also be joined to bioprinting. A novel investigation has illustrated the efficacy of an ultrasound-assisted biofabrication method (figure 13(a')),

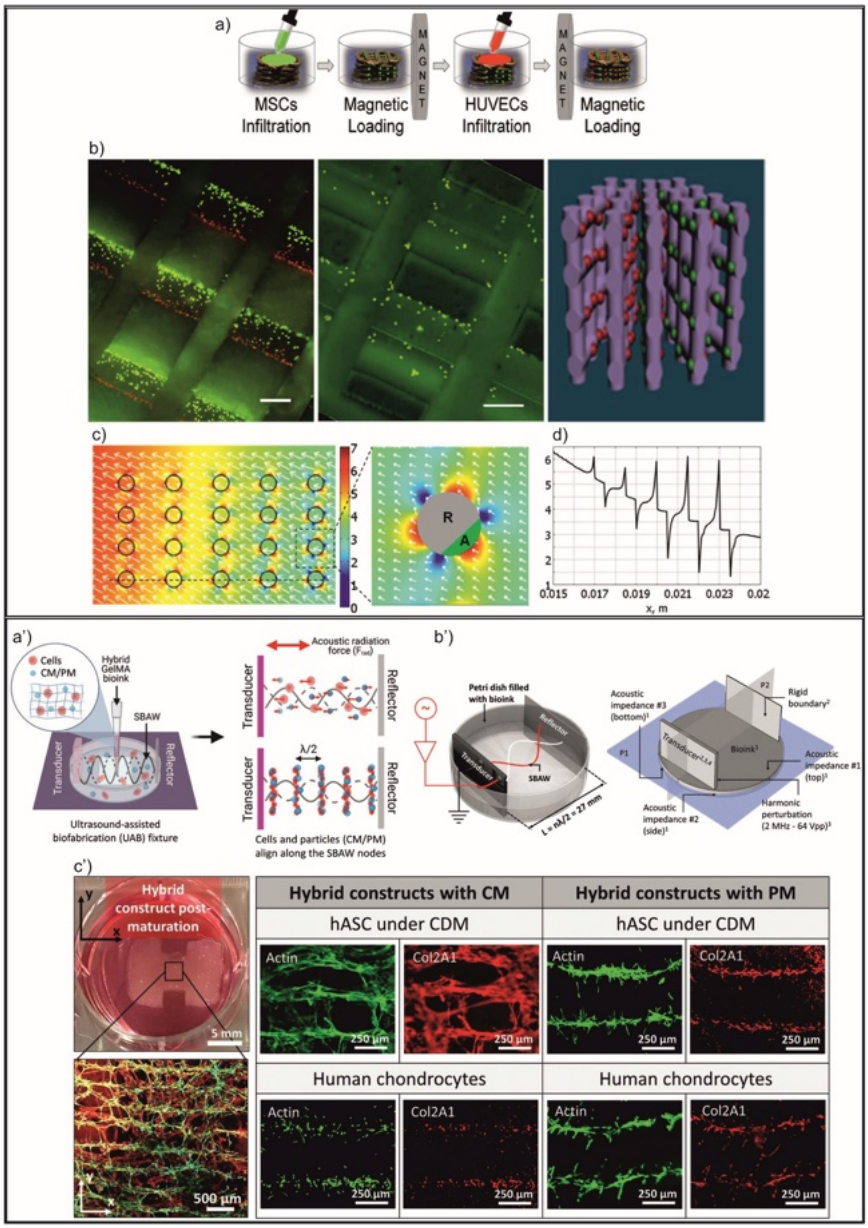

Figure 13. Panel (a) sketched representation of the experimental setup for 3D assembling the magnetically labeled cells inside the magnetic scaffold. Panel (b) from left to right: micro-spatial patterning of magnetically labeled cells in magnetized scaffolds (bar 200 μm): magnetic PCL/FeHA scaffold; non-magnetic PCL/HA scaffold; schematic illustration of magnetically assembled 3D cellular architectures. Panel (c) magnetic gradient in T m^{-1} units: distribution in the scaffold region: color scale indicates the magnitude while arrows show the direction of gradient and hence the direction of magnetic forces; in the dashed box: zooming around one fiber section, where green area delineates the attraction region (A), and gray area indicates the repulsion region (R); Panel (d) gradient distribution along the dashed line in panel c. Reproduced from [260]. CC BY 4.0. Copyright 2020 The Authors, published by Springer Nature. Panel (a') schematic representation of fabrication of anisotropic hybrid hydrogel constructs featuring patterned cells. The hybrid GelMA bioink is added to the ultrasonic patterning chamber (UPC) containing opposing transducer-reflector pairs. The actuation of the transducer at ultrasonic frequencies generates standing bulk acoustic waves (SBAW), which exerts radiation forces on the cells and particles, causing them to pattern along planes (3D patterning) parallel to the transducer/reflector surface. Panel (b") setup for the 3D computational modeling of SBAW generation in UPC including the boundary conditions. The pressure distribution pattern (right) is along straight lines as seen from the planar sections P1 (top view) and P2 (cross-sectional view), which is supportive of the analytical prediction that the cells and particles are patterned along parallel planes. Panel (c') synthesis of anisotropic cartilage *via* maturation (4 weeks in static culture) of constructs featuring ultrasound-assisted biofabrication (UAB) planar patterning of cells forming cell-adhesion. Cell morphology (green, actin) and collagen production (red, Collagen II) of cells under chondrogenic differentiation medium and human chondrocytes after prolonged maturation within hybrid GelMA constructs. Both the cells and cell-derived Col II exhibited aligned morphology, which establishes the effectiveness of UAB method in producing anisotropic musculoskeletal tissues. For human chondrocytes, while the cells failed to establish an aligned morphology, the collagen was predominantly organized along a singular direction around the periphery of the cells. For constructs containing patterned PCL, both cell types demonstrated cellular and Col II alignment. Reproduced with permission from [263]. © 2022 the authors. Advanced healthcare materials published by Wiley- VCH GmbH. All rights reserved, including rights for text and data mining and training of artificial intelligence technologies or similar. CC BY-NC-ND 4.0. Copyright 2022 with permission from Wiley-VCH GmbH.

which employs the force of radiation emanating from superposed ultrasonic bulk acoustic waves. This technique swiftly aligns cellular arrays and various biomaterial additives within hydrogel layers, both single and multiple (figure 13(b')). In this process, ultrasounds are applied with a composite bioink system. This system includes either human adipose tissue-derived stem cells or chondrocytes, along with either collagen microaggregates or polycaprolactone microfibers, all embedded within gelatin methacryloyl hydrogels. The resulting cartilage-like structures exhibit pronounced anisotropy. When crafted under optimal conditions that combine thermo-reversible and photocrosslinking, these hybrid matrices showcase superior mechanical properties such as stiffness and elasticity, as well as increased tensile strength. Additionally, they maintain their intended shape, display an aligned morphology of the encapsulated cells, and promote the secretion of collagen type II during extended culture periods (figure 13 (c')) (table 6) [263].

In conclusion, one of the most significant barriers to clinical translation of nanomaterials and microscaffolds mentioned in this chapter is noncompliance with demanding regulatory frameworks such as the European MDR 2017/745, or the complexity to align with standard as ISO 10993, ISO 13485, and so on. Many of the cited works do not completely comply (or even indicate data in agreement) with standards such as ISO10993, despite their established biocompatibility, which poses considerable challenges to future clinical studies. The apparent disparity between the current level of nanomaterials and microscaffolds research and those regulations emphasizes the need for more robust, compliant approaches to bridge the gap from experimental investigations to clinical application. This may involve the use of refined and more conforming biocompatibility studies, as well as thorough quality control in fabrication protocol systems, to fulfill regulatory criteria and ensure cheaper standardization.

19. Materials for microscaffolds for drug release

Creating polymers capable of delivering drugs for use in 3D-printed microscaffolds for tissue engineering holds significant promise in advancing regenerative medicine. The incorporation of drug-delivering polymers into 3D-printed microscaffolds can significantly enhance tissue regeneration. Drug delivery systems can provide controlled release of growth factors, cytokines, or other bioactive molecules at the site of tissue regeneration, promoting cell proliferation, differentiation, and tissue remodeling. This precise control enables the creation of complex tissue structures with tailored drug release profiles, optimizing therapeutic outcomes. Drug eluting polymers can enhance the biocompatibility of scaffolds by mitigating inflammatory responses and promoting cell adhesion and proliferation. This is crucial for ensuring the integration of the scaffold with the surrounding tissue and supporting tissue regeneration. Tailoring drug release profiles within 3D-printed microscaffolds allows for personalized medicine approaches in tissue engineering. Different patients may require different concentrations or combinations of drugs for optimal tissue regeneration based on their specific physiological conditions and needs. Localized drug delivery at the site of tissue regeneration minimizes systemic side effects associated with conventional systemic drug administration. This targeted approach enhances therapeutic efficacy while reducing the risk of adverse reactions in other tissues or organs. The combination of drug-delivering polymers and 3D-printing technology facilitates the fabrication of complex tissue structures with hierarchical organization and spatially controlled drug gradients. This is particularly relevant for engineering tissues with intricate architecture such as blood vessels, nerves, or organs. Controlled release of bioactive molecules from drug-eluting polymers can accelerate tissue healing processes by promoting angiogenesis, ECM deposition, and tissue remodeling. By providing precise control over drug release, enhancing scaffold biocompatibility, enabling personalized medicine approaches, and promoting accelerated tissue healing, this technology holds great promise for the development of next-generation regenerative therapies. Nonetheless, few works showed this possibility since drug half-life can be limited in time and the fabrication method can lead to degradation of the molecule itself.

In this context, PCL fibers can be loaded with drugs of specific chemical factors. 3D aerogel scaffolds composed of PLCL/gelatin electro-spun nanofiber loaded with statins (i.e. simvastatin) showed promising capability. As an example, Linfeng and colleagues fabricated a scaffold by coaxial electrospinning followed by freezing and drying the nanofiber loaded with Simvastatin. The PLCL coaxial fiber had a diameter distribution of 561 $\pm$ 95 nm without simvastatin and increased to 631 $\pm$ 103 nm when loaded, highlighting an enhanced osteoblast proliferation and osteogenic differentiation [235]. Jaffredo *et al* applied laser-assisted bioprinting techniques *in vivo* in mice, to demonstrate the possibility of vehiculating corticosteroids (i.e. dexamethasone) embedded in a sacrificial thermosensitive gel-based scaffold [244]. Then, inkjet and laser-assisted methods offer the capability to incorporate specific materials into scaffold fabrication. Ten years' old published research demonstrated the feasibility of forming patterns

Table 6. Materials used to fabricate microscaffolds in tissue engineering.

Fabrication Approach	Material	Resolution	Mechanical properties	Targeted organ	Detailed application	References
Bioprinting	PLA + HA + GelMA	40 μm	$E = 3.4$ kPa	Bone	- Implantable multi-material core–shell bone grafts - These grafts are designed to mimic the structure of long bones, featuring a stiffer shell and a softer core - The scaffold incorporates a hybrid composite of hydroxyapatite-coated poly(lactic acid) fiber-reinforced methacryolyl gelatin/alginate hydrogel	[279]
Bioprinting	MeHA	1.34 mm	$E = 3.02$–4.39 kPa	Skin	- Scaffold for the treatment of diabetic foot ulcers - This advanced wound dressing aims to enhance wound repair by providing a controlled release of proangiogenic factors - The scaffold is a patch of methacrylated hyaluronic acid designed to deliver small extracellular vesicles	[245]
Bioprinting & 2PP	Collagen & Collagen + PEGda	80 μm/100 nm	NA	Bone/ Cartilage/ Skin	- Scaffolds designed study disease pathogenesis, drug efficacy, and pharmaceutics in the context of pulmonary diseases - Stem cell expansion and differentiation, bone and cartilage regeneration, retina models etc.	[239, 294, 295]
Bioprinting	PCL + HA + MWCNT	330 μm	90–95 MPa	Bone	- The scaffold is designed to mimic the hierarchical structure of natural bone, aiming to repair damaged bone tissues - Aligned multi-walled carbon nanotubes and nano-hydroxyapatite within a polycaprolactone matrix - The scaffold shows an increased mechanical strength, cell proliferation, osteogenic differentiation, and scaffold mineralization	[280]
Bioprinting	Gel + bioglass	56–384 μm	397 kPa	Vessels	- The scaffold is made of a bioactive gelatin-sheet designed to support prevascularization - The scaffold shown potential for vascularized bone biofabrication, which is crucial for enhancing bone regeneration and healing	[243]

(Continued.)

Table 6. (Continued.)

Fabrication Approach	Material	Resolution	Mechanical properties	Targeted organ	Detailed application	References
Bioprinting	Gel + HA + Genipin	590–1000 μm	NA	Vessels	- The scaffold is designed to support prevascularization - The scaffold may produce bone substitutes that mimic the structure and function of native bone, with a focus on promoting vascularization - This blend demonstrated the ability to support mineralization and vasculogenesis	[247]
Bioprinting	Polydioxanone + silk	360 $\pm$ 35 μm and 420 $\pm$ 42 μm	100–200 MPa	Ligaments/ skin	- The scaffold is specifically aimed at repairing the anterior cruciate ligament - The blend of silk, polydioxanone and poly(lactide-co-caprolactone), has been designed to enhance material properties and improve *in vitro* and *in vivo* biocompatibility - The addition of silk increased tensile properties, degradation rate, and miscibility between phases	[296]
2PP	PCL + cells	Scaffolds diameter 300.4 $\pm$5.7 μm and trusses of 35.4 $\pm$4.0 μm	NA	Bone	- The scaffold allows the creation of single spheroids within each highly porous microscaffold, which can be used as modular building blocks - These tissue units can be combined to build larger tissue constructs through a bottom–up self-assembly process - This strategy can overcome limitations of scaffold-based and scaffold-free methods by using a synergistic approach	[282]
2PP	SZ2080	2.1 $\pm$ 0.4 μm to 1.04 $\pm$ 0.06 μm	1.9–4.4 GPa	Vessels/skin	- The Microatlas scaffold allows for the quantification and identification of cells, as well as the visualization of collagen and microvessels within the tissue, which is crucial for understanding the tissue's response to biomaterials and aiding in the healing process after injury - The Nichoid scaffold allows for stimulating stem cell proliferation while maintaining their stemness - Both scaffolds offer a 3D environment that influences cell growth and proliferation. - SZ2080 was proved to be biocompatible and inert both in *in vitro* and *in vivo* applications	[206, 290–292, 297]

(Continued.)

Table 6. (Continued.)

2PP	IP-L 780	5–12 μm	4.7 GPa	Vessels/skin/bone	- The scaffold is designed to support the growth of osteoblast-like, endothelial, cartilage, fibroblast cells, etc. - A novel work demonstrated the possibility to design, featuring stackable microcontainers. This technology could potentially be tailored for specific applications in drug screening or the creation of artificial organs in a building block approach	[287]
2PP	Poly(trimethylene-carbonate)	22–30 μm	NA	Bone	- The scaffold is made from a biodegradable and biocompatible polymer which is suitable for bone tissue engineering - The scaffold supports the attachment, proliferation, and differentiation of human adipose tissue-derived mesenchymal stem cells towards osteogenic and chondrogenic lineages	[203]
2PP	C, H-insertion crosslinking polymers	2.5 μm	300–550 kPa	Bone	- Scaffold made from one-component, polymer-based photoreactive material that relies on carbon-hydrogen (C, H) insertion crosslinking for bone tissue engineering - The scaffolds were made of woodpile with mesh sizes of 10 μm, 25 μm, and 50 μm with a lateral resolution down to 2.5 μm	[212]
2PP	Polylactide methacry-late + polylactide oligourethanedimethacry-late	NA	140 $\pm$ 40 MPa	Bone	- The scaffold is aided in the healing of bone defects (an alternative to allogeneic mesenchymal stem cell transplantation) - The scaffold structure has been shown to improve osteoinductive properties	[211]
2PP	GelMA + cells	2 μm	NA	Bone	- The scaffold is designed to support the growth and mineralization of dental pulp stem cells - The scaffold functionality is further enhanced by functionalization with bone morphogenetic protein 2, which promotes matrix mineralization, critical aspect of bone tissue engineering	[288]
2PP	B- cyclodextrin acry-lamide + adamantane acrylamide	3–4 μm	7–23 kPa	Skin	- The scaffold is designed to stretch single cells by applying an equibiaxial stretch of up to 25% - The scaffold utilizes a stimuli-responsive photoresist that contains cross-links formed by noncovalent interactions between β-cyclodextrin (host) and adamantane (guest), which can be actuated under physiological conditions - The host-guest interactions are reversible, allowing for controlled manipulation of the scaffold's mechanical properties and enabling the study of cell responses over time	[209]

(Continued.)

Table 6. (Continued.)

Fabrication Approach	Material	Resolution	Mechanical properties	Targeted organ	Detailed application	References
Photodegradation	Poly(ethylene glycol) tetrabicy-clononyne + diazide-functionalized synthetic peptides	10 μm	NA	Vessels	- The scaffold can produce a photothermal effect upon interaction with NIR light, leading to tumor destruction with high spatio-temporal resolution - The scaffold has also a photodynamic effect involving the production of reactive oxygen species which can kill cancer cells - Creating 3D channels and pores for vascularization models - Patterning of biochemical cues to guide cell migration and differentiation	[202]
Cell sheets & Self-assembly & Acoustic Patterning	Cells aggregates	NA	NA	Skin/cartilage/ bone	- Creating 3D tissue constructs with complex geometries for regenerative medicine, developing organ-on-a-chip systems for drug testing - Cell sheets and Self-Assembly organoids are used for repairing or regenerating defective tissues and organs, such as the heart, skin, cornea, cartilage, esophagus, and brain - They have been utilized in various preclinical trials - They contribute to creating scaffold-free tissues, which are crucial for studying cell-to-cell and extracellular matrix interactions	[265, 270–273, 293]
Microfluidics	Hydrogel microspheres	GelMA 100–200 μm Alginate 5–20 μm PAAm 363–571 μm PEG-4MAL 64–105 μm Dextran 150–1000 μm Alginate 90.4 μm PEG 355 μm Chitosan 19.2–31.6 μm pNIPAm 81 μm PEG 50–90 μm GelMA + chitosan 54–350 μm HAMA/HepMA 256.6 μm PEGDA 50–200 μm	NA	Skin/cartilage/bone	- Largely used to manipulate small amounts of materials Principal applications in cell sorting, organ-on-a-chip, spheroid, hydrogel microsphere formation, etc.	[255]

(Continued.)

Table 6. (Continued.)

Magnetophoresis	MNP + cells + PCL + FeHA	100–200 μm	NA	Vessels	- The scaffold is intended to be a precursor for vascularized tissue - The scaffold employs magnetic gradients to orient and trap magnetized cells on chosen sides of the scaffold fibers, facilitating the assembly of cellular constructs organized in biologically adequate arrangements - This method is a versatile solution for controlled seeding - The technology could potentially be used for *in vivo* environments	[260]
Magnetophoresis	Ferucarbotran + cells	NA	NA	Cartilage	- The scaffold is intended for the repair of focal articular cartilage defects - Autologous bone marrow mesenchymal stem cells have been magnetized with ferucarbotran and then controlled and accumulated at the cartilage defect area using a magnetic force - The process aims to enhance the repair of cartilage defects and has been tested for safety and efficacy in a clinical trial setting	[261]
Bioprinting & Acoustic Patterning	PCL + GelMa + cells	50–100 μm	NA	Bone	- The scaffold aims to replicate the microstructural organization of cells and extracellular components - Human adipose tissue-derived stem cells or chondrocytes and functional additives within hydrogel constructs were patterned by means of ultrasound-assisted biofabrication, creating anisotropic structures - Additives that promote cell adhesion were encapsulated within gelatin methacryloyl hydrogels - The process aims to fabricate tissue constructs with enhanced mechanical properties and aligned cell morphology	[263]
Bioprinting	Gel + drugs	NA	NA	Drug vehiculation for cancer	- A proof of concept for a new technique of intracochlear drugs administration in mice is presented - This technique involves delivering dexamethasone phosphate with a thermosensitive hydrogel on the mouse round window membrane - The drug diffusion into the perilymph was confirmed and no significant cochlear damages were highlighted	[244]

(Continued.)

Table 6. (Continued.)

Fabrication Approach	Material	Resolution	Mechanical properties	Targeted organ	Detailed application	References
Electrospinning	PCL + CS	3.4 ± 0.7 μm	2–10 MPa	Bone	- The scaffold aims to support cell adhesion, proliferation, and infiltration, thereby facilitating the restoration of tissue structure and function - The incorporation of chitosan granules into polycaprolactone fibers creates a 3D structure with expanded pores - This design addresses the limitation of small pore sizes in traditional electrospun membranes, which typically prevent cellular infiltration and limit the membranes to behave more like 2D structures	[277]
Electrospinning	PCL + Gel + GO	97–98 μm	14.8–17.2 MPa	Bone	- The scaffold is realized for bone tissue engineering - Nanofiber scaffold used a blend of polycaprolactone/gelatin reinforced with bone morphogenetic protein (BMP)-modified graphene oxide - The scaffold is designed to support bone tissue regeneration by providing a structure that closely resembles bone tissue, offering good biocompatibility, mechanical strength, and antibacterial properties	[281]
Electrospinning	PVA + Gel	100–350 μm	NA	Skin	- The bilayer nanofibrous-hydrogel scaffold is designed to promote wound healing - It has a hydrophilic surface, high swelling ability, and good stability, which are beneficial for maintaining a moist wound environment conducive to healing - The structure includes a top layer of nanofibers and a bottom layer of porous hydrogel, mimicking the extracellular matrix and supporting cell adhesion, proliferation, and tissue integration	[234]

(Continued.)

Table 6. (Continued.)

Electrospinning	CS + Nanodiamonds	80–190 nm	353–405 MPa	Skin	- The electrospun nanofibrous scaffold, modified with medical grade nanodiamonds, is designed to mimic the properties of natural skin - The scaffold aims to improve mechanical durability, hydrophilicity, and water vapor permeability, making it suitable for wound healing applications - The inclusion of MND is intended to enhance the mechanical strength of the membranes, decrease fiber diameters, and provide a platform for drug and growth factor conjugation for controlled release	[298]
Electrospinning	PCL + silk + CNT + GelMa	24–105 μm	NA	Skin	- The core–shell scaffold, based on aligned conductive nanofiber yarns within a hydrogel, is designed to mimic hierarchically aligned biological structures - This scaffold aims to enhance aligned neuronal outgrowth without external stimulation	[283]
Electrospinning	Polyethersulfone + Collagen	0.4–1.5 μm	NA	Vessels	- The scaffold is for the hepatogenic differentiation of induced pluripotent stem cells into hepatocyte-like cells - The scaffold is made of aligned polyethersulfone/collagen nanofibers	[285]
Electrospinning	PCL + Gel	NA	NA	Neural/ Wound healing	- The scaffold facilitates the formation of biological elongated networks by providing aligned electrospun fibers that guide the directional growth of cells	[286]
Electrospinning	PLCL + drugs	0.56–0.34 μm	NA	Drug vehiculation for cancer	- Simvastatin-loaded PLCL/gelatin electrospun nanofiber, which is being studied for its biocompatibility and efficacy in cell proliferation and ossification differentiation, forms up the scaffold - This scaffold aims to emulate the microstructure and compositional framework of natural bone, addressing the shortcomings of current bone repair materials - It shows potential in enhancing osteoblast proliferation and osteogenic differentiation, making it a promising material for treating bone defects	[235]

(Continued.)

Table 6. (Continued.)

Fabrication Approach	Material	Resolution	Mechanical properties	Targeted organ	Detailed application	References
Electrospinning & Cells Origami	PCL + nHA + cells	200 μm	NA	Bone	- The 3D nanofiber scaffold/cells complex created by combining electrospinning technology and origami techniques is intended for use in bone tissue engineering - Human fetal osteoblasts are grown on the scaffold and are anticipated to secrete extracellular matrix to promote the bonding of neighboring nanofiber films - The origami technique allows for the construction of a 3D block composed of electrospun nanofiber scaffold and cells, which can mimic the structure of natural bone tissue - The successful integration of nanohydroxyapatite particles into the scaffold aims to improve mechanical properties	[269]
Electrospinning & Bioprinting	PCL + drugs	2–4 μm	NA	Bone	- The scaffold is intended for bone tissue engineering - The scaffold is a bilayer electroconductive designed to provide an electrically conductive environment for cells - It incorporates conductive polyaniline bioactive particles, and drugs within an electrospun polycaprolactone/gelatin composite to enhance bioactivity and support cellular functions such as attachment, proliferation, migration, and differentiation - The conductive patterns are created using bioprinting method on the surface of the electrospun scaffolds	[299]

with conductive polymers atop electrospun scaffolds *via* inkjet printing to activate cellular responses. In such research, gelatin, enhanced with calcium phosphate NPs, and polycaprolactone, integrated with the Osteogenon medication, were utilized to construct a composite bilayer scaffold. This scaffold was prepared by collecting electrospun PCL/Osteo and gel fibers successively in the same collector. Subsequently, thin polyaniline patterns were applied to the hybrid scaffold's surface using inkjet printing. Their objective was to develop a bioactive, hybrid scaffold system by combining conductive polyaniline with bioactive particles and drugs within an electrospun composite scaffold. This system aimed to provide an electrically conductive environment for cells, but no further advancements can be found in recent years [299].

In conclusion, to date the use of inkjet printing as an additive manufacturing process for creating personalized medicine, using pharma-inks containing drugs and excipients for precise material deposition can be employed repeatedly. In the field of pharmaceutical inks, a notable categorization distinguishes between aqueous and nonaqueous formulations. Additionally, pharmaceutical inks can be categorized by their composition into polymer-, lipid-, and NP-based formulations. Each category of pharmaceutical ink necessitates specific excipients to enhance ink characteristics and drug delivery features. However, few studies reported their use in microscaffold printing and only with limited applicability in hydrogel-based materials.

20. Tissue engineering from basic research to clinical translation

The integration of various research fields such as biology, biomedical engineering, and materials science has led to the development of tissue engineering innovative strategies for combining cells, scaffolds, and mechanical and biochemical signals, as reported in this topical review. Even though tissue engineering was introduced three decades ago and has been extensively researched globally, its clinical applications are still in the early stages, with experimental, ethical, and regulatory issues posing ongoing challenges worldwide.

While there have been advancements in clinical protocols for the creation of bidimensional and small 3D tissue portions (up to few hundred micrometers), the production of fully functional 3D organs remains a complex task. In particular, the development of revascularized tissues with physiological capillary networks, which are essential for oxygen and nutrient distribution within, presents numerous obstacles. Several applications have been devised to address this issue before moving on to *in vivo* procedures, thereby reducing the risk of tissue necrosis [300].

Most clinical advancements in tissue-engineered products have been observed in the repair of elastic and articular cartilage, as well as in the treatment of cardiovascular and urological damages. Currently, cell-based therapies are entering clinical trials, and there is a growing demand for the standardization of potential tissue engineering approaches to facilitate their commercialization. Currently, 75 studies are reported in the U.S. clinical trials database under the keyword 'tissue* engineering', the vast majority of which are based on cell applications to treat specific diseases with 8 of them having reached phase III, and only one phase IV [301]. Similarly, 301 studies can be highlighted by searching the database for 'scaffold*'.

Nanomedicine has undergone extensive development starting from the discovery of liposome structure, passing through the approval of the first nanodrug Doxil® by the FDA in 1995 [302], up to the clinical validation and commercialization of many nanoformulations. The most recent evolution in this field focused on making nanomaterials responsive to specific stimuli, to warrant precision medicine and reduce not specific responses and toxicity [261]. Most nanomaterials have been devised for the diagnosis and treatment of cancer [40, 303, 304], and more recently have demonstrated high potential for other diseases (e.g. cardiovascular), and infections [305, 306]. Clinical trials involving the use of nanomaterials in tissue regeneration are extremely limited and up to now only two of them have been reported. Interestingly, one clinical trial investigated the osteogenic effects promoted by Wnt3a delivery by comparing hydroxyapatite NPs with viral administration and was completed in 2013 [307]. Another study, completed in 2019, evaluated the safety of a resorbable PLLA implant for regenerating the anterior cruciate ligament [308].

In the last 14 years, scaffolds have been employed in various clinical trials for tissue engineering and regenerative medicine. For instance, studies mainly highlighted the use of microscaffolds for regenerative therapy in spinal cord injury [309]. These scaffolds, in some cases bioprinted, while in the majority realized with additive manufacturing techniques, were used as drug and/or cell delivery systems to facilitate favorable cell-material interactions and neuroprotection. In other studies, the use of 3D structured

scaffolds and hydrogels, alone or combined with bioactive molecules or genes and cells, for tissue engineering applications was evaluated. These scaffolds were able to guide the development of functionally engineered tissues and provide mechanical support during *in vivo* implantation [310]. By considering the bone and cartilage frameworks, we can highlight 13 studies with different statuses of completion but having a poor focus on bioprinted and microfabricated ones [311–323]. Breast cancer clinical trials highlighted the use of a medical grade polycaprolactone scaffold implanted and combined with the patient's own fat cells to support soft tissue regeneration [324]. Similarly, few studies have used 3D-printed PCL scaffold for horizontal ridge augmentation in aesthetic zones [325, 326]. Despite the promising advancements, the scarcity of studies focusing on 3D microscaffolds compared to layer-by-layer approaches indicates a need for further research to optimize scaffold design, material selection, and biocompatibility to achieve functional skin reconstruction. In this regard, in the last 14 years, only three cases can be found in skin reconstruction [327–329].

21. Regulatory pathways and open challenges for clinical translation

As outlined in section 20, the number of nanomaterial- and scaffold-based products that have reached clinical use remains small relative to the volume of preclinical research. Therefore, a primary reason is regulatory since the engineered systems described in this topical review do not map neatly onto the established product categories of drug, medical device, and biologic, and the category assigned to a given construct determines its entire approval pathway, evidence burden, and timeline.

The regulatory route depends on the construct's principal mode of action rather than on its composition. An acellular scaffold whose action is essentially structural is normally treated as a medical device. A scaffold that elutes a drug or growth factor, or a therapeutic nanocarrier such as a liposome, polymeric micelle, dendrimer, or iron-oxide NP (sections 3–13; figures 7–9–10), exerts a pharmacological action and is regulated as a medicinal product/biologic, or, when an integral device component is present, as a combination product. A cell-loaded scaffold, as a cellularized construct, including the spheroid- and cell-sheet-based constructs discussed in section 16, is regulated as a cell-based/tissue-engineered product. The most demanding cases are the borderline and combination products that dominate this field, where even the responsible authority is not obvious at the outset.

21.1. United States (FDA pathways)

Devices, drugs, and biologics are reviewed by distinct centers (CDRH, Center for Devices and Radiological Health, CDER, Center for Drug Evaluation and Research and CBER, Center for Biologics Evaluation and Research, respectively). Additionally, for combination products, the Office of Combination Products assigns a lead center according to the primary mode of action. For example, acellular devices/scaffolds follow the validation paths '510(k)', 'De Novo', or 'premarket-approval routes', with a humanitarian device exemption available for rare conditions, as the pathway used for the first 3D-printed implant cleared in 2021. Cell-loaded constructs/scaffolds are regulated as human cells, tissues, and cellular and tissue-based products under '21 CFR' part 1271. Since those that are minimally manipulated and intended for a homologous use fall under section 361 and require no premarket approval, more than minimally manipulated products such as biologics require an 'Investigational New Drug' application and a 'Biologics License Application'. Such regenerative products, cell therapies, therapeutic tissue-engineered products, and combinations thereof, may qualify for the 'Regenerative Medicine Advanced Therapy' designation introduced by the '21st Century Cures Act' in 2016, which offers accelerated approval on surrogate or intermediate endpoints together with early and frequent engagement with the agency. For the nanomaterials considered in this topical review, the FDA's 2022 guidance drug products, including biological products, that contain nanomaterials, is the key reference document, setting expectations for physicochemical characterization, critical quality attributes, and the nonclinical and clinical data needed across development. Fabrication is addressed by the guidance on additive-manufactured devices and the 2021 discussion paper on 3D printing at the point of care. Notably, bioprinted constructs remain outside the scope of current device guidance and occupy a regulatory gray zone.

21.2. European Union (EMA pathways)

Acellular devices, including microfabricated scaffolds, fall under the MDR 2017/745, whose classification scheme and conformity-assessment requirements are described in section 17. Nonetheless two requirements are particularly relevant to be discussed in the present topical review: under article 117, a basic drug–device combination is regulated as a medicinal product and still requires a notified body opinion

on the device component. Additionally, under article 5.5 ('health-institution exemption'), devices manufactured and used in house by a health institution are partially exempted, and particularly relevant for the academic and hospital fabrication of microscaffolds. Cell-based and tissue-engineered constructs are instead governed by the advanced therapy medicinal products (ATMP) regulation (EC) No 1394/2007, which defines tissue-engineered products and combined ATMPs and requires a centralized marketing authorization assessed by EMA's committee for advanced therapies. Therefore, it is noteworthy that a construct which combines viable cells with a scaffold is regulated as an ATMP unless the cellular component is non-viable and merely auxiliary to the device. To resolve borderline cases, the optional classification procedure (article 17) provides a scientific recommendation within 60 d, and a dedicated certification scheme supports small and medium-sized developers (article 18). The E.U. has no nanomedicine-specific regulation and therefore nanomaterials are handled case-by-case under the medicinal-product framework, supplemented by EMA reflection papers on individual product classes.

22. Conclusions and future perspectives

Nanomaterials and microstructures represent the new frontiers of tissue engineering. The possibility of exploiting the intrinsic properties of biomaterials combined with the design of innovative biocompatible microstructures has revolutionized the field of regenerative medicine. In the last decade, several strategies to improve the interaction with living cells at the nano/microscale have evolved and the first applications in clinical settings are starting to become reality. Ranging from inorganic to organic NPs, much research has focused on facilitating the delivery and release of bioactive molecules, immunomodulation, and support for cell proliferation and differentiation. Although many promising results obtained, however, improvements are still required concerning, for instance, the expensive and time-consuming fabrication protocols. The creation of nanomaterials and polymers with the ability to incorporate drugs into 3D-printed microscaffolds has the potential to improve tissue regeneration. These drug-delivering polymers can stimulate cell proliferation, differentiation, and tissue remodeling by carefully regulating the release of bioactive compounds at the site of tissue regeneration. Personalized medicine techniques may also be used to create customized medication release profiles, which maximize therapeutic effectiveness and reduce systemic adverse effects. There are still issues, though, such as the short half-lives of medications and possible deterioration during manufacturing. However, developments in both top–down and bottom–up fabrication techniques present chances to get over these obstacles and give exact control over drug deposition in scaffold materials. Successful tissue healing and immune response modulation will be greatly aided by nanomaterials and microstructures. Engineered microstructures that may reduce immune cell involvement can be successfully incorporated into the body to replace damaged tissues and organs through the development of biocompatible nanomaterials. Whether 2.5 or 3D, microscaffolds offer a regulated microenvironment to influence macrophage activity and regulate inflammation. Specifically, inkjet bioprinting provides accurate control over drug deposition, making it possible to create intelligent scaffolds for tailored treatments.

Bridging the gap from laboratories to clinical applications will require early and structured regulatory engagement, pre-submission meetings and scientific advice, *ad hoc* classification in the E.U. framework and combination-product determinations in the U.S., together with a quality by design development, standardized nanomaterial characterization, and a design for compliance. In these, ISO 10993 and ISO 13 485 normative should be embedded from the beginning rather than retrofitted, as we emphasized in section 17. The development of a guidance for nanomaterial- and scaffold for tissue engineering, and a continued international harmonization through the International Council for Harmonisation and the relevant ISO additive-manufacturing standards, will be decisive in converting the experimental advances reviewed here into approved and long-lasting impacting therapies. Even though there are still difficulties with clinical translation on scaffold implantation and their general usage in human patients, further research promises to enhance scaffold design, material choice, and biocompatibility, which will eventually result in functional tissue restoration and better patient outcomes.

Acknowledgments

This research is funded by European Commission (EU, H2020 IN2SIGHT, G.A. 964481), by European Research Council (ERC, HE BEACONSANDEGG, G.A. 101053122) and by European Research Council (ERC, HE ALFRED, G.A. 101221323). Views and opinions expressed are however those of the authors

only and do not necessarily reflect those of the European Union or the European Research Council. Neither the European Union nor the granting authority can be held responsible for them.

Data availability statement

No new data were created or analysed in this study.

Conflict of interest

Manuela T. Raimondi is founder of the university spinoff company MOAB S.r.l. and holds shares. The other authors declare no competing financial interest.

Author contributions

Chiara Martinelli 0000-0001-9360-1689
Conceptualization (equal), Data curation (equal), Investigation (equal), Methodology (equal), Resources (equal), Software (equal), Supervision (equal), Visualization (equal), Writing – original draft (equal), Writing – review & editing (equal)

Claudio Conci 0000-0002-2335-9046
Conceptualization (equal), Data curation (equal), Funding acquisition (equal), Investigation (equal), Methodology (equal), Project administration (equal), Resources (equal), Software (equal), Supervision (equal), Visualization (equal), Writing – original draft (equal), Writing – review & editing (equal)

Manuela Teresa Raimondi 0000-0003-2585-7206
Conceptualization (equal), Funding acquisition (equal), Project administration (equal), Supervision (equal), Writing – original draft (supporting), Writing – review & editing (supporting)

References

[1] Sidhu P, Kumar S K K, Vyas V, Vyas R, Dhillon P S and Kaur T 2020 *Biomed. J. Sci. Tech. Res.* **26** 19733–9
[2] Health Resources & Services Administration Organ Donation Statistics (available at: www.organdonor.gov/learn/organ-donation-statistics) (Accessed March 2026)
[3] Eurotransplant Statistics Report Library (available at: https://statistics.eurotransplant.org/) (Accessed March 2026)
[4] Zion Market Research 2024 Tissue engineering market by application (gynecology, cell banking & cord blood, dental, urology, integumentary & skin, cardiology, neurology, musculoskeletal, orthopedics, & spine, and others), and by region - Global and regional industry overview, market intelligence, comprehensive analysis, historical data, and forecasts 2024-2032 (available at: https://www.zionmarketresearch.com/sample/tissue-engineering-market) (Accessed March 2026)
[5] Hasan A, Paul A, Memic A and Khademhosseini A 2015 *Biomed. Microdevices* 1788
[6] Paul A *et al* 2016 *J. Mater. Chem. B* **4** 3544–54
[7] Gaharwar A K, Singh I and Khademhosseini A 2020 *Nat. Rev. Mater.* **5** 686–705
[8] Zorlutuna P, Vrana N E and Khademhosseini A 2013 *IEEE Rev. Biomed. Eng.* **6** 47–62
[9] Li T, Chang J, Zhu Y and Wu C 2020 *Adv. Healthcare Mater.* **9** 2000208
[10] Yu L, Cai Y, Wang H, Pan L, Li J, Chen S, Liu Z, Han F and Li B 2020 *Acta Biomater.* **112** 75–86
[11] Han F *et al* 2022 *Adv. Healthcare Mater.* **11** 19e2200895
[12] Nicolas J, Magli S, Rabbachin L, Sampaolesi S, Nicotra F and Russo L 2020 *Biomacromolecules* 21 1968–94
[13] Wang S, Li J, Zhou Z, Zhou S and Hu Z 2018 *Molecules* **24**
[14] Werner M, Kurniawan N A and Bouten C V C 2020 *Materials* **13** 963
[15] Carotenuto F, Politi S, Ul Haq A, De Matteis F, Tamburri E, Terranova M L, Teodori L and Pasquo A 2022 *Micromachines* **13** 780
[16] Singh A P, Biswas A, Shukla A and Maiti P 2019 *Signal Transduct. Target. Ther.* **4**
[17] Cooke J P 2019 *Circ. Res.* **124** 1166–8
[18] Anderson J M, Rodriguez A and Chang D T 2008 *Semin. Immunol.* **20** 86–100
[19] Oishi Y and Manabe I 2018 *Int. Immunol.* **30** 511–28
[20] El-Sherbiny I M and Yacoub M H 2013 *Glob. Cardiol. Sci. Pract* **3** 316–42
[21] Dagtekin G, Schiffer R, Klein B, Jahnen-Dechent W and Zwadlo-Klarwasser G 2003 *Biomaterials* **24** 3395–401
[22] Théry C, Zitvogel L and Amigorena S 2002 Nat *Rev. Immunol.* **2** 569–79
[23] Cancedda R, Bollini S, Descalzi F, Mastrogiacomo M and Tasso R 2017 *Front. Bioeng. Biotechnol.* **5** 28
[24] Deng Z J, Liang M, Monteiro M, Toth I and Minchin R F 2011 *Nat. Nanotechnol.* **6** 39–44
[25] Schinwald A, Chernova T and Donaldson K 2012 *Part. Fibre Toxicol* **9** 47
[26] Xie J, MacEwan M R, Ray W Z, Liu W, Siewe D Y and Xia Y 2010 *ACS Nano* **4** 5027–36
[27] Park W, Shin H, Choi B, Rhim W K, Na K and Han D K 2020 *Prog. Mater. Sci.* **114** 100686
[28] Singh R, Kumawat M, Gogoi H, Madhyastha H, Lichtfouse E and Daima H K 2024 *ACS Appl. Bio Mater.* **7** 727–51

[29] Xiong J, Xiao R, Zhao J, Zhao Q, Luo M, Li F, Zhang W and Wu M 2024 *J. Transl. Med.* **22** 85
[30] Jafarinia H, Khalilimeybodi A, Barrasa-Fano J, Fraley S I, Rangamani P and Carlier A 2024 *npj Syst. Biol. Appl.* **10** 90
[31] Yu D, Xu C, Jiang J, Shen W and Zhu H 2025 *J. Zhejiang Univ. Sci. B* **27** 129–48
[32] Guan Y, Racioppi L and Gerecht S 2023 *Nat. Rev. Mater.* **8** 688–99
[33] Xu Z, Xu F and Cheng B 2024 *Mechanobiol. Med.* **2** 100067
[34] Ingber D E 1993 *J. Cell Sci.* **104** 613–27
[35] Khounsaraki G M, Movahedi M, Oscuii H N and Voloshin A 2024 *Ann. Biomed. Eng.* **52** 1213–21
[36] Donati L, Valicenti M L, Giannoni S, Morena F and Martino S 2024 *Int. J. Mol. Sci.* **25** 10386
[37] Carou-Senra P, Rodríguez-Pombo L, Awad A, Basit A W, Alvarez-Lorenzo C and Goyanes A 2024 *Adv. Mater.* **36** e2309164
[38] Ikada Y 2006 *J. R. Soc. Interface* **3** 589–601
[39] Kutluk H, Bastounis E E and Constantinou I 2023 *Adv. Healthcare Mater.* **12** 2203256
[40] Martinelli C, Pucci C and Ciofani G 2019 *APL Bioeng.* **3** 011502
[41] Colson Y L and Grinstaff M W 2012 *Adv. Mater.* **24** 3878–86
[42] Martinelli C, Pucci C, Battaglini M, Marino A and Ciofani G 2020 *Adv. Healthcare Mater.* **9** 1901589
[43] Amini A R, Laurencin C T and Nukavarapu S P 2012 *Crit. Rev. Biomed. Eng.* **40** 363–408
[44] Ju Y, Liao H, Richardson J J and Caruso F 2022 *Chem. Soc. Rev.* **51** 4287–336
[45] Liu X *et al* 2022 *J. Orthop. Transl.* **37** 152–62
[46] Wu P and Liang Y 2021 *Biomater. Transl.* **2** 61–71
[47] Gu Z, Wang J, Fu Y, Pan H and He H 2023 *Adv. Funct. Mater.* **33** 2212561
[48] Ezhilarasu H, Sadiq A, Ratheesh G, Sridhar S, Ramakrishna S, Ab Rahim M H, Yusoff M M and Jose R 2019 *Nanomedicine* **14** 201–14
[49] Martinelli C, Battaglini M, Pucci C, Gioi S, Caracci C, Macaluso G, Doccini S, Santorelli F M and Ciofani G 2020 *ACS Omega* **5** 12451–66
[50] Trofimov A, Ivanova A, Zyuzin M and Timin A 2018 *Pharmaceutics* **10** 167
[51] Zhong Q, Li W, Su X, Li G, Zhou Y, Kundu S C, Yao J and Cai Y 2016 *Colloids Surf. B* **143** 56–63
[52] Bobo D, Robinson K J, Islam J, Thurecht K J and Corrie S R 2016 *Pharm. Res.* **33** 2373–87
[53] Arias L, Pessan J, Vieira A, Lima T, Delbem A and Monteiro D 2018 *Antibiotics* **7** 46
[54] Kim J, Mahapatra C, Hong J, Kim M S, Leong K W, Kim H and Hyun J K 2017 *Adv. Sci.* **4** 1700034
[55] Lu Z, Yu D, Nie F, Wang Y and Chong Y 2023 *Pharmaceutics* **15** 2327
[56] Carvalho T, Bártolo R, Pedro S N, Valente B F A, Pinto R J B, Vilela C, Shahbazi M A, Santos H A and Freire C S R 2023 *ACS Appl. Mater. Interfaces* **15** 25860–72
[57] Zhang Y, Wang P, Mao H, Zhang Y, Zheng L, Yu P, Guo Z, Li L and Jiang Q 2021 *Mater. Des.* **197** 109231
[58] Wang Y, Shen B, Zhang Z, Chen Y, Zhu L, Zhang Y, Huang H and Jiang L 2022 *Biomater. Adv.* **137** 212841
[59] Peilin W *et al* 2023 *Mater. Today Bio.* **21** 100700
[60] Dong Y, Wang Z, Wang J, Sun X, Yang X and Liu G 2024 *J. Biol. Eng* **18**
[61] Popescu I, Constantin M, Solcan G, Ichim D L, Rata D M, Horodincu L, Solcan C and Solcan G 2023 *Gels* **9** 654
[62] Zhang Y, Kang J, Chen X, Zhang W, Zhang X, Yu W and Yuan W E 2023 *J. Nanobiotechnol.* **21** 435
[63] Tavares F J T M, Soares P I P, Silva J C and Borges J P 2023 *Int. J. Mol. Sci.* **24** 1128
[64] Zhou C, Wang C, Xu K, Niu Z, Zou S, Zhang D, Qian Z, Liao J and Xie J 2023 *Bioact. Mater.* **25** 615–28
[65] Suryadevara V *et al* 2023 *Theranostics* **13** 2710–20
[66] Kurian A G, Singh R K, Lee J H and Kim H W 2022 *ACS Appl. Bio Mater.* **5** 1130–8
[67] Singh H *et al* 2022 *Biomater. Adv.* **137** 212806
[68] Gong X, Luo M, Wang M, Niu W, Wang Y and Lei B 2022 *Regen. Biomater.* **9** rbab074
[69] Nakamura M, Araki H, Tsurushima H and Oyane A 2023 *Colloids Surf. B* **230** 113502
[70] Tenkumo T, Kruse B, Kostka K, Sokolova V, Ogawa T, Yoda N, Prymak O, Suzuki O, Sasaki K and Epple M 2024 *Regen. Ther* **25** 49–60
[71] Zhou Z, Zhou A, Jalil A T, Saleh M M and Huang C 2023 *Bioprocess Biosyst. Eng.* **46** 577–88
[72] Ghataty D S, Amer R I, Amer M A, Abdel Rahman M F and Shamma R N 2023 *Pharmaceutics* **15** 234
[73] Arambula-Maldonado R, Liu Y, Xing M and Mequanint K 2023 *Biomater. Adv.* **154** 213616
[74] Turkevich J, Stevenson P C and Hillier J 1951 *Discuss. Faraday Soc.* **11** 55–75
[75] Alivisatos A P, Johnsson K P, Peng X, Wilson T E, Loweth C J, Bruchez M P and Schultz P G 1996 *Nature* **382** 609–11
[76] Boisselier E and Astruc D 2009 *Chem. Soc. Rev.* **38** 1759–82
[77] Vial S and Reis R L 2017 *Curr. Opin. Solid State Mater. Sci* **21** 92–112
[78] Ostovari M, Riahi Alam N, Zabihzadeh M, Gharibvand M M and Hoseini-Ghahfarokhi M 2018 *J. Biomed. Phys. Eng.* **8** 241–50
[79] Chan K Y, Yang D, Demir B, Mouritz A P, Lin H, Jia B and Lau K T 2019 *Compos. Part B Eng.* **178** 107480
[80] Singh S, Gupta A, Qayoom I, Teotia A K, Gupta S, Padmanabhan P, Dev A and Kumar A 2020 *J. Nanoparticle Res.* **22** 152
[81] Prakash J, Prema D, Venkataprasanna K S, Balagangadharan K, Selvamurugan N and Venkatasubbu G D 2020 *Int. J. Biol. Macromol.* **154** 62–71
[82] Ehnert S, Schröter S, Aspera-Werz R H, Eisler W, Falldorf K, Ronniger M and Nussler A K 2019 *J. Clin. Med.* **8** 2028
[83] Ko W K, Heo D N, Moon H J, Lee S J, Bae M S, Lee J B, Sun I C, Park H K and Kwon I K 2015 *J. Colloid Interface Sci.* **438** 68–76
[84] Chen Q *et al* 2016 *Cell Death Differ.* **23** 1128–39
[85] Yi C, Liu D, Fong C C, Zhang J and Yang M 2010 *ACS Nano* **4** 6439–48
[86] Shi Y, Han X, Pan S, Wu Y, Jiang Y, Lin J, Chen Y and Jin H 2021 *Front. Chem.* **9** 724188
[87] Heo D N 2014 *ACS Nano* **8** 12049–62
[88] Yuan M and Wang Y 2017 *J. Biomed. Mater. Res. A* **105** 3350–9
[89] Pourjavadi A, Doroudian M, Ahadpour A and Azari S 2019 *Int. J. Biol. Macromol.* **126** 310–7
[90] Xu X, Ding Y, Hadianamrei R, Lv S, You R, Pan F, Zhang P, Wang N and Zhao X 2022 *Colloids Surf. B* **220** 112887
[91] He X, Dai L, Ye L, Sun X, Enoch O, Hu R, Zan X, Lin F and Shen J 2022 *Adv. Sci.* **9** e2105223
[92] Rezaei Kolarijani N, Cheraghali D, Khastar H, Ehterami A, Alizade M, Vaez A, Amini S M and Salehi M 2023 *Wound Repair Regen* **31** 804–15
[93] Sánchez-López E *et al* 2020 *Nanomaterials* **10** 292
[94] Wang Y, Dou C, He G, Ban L, Huang L, Li Z, Gong J, Zhang J and Yu P 2018 *Nanomaterials* **8** 324
[95] Rodríguez-Acosta H *et al* 2022 *J. Tissue Viability* **31** 173–9

[96] Sanmugam A, Shanthi D, Sairam A B, Kumar R S, Almansour A I, Arumugam N, Kavitha A, Kim H S and Vikraman D 2024 *Int. J. Biol. Macromol.* **257** 128598
[97] Dreanca A *et al* 2023 *Biomed. Mater.* **18** 055014
[98] Gupta A K and Gupta M 2005 *Biomaterials* **26** 3995–4021
[99] Xu H, Cheng L, Wang C, Ma X, Li Y and Liu Z 2011 *Biomaterials* **32** 9364–73
[100] Kudr J, Haddad Y, Richtera L, Heger Z, Cernak M, Adam V and Zitka O 2017 *Nanomaterials* **7** 243
[101] Li Z, Zhang Y, Ye Q, Wang L, Chen H, Xu C, Wang P and Sun J 2023 *Front. Bioeng. Biotechnol.* **11** 1259904
[102] Chircov C, Bejenaru I T, Nicoară A I, Bîrcă A C, Oprea O C and Tihăuan B 2022 *Pharmaceutics* **14** 2620
[103] Daya R, Xu C, Nguyen N Y T and Liu H H 2022 *ACS Appl. Mater. Interfaces* **14** 11051–67
[104] Celardo I, Pedersen J Z and Ghibelli L 2011 *Nanoscale* **3** 1411–20
[105] Genchi G G *et al* 2021 *ACS Appl. Mater. Interfaces* **13** 40200–13
[106] Purohit S D, Singh H, Bhaskar R, Yadav I, Chou C F, Gupta M K and Mishra N C 2020 *Mater. Sci. Eng. C* **116** 111111
[107] Li F, Li J, Song X, Sun T, Mi L, Liu J, Xia X, Bai N and Li X 2022 *Int. J. Nanomedicine* **17** 6561–78
[108] Dulany K, Hepburn K, Goins A and Allen J B 2020 *J. Biomed. Mater. Res. A* **108** 301–15
[109] Yildizbakan L, Iqbal N, Ganguly P, Kumi-Barimah E, Do T, Jones E, Giannoudis P V and Jha A 2023 *Antibiotics* **12** 1004
[110] Andrabi S M, Majumder S, Gupta K C and Kumar A 2020 *Colloids Surf. B* **195** 111263
[111] Lv Y, Xu Y, Sang X, Li C, Liu Y, Guo Q, Ramakrishna S, Wang C, Hu P and Nanda H S 2022 *J. Mater. Chem. B* **10** 1116–27
[112] He J, Meng X, Meng C, Zhao J, Chen Y, Zhang Z and Zhang Y 2022 *Molecules* **27** 1830
[113] Ebrahimi M, Botelho M, Lu W and Monmaturapoj N 2019 *J. Biomed. Mater. Res. A* **107** 1654–66
[114] Cao X, Wang G, Wang K, Guo L, Cao Y, Cao X and Yang Y 2020 *Nanoscale Res. Lett.* **15** 69
[115] Zhou P, Wu J, Xia Y, Yuan Y, Zhang H, Xu S and Lin K 2019 *Int. J. Nanomedicine* **14** 2753–4
[116] Wang D, Tabassum A, Wu G, Deng L, Wismeijer D and Liu Y 2017 *Clin. Oral Implants Res.* **28** 251–60
[117] Kinloch I A, Suhr J, Lou J, Young R J and Ajayan P M 2018 *Science* **362** 547–53
[118] Moniruzzaman M, Dutta S, Hexiu J, Ganguly K, Lim K T and Kim J 2022 *Biomater. Sci.* **10** 3527–39
[119] Cheng H *et al* 2023 *Int. J. Nanomedicine* **18** 6813–28
[120] Majood M *et al* 2024 *Biomater. Adv.* **157** 213730
[121] Kumari S, Singh D, Srivastava P, Singh B N and Mishra A 2022 *Biomed. Mater.* **17** 6
[122] Chen M, Li Y, Hou W X, Peng D Y, Li J K and Zhang H X 2023 *Int. J. Nanomedicine* **18** 1365–80
[123] Zhang L, Beatty A, Lu L, Abdalrahman A, Makris T M and Wang G 2020 *Mater. Sci. Eng. C* **111** 110768
[124] Caldorera-Moore M, Vela Ramirez J E and Peppas N A 2019 *J. Drug Target.* **27** 582–9
[125] Ulery B D, Nair L S and Laurencin C T 2011 *J. Polym. Sci. B* **49** 832–64
[126] Niza E, Ocaña A, Castro-Osma J A and Alonso-Moreno C 2021 *Cancers* **13** 3387
[127] Rezvantalab S, Drude N I, Moraveji M K, Güvener N, Koons E K, Shi Y, Lammers T and Kiessling F 2018 *Front. Pharmacol.* **9** 1260
[128] Essa D, Kondiah P P D, Choonara Y E and Pillay V 2020 *Front. Bioeng. Biotechnol.* **8** 48
[129] Paul P S, Cho J Y, Wu Q, Karthivashan G, Grabovac E, Wille H, Kulka M and Kar S 2022 *J. Nanobiotechnol.* **20** 67
[130] Udayar V, Chen Y, Sidransky E and Jagasia R 2022 *Trends Neurosci.* **45** 184–99
[131] Liu J, Shi L, Deng Y, Zou M, Cai B, Song Y, Wang Z and Wang L 2022 *Biomaterials* **287** 121638
[132] Ode Boni B O, Bakadia B M, Osi A R, Shi Z, Chen H and Gauthier M 2022 *Macromol. Biosci.* **22** e2100292
[133] Jena K, Pandey J P, Kumari R, Sinha A K, Gupta V P and Singh G P 2018 *Int. J. Biol. Macromol.* **120** 255–62
[134] Suktham K, Koobkokkruad T, Wutikhun T and Surassmo S 2018 *Int. J. Pharm.* **537** 48–56
[135] Chaisabai W, Khamhaengpol A and Siri S 2018 *Artif. Cells Nanomed. Biotechnol.* **46** 536–43
[136] Yang M, Shuai Y, Zhang C, Chen Y, Zhu L, Mao C and OuYang H 2014 *Biomacromolecules* **15** 1185–93
[137] Minhua T, Dashan W, Xinyan S, Xiao Y, Xiaojing L and Baodong Z 2022 *Bioengineered* **13** 1013–24
[138] Toita R, Kang J H and Tsuchiya A 2022 *Acta Biomater.* **154** 583–96
[139] Kiani M, Moraffah F, Khonsari F, Kharazian B, Dinarvand R, Shokrgozar M A and Atyabi F 2023 *Biomater. Adv.* **154** 213658
[140] Kurian A G, Mandakhbayar N, Singh R K, Lee J H, Jin G and Kim H W 2023 *Mater. Today Bio.* **20** 100664
[141] Liu F, Wang X, Li Y, Ren M, He P, Wang L, Xu J, Yang S and Ji P 2022 *Stem Cell Res. Ther.* **13** 26
[142] Cisneros K, Chowdhury N, Coleman E, Ferdous T, Su H, Jennings J A, Bumgardner J D and Fujiwara T 2021 *Macromol. Biosci.* **21** e2100123
[143] Shah S A, Sohail M, Karperien M, Johnbosco C, Mahmood A and Kousar M 2023 *Int. J. Biol. Macromol.* **227** 1203–20
[144] Karimi-Soflou R, Mohseni-Vadeghani E and Karkhaneh A 2022 *J. Biomed. Mater. Res. A* **110** 21–30
[145] Fu Z, Li D, Lin K, Zhao B and Wang X 2023 *Int. J. Biol. Macromol.* **226** 1079–87
[146] Danagody B, Bose N, Rajappan K, Iqbal A and Ramanujam G M 2024 *ACS Biomater. Sci. Eng.* **10** 468–81
[147] Pan H, Wei Y, Zeng C, Yang G, Dong C, Wan W and Chen S 2024 *Small* **20** e2309868
[148] Liu J, Tang C, Huang J, Gu J, Yin J, Xu G and Yan S 2023 *Adv. Healthcare Mater.* **12** e2302293
[149] Xiao L *et al* 2020 *Oxid. Med. Cell. Longev.* **2020** 6797154
[150] Lee C-S, Hsu G C-Y, Sono T, Lee M and James A W 2021 *Mol. Pharm.* **18** 1677–89
[151] Liu M, Chen W, Zhang X, Su P, Yue F, Zeng S and Du S 2020 *Eur. J. Pharm. Sci.* **151** 105373
[152] Ebrahimzade M, Mirdoraghi M, Alikarami A and Heidari S 2021 *Endocr. Metab. Immune Disord. Drug Targets* **21** 866–77
[153] Alquraishi R *et al* 2023 *Biomed. Chromatogr.* **37** e5716
[154] Yu J R, Varrey P, Liang B J, Huang H C and Fisher J P 2021 *ACS Biomater. Sci. Eng.* **7** 5230–41
[155] Li S, Wang Y, Wang S and Xie J 2023 *Front. Bioeng. Biotechnol.* **11** 1189010
[156] Cui Z *et al* 2024 *J. Control. Release* **366** 297–311
[157] Mancino C, Pasto A, De Rosa E, Dolcetti L, Rasponi M, McCulloch P and Taraballi F 2023 *Heliyon* **9** e16640
[158] Kryuchkova A, Savin A, Kiseleva A, Dukhinova M, Krivoshapkina E and Krivoshapkin P 2023 *Int. J. Biol. Macromol.* **253** 127246
[159] Tomalia D A and Fréchet J M J 2002 *J. Polym. Sci. A* **40** 2719–28
[160] Yang L *et al* 2020 *ACS Appl. Mater. Interfaces* **12** 37873–84
[161] Roumani S, Jeanneau C, Giraud T, Cotten A, Laucournet M, Sohier J and Pithioux M 2023 *Materials* **16** 862
[162] Zhu J, Tian J, Yang C, Chen J, Wu L, Fan M and Cai X 2021 *Small* **17** e2101495
[163] Elsabahy M, Perron M È, Bertrand N, Yu G and Leroux J C 2007 *Biomacromolecules* **8** 2250–7
[164] Liu T, Romanova S, Wang S, Hyun M A, Zhang C, Cohen S M, Singh R K and Bronich T K 2019 *Mol. Pharm.* **16** 2872–83

[165] Dahmana N, Mugnier T, Gabriel D, Favez T, Kowalczuk L, Behar-Cohen F, Gurny R and Kalia Y N 2021 *Int. J. Pharm.* **604** 120773
[166] Shi R, Li H, Jin X, Huang X, Ou Z, Zhang X, Luo G and Deng J 2022 *Acta Biomater.* **152** 425–39
[167] Gradinaru L M, Bercea M, Lupu A and Gradinaru V R 2023 *Polymers* **15** 1697
[168] Xue J, Wu T, Dai Y and Xia Y 2019 *Chem. Rev.* **119** 5298–415
[169] Doshi J and Reneker D H 1995 *J. Electrostat.* **35** 151–60
[170] Taskin M B, Ahmad T, Wistlich L, Meinel L, Schmitz M, Rossi A and Groll J 2021 *Chem. Rev.* **121** 11194–237
[171] Dash T K and Konkimalla V B 2012 *J. Control. Release* **158** 15–33
[172] Seo H J, Lee M H, Kwon B J, Kim H L, Lee S J, Kim B J, Wang K K, Kim Y R and Park J C 2013 *J. Appl. Phys.* **114** 071101
[173] Cheng G, Ma X, Li J, Cheng Y, Cao Y, Wang Z, Shi X, Du Y, Deng H and Li Z 2018 *Int. J. Pharm.* **547** 656–66
[174] Li R, Ma Y, Zhang Y, Zhang M and Sun D 2018 *Colloids Surf. B* **169** 384–94
[175] Cheng G *et al* 2019 *ACS Nano* **13** 6372–82
[176] Xu R, Zhang Z, Toftdal M S, Møller A C, Dagnaes-Hansen F, Dong M, Thomsen J S, Brüel A and Chen M 2019 *J. Control. Release* **301** 129–39
[177] Wang J, Shao L, Wu X, Liu C, Ni S, Dai T, Liu H and Zhao H 2023 *Mater. Today Bio.* **23** 100794
[178] Wang Y, Yuan Z, Pang Y, Zhang D, Li G, Zhang X, Yu Y, Yang X and Cai Q 2023 *ACS Appl. Mater. Interfaces* **15** 20661–76
[179] da Silva T N, Gonçalves R P, Rocha C L, Archanjo B S, Barboza C A G, Pierre M B R, Reynaud F and Picciani P H D S 2019 *Mater. Sci. Eng. C* **97** 602–12
[180] Movahedi M, Asefnejad A and Rafienia M 2020 *Int. J. Biol. Macromol.* **146** 627–37
[181] Hadisi Z, Farokhi M, Bakhsheshi-Rad H R, Jahanshahi M, Hasanpour S, Pagan E, Dolatshahi-Pirouz A, Zhang Y S, Kundu S C and Akbari M 2020 *Macromol. Biosci.* **20** e1900328
[182] Mirmajidi T, Chogan F, Rezayan A H and Sharifi A M 2021 *Int. J. Pharm.* **596** 120213
[183] Wang F, Wang X, Hu N, Qin G, Ye B and He J-S 2022 *J. Biomed. Nanotechnol.* **18** 77–86
[184] Tavakoli M *et al* 2023 *ACS Appl. Mater. Interfaces* **15** 55276–86
[185] Wen J *et al* 2023 *Int. J. Biol. Macromol.* **248** 125557
[186] Li X, Sun S, Yang A, Li X, Jiang Z, Wu S and Zhou F 2023 *Int. J. Biol. Macromol.* **253** 127601
[187] Wang S, Zhu H and Meng Q 2022 *Int. J. Mol. Sci.* **23** 14055
[188] Kazemi M H, Sajadimajd S and Gorgin Karaji Z 2023 *Int. J. Biol. Macromol.* **253** 126602
[189] Albanese A, Tang P S and Chan W C W 2012 *Annu. Rev. Biomed. Eng.* **14** 1–16
[190] Blanco E, Shen H and Ferrari M 2015 *Nat. Biotechnol* **33** 941–51
[191] Oberdörster G, Oberdörster E and Oberdörster J 2005 *Environ. Health Perspect.* **113** 823–39
[192] Nel A, Xia T, Mädler L and Li N 2006 *Science* **311** 622–7
[193] Wilhelm S, Tavares A, Dai Q, Ohta S, Audet J, Dvorak H F and Chan W C W 2016 *Nat. Rev. Mater.* **1** 16014
[194] Monopoli M P, Åberg C, Salvati A and Dawson K A 2012 *Nat. Nanotechnol.* **7** 779–86
[195] Fadeel B and Garcia-Bennett A E 2010 *Adv. Drug Deliv. Rev.* **62** 362–74
[196] Decuzzi P, Godin B, Tanaka T, Lee S Y, Chiappini C, Liu X and Ferrari M 2010 *J. Control. Release* **141** 320–7
[197] Gabbai-Armelin P R *et al* 2017 *J. Tissue Eng. Regen. Med.* **11** 1141–51
[198] Jovic T H, Kungwengwe G, Mills A C and Whitaker I S 2019 *Front. Mech. Eng.* **5** 19
[199] Ebrahimi M 2021 *Front. Mater. Sci.* **15** 352–73
[200] Witherel C E, Abebayehu D, Barker T H and Spiller K L 2019 *Adv. Healthcare Mater.* **8** 1801451
[201] Leclech C and Villard C 2020 *Front. Bioeng. Biotechnol.* **8** 551505
[202] Arakawa C K, Badeau B A, Zheng Y and DeForest C A 2017 *Adv. Mater.* **29** 1703156
[203] Weisgrab G, Guillaume O, Guo Z, Heimel P, Slezak P, Poot A, Grijpma D and Ovsianikov A 2020 *Biofabrication* **12** 045036
[204] Galeano J, Zarzycki A, Garzón Reyes J and Moncada M E 2020 *Biomed. Signal Process. Control* **62** 102087
[205] Lepore M, Portaccio M, Delfino I, Sironi L, La Gatta A, D'Agostino A, Izzo E and Schiraldi C 2017 *J. Appl. Polym. Sci.* **134** e45243
[206] Conci C, Jacchetti E, Sironi L, Gentili L, Cerullo G, Osellame R, Chirico G and Raimondi M T 2022 *Adv. Opt. Mater.* **10** 2101103
[207] Colombo F *et al* 2024 *Adv. Funct. Mater.* **34** 2303601
[208] Eivazzadeh-Keihan R *et al* 2024 *Nanoscale Adv.* **6** 337–66
[209] Hippler M *et al* 2020 *Sci. Adv.* **6** eabc2648
[210] Zhao H, Liu M, Zhang Y, Yin J and Pei R 2020 *Nanoscale* **12** 14976–95
[211] Rodimova S *et al* 2023 *Stem Cell Res. Ther.* **14** 81
[212] Song D, Husari A, Kotz-Helmer F, Tomakidi P, Rapp B E and Rühe J 2023 *Small* **20** 2306682
[213] Duan Q *et al* 2023 *ACS Appl. Mater. Interfaces* **15** 26472–83
[214] Thompson J R *et al* 2019 *Acta Biomater.* **94** 204–18
[215] Florian B, Michel K, Steffi G, Nicole H, Frant M, Klaus L and Henning S 2019 *Biomed. Mater.* **14** 035001
[216] Broguiere N, Lüchtefeld I, Trachsel L, Mazunin D, Rizzo R, Bode J W, Lutolf M P and Zenobi-Wong M 2020 *Adv. Mater.* **32** 1908299
[217] Wang H *et al* 2023 *Adv. Funct. Mater.* **33** 2214211
[218] Liu K, Ding H, Li S, Niu Y, Zeng Y, Zhang J, Du X and Gu Z 2022 *Nat. Commun* **13** 4563
[219] Jing X, Fu H, Yu B, Sun M and Wang L 2022 *Front. Bioeng. Biotechnol.* **10** 994355
[220] Spiegel C A, Hippler M, Münchinger A, Bastmeyer M, Barner-Kowollik C, Wegener M and Blasco E 2020 *Adv. Funct. Mater.* **30** 1907615
[221] Turunen S, Joki T, Hiltunen M L, Ihalainen T O, Narkilahti S and Kellomäki M 2017 *ACS Appl. Mater. Interfaces* **9** 25717–30
[222] Harberts J, Fendler C, Teuber J, Siegmund M, Silva A, Rieck N, Wolpert M, Zierold R and Blick R H 2020 *ACS Nano* **14** 13091–102
[223] Lesani P, Singh G, Viray C M, Ramaswamy Y, Zhu D M, Kingshott P, Lu Z and Zreiqat H 2020 *ACS Appl. Mater. Interfaces* **12** 18395–406
[224] Sharaf A, Roos B, Timmerman R, Kremers G-J, Bajramovic J J and Accardo A 2022 *Front. Bioeng. Biotechnol.* **10** 926642
[225] Buchberger G, Muck M, Plamadeala C and Heitz J 2023 *Ultrafast Laser Nanostructuring: The Pursuit of Extreme Scales* 1st edn vol 239, ed R Stoian and J Bonse (*Springer Series in Optical Sciences*)(Springer) pp 1105–65
[226] Alghauli M A, Almutairi S, Aljohani R, Aljohani W and Alqutaibi A Y 2025 *Bioprinting* **46** e00395
[227] Flamourakis G, Kordas A, Barmparis G D, Ranella A and Farsari M 2021 *Opt. Mater. Express* **11** 801
[228] LeValley P J, Noren B, Kharkar P M, Kloxin A M, Gatlin J C and Oakey J S 2018 *ACS Biomater. Sci. Eng.* **4** 3078–87

[229] Nouri-Felekori M, Nezafati N, Moraveji M, Hesaraki S and Ramezani T 2021 *Int. J. Biol. Macromol.* **183** 2030–43
[230] Belgio B, Boschetti F and Mantero S 2021 *Bioengineering* **8** 18
[231] Mukasheva F, Zhanbassynova A and Erisken C 2024 *Biomed. Mater. Eng.* **35** 1–13
[232] Qiu B *et al* 2024 *Langmuir* **40** 4709–18
[233] Zheng T, Gao H, Liu Y, Sun S, Guan W, Wu L, Yang Y and Li G 2024 *Bioact. Mater.* **35** 401–15
[234] Khan R, Khan M U A, Stojanović G M, Javed A, Haider S and Abd Razak S I 2024 *ACS Omega* **9** 6527–36
[235] Linfeng L, Xiaowei Z, Xueqin C and Xianfeng Z 2024 *Biomed. Mater. Eng.* **35** 1–11
[236] Li X, Liu B, Pei B, Chen J, Zhou D, Peng J, Zhang X, Jia W and Xu T 2020 *Chem. Rev.* **120** 10793–833
[237] Dufour A, Gallostra X B, O'keeffe C, Eichholz K, Von Euw S, Garcia O and Kelly D J 2022 *Biomaterials* **283** 121405
[238] Kim W, Lee Y, Kang D, Kwak T, Lee H R and Jung S 2023 *ACS Biomater. Sci. Eng.* **9** 2806–15
[239] Kang D, Park J A, Kim W, Kim S, Lee H, Kim W, Yoo J and Jung S 2021 *Adv. Sci.* **8** 2004990
[240] Compaan A M, Christensen K and Huang Y 2017 *ACS Biomater. Sci. Eng.* **3** 1519–26
[241] Hakobyan D, Kerouredan O, Remy M, Dusserre N, Medina C, Devillard R, Fricain J-C and Oliveira H 2020 *3D Bioprint.* **2140** 135–44
[242] Koch L, Brandt O, Deiwick A and Chichkov B 2017 *Int. J. Bioprinting* **3** 42
[243] Kérourédan O, Washio A, Handschin C, Devillard R, Kokabu S, Kitamura C and Tabata Y 2024 *Biomed. Mater.* **19** 25038
[244] Jaffredo M, Duchamp O, Touya N, Bouleau Y, Dulon D, Devillard R and Bonnard D 2023 *Hear. Res* **438** 108880
[245] Ferroni L *et al* 2023 *J. Nanobiotechnology* **21** 469
[246] Wu J, Wu C, Zou S, Li X, Ho B, Sun R, Liu C and Chen M 2023 *Bioengineering* **10** 1358
[247] Khatun M R, Bhattacharyya A, Gunbayar M, Jung M and Noh I 2023 *Gels* **9** 601
[248] Vijayaraghavan R, Loganathan S and Valapa R B 2024 *Macro Molecular Bioscience* **264** 130472
[249] Cui X, Li J, Hartanto Y, Durham M, Tang J, Zhang H, Hooper G, Lim K and Woodfield T 2020 *Adv. Healthcare Mater.* **9** e1901648
[250] Adhikari J, Roy A, Das A, Ghosh M, Thomas S, Sinha A, Kim J and Saha P 2021 *Macromol. Biosci.* **21** e2000179
[251] Yu Y, Shang L, Guo J, Wang J and Zhao Y 2018 *Nat. Protoc.* **13** 2557–79
[252] Sanjay S T, Zhou W, Dou M, Tavakoli H, Ma L, Xu F and Li X 2018 *Adv. Drug Deliv. Rev.* **128** 3–28
[253] Zhou W, Dou M, Timilsina S S, Xu F and Li X 2021 *Lab Chip* **21** 2658–83
[254] Kung C-T, Gao H, Lee C-Y, Wang Y-N, Dong W, Ko C-H, Wang G and Fu L-M 2020 *Chem. Eng. J.* **399** 125748
[255] Chen Z, Lv Z, Zhang Z, Weitz D A, Zhang H, Zhang Y and Cui W 2021 *Exploration* **1** 20210036
[256] Highley C B, Song K H, Daly A C and Burdick J A 2019 *Adv. Sci.* **6** 1801076
[257] Zhang S, Wan Z and Kamm R D 2021 *Lab Chip* **21** 473–88
[258] Ko J, Ahn J, Kim S, Lee Y, Lee J, Park D and Jeon N L 2019 *Lab Chip* **19** 2822–33
[259] Brassard J A, Nikolaev M, Hübscher T, Hofer M and Lutolf M P 2021 *Nat. Mater.* **20** 22–29
[260] Goranov V *et al* 2020 *Sci. Rep.* **10** 2289
[261] Kamei N, Ochi M, Adachi N, Ishikawa M, Yanada S, Levin L S, Kamei G and Kobayashi T 2018 *Knee Surg. Sports Traumatol. Arthrosc.* **26** 3626–35
[262] Chakraborty J *et al* 2024 *Cell Rep. Phys. Sci.* **5** 101819
[263] Chansoria P, Asif S, Gupta N, Piedrahita J and Shirwaiker R A 2022 *Adv. Healthcare Mater.* **11** 2102351
[264] Ma Y, Poole K, Goyette J and Gaus K 2017 *Front. Immunol.* **8** 1513
[265] Comeau E S, Vander Horst M A, Raeman C H, Child S Z, Hocking D C and Dalecki D 2023 *Sci. Rep.* **13** 16082
[266] Primo G A and Mata A 2021 *Adv. Funct. Mater.* **31** 2009574
[267] Serpooshan V *et al* 2017 *Biomaterials* **131** 47–57
[268] Davis D, Chen B, Dickey M D and Genzer J 2016 *J. Mech. Robot.* **8** 031014
[269] Song J, Zhu G, Gao H, Wang L, Li N, Shi X and Wang Y 2018 *Bio-Des. Manuf.* **1** 254–64
[270] Thummarati P, Laiwattanapaisal W, Nitta R, Fukuda M, Hassametto A and Kino-oka M 2023 *Bioengineering* **10** 211
[271] Imashiro C and Shimizu T 2021 *Int. J. Mol. Sci.* **22** 425
[272] Mito K, Lachnish J, Le W, Chan C, Chang Y-L and Yao J 2024 *Tissue Eng. A* **30** 107–14
[273] Decoene I *et al* 2024 *Stem Cells Transl. Med.* **13** 278–92
[274] Gjorevski N, Nikolaev M, Brown T E, Mitrofanova O, Brandenberg N, DelRio F W, Yavitt F M, Liberali P, Anseth K S and Lutolf M P 2022 *Science* **375** eaaw9021
[275] Liu J, Shahriar M, Xu H and Xu C 2022 *Biofabrication* **14** 045020
[276] Huang Q *et al* 2024 *Lab Chip* **24** 1715–26
[277] Vieira T, Rebelo A M, Borges J P, Henriques C and Silva J C 2024 *Polymers* **16** 527
[278] He Q, Okajima T, Onoe H, Subagyo A, Sueoka K and Kuribayashi-Shigetomi K 2018 *Sci. Rep.* **8** 4556
[279] Moghimi N, Kamaraj M, Zehtabi F, Amin Yavari S, Kohandel M, Khademhosseini A and John J V 2024 *J. Mater. Chem. B* **12** 2818–30
[280] Huang B, Vyas C, Byun J J, El-Newehy M, Huang Z and Bártolo P 2020 *Mater. Sci. Eng. C* **108** 110374
[281] Kadhim M M, Bokov D O, Ansari M J, Suksatan W, Jawad M A, Chupradit S, Fenjan M N and Kazemnejadi M 2022 *Bioprocess Biosyst. Eng.* **45** 981–97
[282] Guillaume O, Kopinski-Grünwald O, Weisgrab G, Baumgartner T, Arslan A, Whitmore K, Van Vlierberghe S and Ovsianikov A 2023 *Acta Biomater.* **165** 72–85
[283] Wang L, Wu Y, Hu T, Ma P X and Guo B 2019 *Acta Biomater.* **96** 175–87
[284] Kim J H, Choi Y-J, Yi H-G, Wang J H, Cho D-W and Jeong Y H 2017 *Biomed. Mater.* **12** 055010
[285] Mahmoodinia Maymand M, Soleimanpour-Lichaei H R, Ardeshirylajimi A, Soleimani M, Enderami S E, Nojehdehi S, Behjati F and Kabir Salmani M 2018 *Artif. Cells Nanomedicine Biotechnol.* **46** 853–60
[286] Soliman E, Bianchi F, Sleigh J N, George J H, Cader M Z, Cui Z and Ye H 2018 *Biotechnol. Lett.* **40** 601–7
[287] Larramendy F, Yoshida S, Maier D, Fekete Z, Takeuchi S and Paul O 2019 *Lab Chip* **19** 875–84
[288] Parkatzidis K, Chatzinikolaidou M, Kaliva M, Bakopoulou A, Farsari M and Vamvakaki M 2019 *ACS Biomater. Sci. Eng.* **5** 6161–70
[289] Nava M M, Di Maggio N, Zandrini T, Cerullo G, Osellame R, Martin I and Raimondi M T 2017 *J. Tissue Eng. Regen. Med.* **11** 2836–45
[290] Parodi V, Jacchetti E, Bresci A, Talone B, Valensise C M, Osellame R, Cerullo G, Polli D and Raimondi M T 2020 *Int. J. Mol. Sci.* **21** 8498

[291] Mačiulaitis J et al 2015 Biofabrication 7 015015
[292] Conci C et al 2024 APL Bioeng. 8 016102
[293] Forghani A, Kriegh L, Hogan K, Chen C, Brewer G, Tighe T B, Devireddy R and Hayes D 2017 J. Biomed. Mater. Res. A 105 1346–54
[294] Nakayama A, Kumamoto Y, Minoshima M, Kikuchi K and Fujita K 2022 Adv. Opt. Mater. 10 2200474
[295] Păun I A, Mustăciosu C C, Popescu R C, Călin B Ş and Mihăilescu M 2020 Int. J. Mol. Sci. 21 6426
[296] Shiroud Heidari B et al 2023 Bioact. Mater. 25 291–306
[297] Zandrini T, Shan O, Parodi V, Cerullo G, Raimondi M T and Osellame R 2019 Sci. Rep. 9 11761
[298] Mahdavi M, Mahmoudi N, Rezaie Anaran F and Simchi A 2016 Drugs 14 128
[299] Rajzer I, Rom M, Menaszek E and Pasierb P 2015 Mater. Lett. 138 60–63
[300] Den Hondt M, Vanaudenaerde B M, Verbeken E K and Vranckx J J 2018 Interact. Cardiovasc. Thorac. Surg. 26 753–60
[301] ClinicalTrials.gov (available at: https://clinicaltrials.gov) (Accessed March 2026)
[302] FDA (available at: www.accessdata.fda.gov/scripts/cder/daf/index.cfm?event=overview.process&ApplNo=050718) (Accessed March 2026)
[303] Zhang Y, Li M, Gao X, Chen Y and Liu T 2019 J. Hematol. Oncol. 12 137
[304] Martinelli C and Biglietti M 2020 Cancer Drug Resist. 3 1003–20
[305] Chandarana M, Curtis A and Hoskins C 2018 Appl. Nanosci. 8 1607–19
[306] Anselmo A C and Mitragotri S 2019 Bioeng. Transl. Med. 4 e10143
[307] ClinicalTrials.gov (available at: https://clinicaltrials.gov/study/NCT01323894) (Accessed March 2026)
[308] ClinicalTrials.gov (available at: https://clinicaltrials.gov/study/NCT01634711) (Accessed March 2026)
[309] Suzuki H, Imajo Y, Funaba M, Ikeda H, Nishida N and Sakai T 2023 Int. J. Mol. Sci. 24 2528
[310] Pina S, Ribeiro V P, Marques C F, Maia F R, Silva T H, Reis R L and Oliveira J M 2019 Materials 12 1824
[311] ClinicalTrials.gov (available at: https://clinicaltrials.gov/study/NCT01301664) (Accessed March 2026)
[312] ClinicalTrials.gov (available at: https://clinicaltrials.gov/study/NCT01791062) (Accessed March 2026)
[313] ClinicalTrials.gov (available at: https://clinicaltrials.gov/study/NCT01879046) (Accessed March 2026)
[314] ClinicalTrials.gov (available at: https://clinicaltrials.gov/study/NCT01813188) (Accessed March 2026)
[315] ClinicalTrials.gov (available at: https://clinicaltrials.gov/study/NCT02033226) (Accessed March 2026)
[316] ClinicalTrials.gov (available at: https://clinicaltrials.gov/study/NCT02513368) (Accessed March 2026)
[317] ClinicalTrials.gov (available at: https://clinicaltrials.gov/study/NCT00900718) (Accessed March 2026)
[318] ClinicalTrials.gov (available at: https://clinicaltrials.gov/study/NCT02859025) (Accessed March 2026)
[319] ClinicalTrials.gov (available at: https://clinicaltrials.gov/study/NCT03076138) (Accessed March 2026)
[320] ClinicalTrials.gov (available at: https://clinicaltrials.gov/study/NCT01605201) (Accessed March 2026)
[321] ClinicalTrials.gov (available at: https://clinicaltrials.gov/study/NCT02673905) (Accessed March 2026)
[322] ClinicalTrials.gov (available at: https://clinicaltrials.gov/study/NCT02090140) (Accessed March 2026)
[323] ClinicalTrials.gov (available at: https://clinicaltrials.gov/study/NCT03103295) (Accessed March 2026)
[324] ClinicalTrials.gov (available at: https://clinicaltrials.gov/study/NCT05437757) (Accessed March 2026)
[325] ClinicalTrials.gov (available at: https://clinicaltrials.gov/study/NCT05241548) (Accessed March 2026)
[326] ClinicalTrials.gov (available at: https://clinicaltrials.gov/study/NCT03735199) (Accessed March 2026)
[327] ClinicalTrials.gov (available at: https://clinicaltrials.gov/study/NCT02059252) (Accessed March 2026)
[328] ClinicalTrials.gov (available at: https://clinicaltrials.gov/study/NCT04389164) (Accessed March 2026)
[329] ClinicalTrials.gov (available at: https://clinicaltrials.gov/study/NCT03960164) (Accessed March 2026)